Desarrollo de péptidos fotoconmutables para el control de la actividad celular

Andrés Martín Quirós

Programa de Doctorado en Biotecnología
2008 -2014

Desarrollo de péptidos fotoconmutables para el control de la actividad celular

Memoria presentada por Andrés Martín Quirós para optar al título de Doctor por la Universidad de Barcelona.

Andrés Martín Quirós

Nanoprobes and Nanoswitches Group
Institute for Bioengineering of Catalonia

Directors:

Prof. Pau Gorostiza Langa

ICREA Research Professor
Nanoprobes and Nanoswitches Group
Institute for Bioengineering of Catalonia

Prof. Fausto Sanz Carrasco

Universidad de Barcelona
Nanoprobes and Nanoswitches Group
Institute for Bioengineering of Catalonia

Barcelona, Julio 2014

Development of photoswitchable peptides for control of cell activity

Doctoral thesis

Andrés Martín Quirós

Directors:

Prof. Pau Gorostiza Langa
ICREA Research Professor
Nanoprobes and Nanoswitches Group
Institute for Bioengineering of Catalonia

Prof. Fausto Sanz Carrasco
Universidad de Barcelona
Nanoprobes and Nanoswitches Group
Institute for Bioengineering of Catalonia

"Es improbable que uno alcance la comprensión a partir de las explicaciones de otro."

"Este día no volverá.

Cada minuto es una joya de valor incalculable."

- Takuan Soho (1527-1???)

Para Sera y Paqui

Agradecimientos

Es prácticamente imposible citar a todos quienes merecen agradecimiento en esta página inicial. Vaya por delante mi agradecimiento más sincero para todos aquellos cuyo trabajo o parte de él era hacer posible y mejor esta tesis y lo han cumplido. Agradezco también la beca FPU del Ministerio de Educación, Cultura y Deporte (MECD) AP2006-01279 que me ha permitido realizar este trabajo. Pasando a aquellos que se apartaron de su camino, fueron más allá del deber y/o padecieron conmigo (o más bien por mi causa) los momentos difíciles, se impone una disculpa: temo que ningún trabajo que yo pueda hacer esté a la altura de vuestra generosidad. En esa lista, los primeros son mis padres, que mantuvieron viva la curiosidad que inclina a las personas hacia la ciencia y no escatimaron nunca esfuerzos para posibilitar que pudiera seguir este camino. Mi hermano Sera siempre me ha apoyado y me ha acompañado cuando he necesitado apartarme por un rato de la investigación sin importar la hora. Maribel ha sido la mejor compañera que se puede desear y su valor ha alcanzado a adentrarse conmigo en la maternidad de Héctor mientras realizaba su propia tesis y no dejaba de apoyarme en la mía. Roque, Pili, Javi y Lisen también han estado animando siempre; a ellos también gracias. Y gracias a los amigos: roleros, del instituto o de la calle. A todos os he pagado vuestro apoyo con ausencias y nunca lo habéis retirado. Esto es lo que estaba haciendo. De la gente del laboratorio siempre tendré un recuerdo agradecido para Ernest Giralt y buena parte de su equipo que generosamente me acogieron en su laboratorio en algunos tramos del trabajo. Peter Tremmel me introdujo en la fase más temprana a la síntesis orgánica real y al humor, algo negro, que ayuda a sobrellevar los fracasos y decepciones que vienen con la experimentación. Laura Nevola es la más dedicada, metódica y concienzuda experimentadora que he conocido; me faltarán muchos años para llegar a su altura. En el grupo de Anna Aragay también me han dedicado siempre tiempo, aunque nunca conseguí hacer funcionar aquellos experimentos. Mis compañeros originales de laboratorio, ahora repartidos por el mundo han compartido la mayor parte de lo bueno y lo malo del día a día y una infinidad de cafés y bebidas estimulantes de cebada; Lorena, Marcel, Juan Ma, Marina y Michel: ha sido un privilegio compartir laboratorio con vosotros. De los estudiantes que han pasado por el laboratorio en

estos años y con quienes he trabajado siempre he aprendido algo: Mercè (que se quedó y ahora es doctora), Álex, Alfredo, Coral, Simone, Carmen, gracias. La gente de Bellvitge, tan cerca y tan lejos, siempre ha sido una especie de patria en la distancia, ayudando con las partes más "bio" del trabajo Núria y Ari, poderosas y aparentemente incansables, Silvia, Santi y Natalia, siempre dando alegría al trabajo. Isabel Oliveira ha sido como una mamá del laboratorio y Cris sigue por ese camino. La nueva generación del laboratorio, Montse, Marta, Berta y Albert, ha sido una estupenda compañía en la fase final de la tesis. Todos vosotros y alguno más que me dejo (sabéis quiénes sois) formáis ya una parte muy positiva de mi vida.

Gracias.

Table of contents

Table of contents 9
Structure of the thesis 13
1. General introduction 15
1.1. Protein-protein interactions and functional interactomics 15
1.2. Synthetic photoswitches to regulate biological activity 16
1.2.1. Azobenzene 17
1.2.2. Other switches 19
1.3. Peptide inhibitors of protein-protein interactions 21
1.4. Photoswitchable peptide inhibitors and proteins 21
1.4.1. Regulation of secondary structure with chemical photoswitches 21
1.4.2. Genetically encoded photoswitches 24
1.5. Clathrin-mediated endocytosis and the endocytic interactome 26
1.5.1. Clathrin-Mediated Endocytosis 26
1.5.2. Adaptor proteins in CME: AP-2, β- adaptin 2 and β-arrestin 27
1.5.3. β-arrestin peptide-long 30
1.6. Objectives of the thesis 32
2. Design of photoswitchable inhibitors of the interaction of β-adaptin 2 with β-arrestin 33
2.1. Contributions 33
2.2. Introduction 33
2.3. Results and discussion 34
2.3.1. Design, crosslinking, and photoswitching of PIPPI peptides 34
2.3.2. Interaction with β-adaptin. 45
2.3.3. Effect of non-proteinogenic amino acids. 46
2.3.4. Photoswitchable ligand binding model 49
2.4. Conclusion 56

3. Control of clathrin-mediated endocytosis using light 59
3.1. Contributions 59
3.2. Introduction 59
3.3. Results and discussion 60
3.3.1. Peptide design summary 60
3.3.2. Photocontrolled inhibition of BAP-long/β-adaptin 2 interaction 63
3.3.3. Spontaneous uptake of TL peptides by cells 66
3.3.4. Photocontrolled inhibition of transferrin receptor endocytosis 67
3.3.5. Effects of TLs on clathrin-coated pit dynamics 69
3.4. Conclusion 78
4. General conclusions 79
5. Resumen en castellano 81
5.1. Introducción 81
5.2. Diseño de inhibidores fotoconmutables de la interacción de β-adaptina 2 con β-arrestina 87
5.3. Control óptico de la endocitosis mediada por clatrina 90
5.4. Conclusiones 92
Appendix I - Technical notes 95
Azobenzene crosslinker synthesis 95
Peptide preparation 98
Irradiation systems 100
Determination of cis-to-trans relaxation τ of azobenzene. 100
Circular dichroism measurements 100
Molecular dynamics simulations 102
Fluorescence polarization binding assay. 109
Cell lines and gene constructs 110
TL uptake assays in living cells 110
MTT cell viability assay 111
Transferrin receptor uptake 112

TIRF Microscopy 113
Appendix II - Publications and communications 115
Appendix III - References 117
Appendix IV - Abbreviations 131

Structure of the thesis

The introductory section lays out the bases for the work presented in the other two main sections, namely protein-protein interactions, photoswitchable synthetic molecules, the use of peptides to inhibit protein-protein interactions and the progresses made in the combination of these three areas to produce photoswitchable molecules, with a focus on peptides addressing the inhibition of protein-protein interactions. The last part of the introduction consists of a brief primer to clathrin-mediated endocytosis and the specific molecular interaction that the molecules developed in this thesis target. The first section closes with the objectives of the thesis.

The other two main sections present in a progressive and cumulative manner the works carried out to meet the objectives of the thesis. They are structured in introduction, results and discussion and conclusions to facilitate a relatively independent reading of each section. Section 2 addresses the photocontrol of affinity and ability to inhibit protein-protein interaction of peptides from the β-arrestin/β-adaptin 2 interaction surface and derives design feature from the comparison of a panel of candidate peptides to photoswitchable inhibitor of this interaction. Section 3 presents the testing of a small sub-family of the peptides presented in the previous section in living cells, revisiting design considerations with a more specific scope and showing for the first time reversibly photocontrolled interference with cellular functions via application of cell-permeable, photochrome derivatized, peptides derived from a known protein-protein interaction. Section 4 lists the general conclusions of the thesis and Section 5 presents a brief summary of the thesis in Spanish.

Experimental methods are described briefly in the main text and extended when needed in Appendix I. For well-established and broadly extended methods, the reader is referred to the appropriate literature. Appendix II lists the ways in which the works presented have been communicated to the scientific community. References for all the sections are grouped in Appendix III and sorted alphabetically by the first surname of the first author. A list of non-obvious abbreviations used throughout the text has been included as Appendix IV for the reader's reference.

1. General introduction

1.1. Protein-protein interactions and functional interactomics

Protein-protein interactions (PPIs)(Arkin & Wells, 2004) are key processes in the majority of biological functions, from the assembly of protein complexes to signal transduction. The study of PPIs with biochemical, biophysical and bioinformatics techniques has given rise to the fields of proteomics and interactomics, and has led to the **identification of important pharmacological targets** (Mullard, 2012). In order to map the interactome, the yeast two hybrid system is often used to identify the binary interactions among two proteins at a time. However, yeast two hybrid screens include false positive interactions between proteins that are never expressed in the same time and place, and must be complemented by affinity purification and subsequent mass spectrometry of protein complexes.

In order to validate and fully characterize individual, functional PPIs in vivo, new molecular manipulation methods are required that operate at the cellular and subcellular level with **pharmacological selectivity and spatiotemporal selectivity** and take into account the polarization and compartmentalization of PPIs in the cell, i.e. the subcellular localization patterns of the different protein partners involved in a biochemical process. Light is particularly convenient for this purpose because it can be focused with very high resolution in space by optical microscopy equipment and controlled with very high resolution in time with current electronics. Light itself is also non-invasive when compared to other means to gain access to the interior of cells, such as electrophysiology, transfection, microinjection or direct cell disruption.

Optically controlled, or **photoswitchable inhibitors of PPIs (PIPPIs)** would allow for the manipulation with light of PPIs with the pharmacologic selectivity of an inhibitor and the spatial and temporal selectivity of an optical tool. In this way, it would be possible to establish patterns of inhibition of specific PPIs along time and in the chosen subcellular compartments or regions in the cells of interest. Such tools would be appropriate for the validation and investigation of the molecular mechanisms behind the functions assigned to PPIs by conventional

molecular biology methods. They would also open the way for studies on the function of molecular interaction networks and pathways with a high temporal and spatial resolution.

1.2. **Synthetic photoswitches to regulate biological activity**

Photochromism is the reversible transformation of a single chemical species induced in one or both directions by electromagnetic radiation between two states with different absorption properties (Dürr & Bouas-Laurent, 2003). It has been known since the late XIX century, although its chemistry has been studied extensively since the 1940s and has been developed and applied mainly in recent decades. These reversible changes in optical behavior are often accompanied by changes in other properties depending on the molecular rearrangement underlying the photochromism. Thus, photochromic molecules and complexes (photochromes) are also dubbed **photoswitches or optical switches**, as a subclass of the more generic concept of molecular switches. The term “photoswitch” is preferred in this work.

Each of the states of a photoswitch has its own **absorption spectrum**, sometimes including a band that will promote conversion into the other state (which in the cases where the two states are isomers of the photoswitch is called **photoisomerization**). Thus, under every set of conditions of light intensity, light wavelength composition, concentration of photoswitch, temperature, pressure and chemical environment a specific equilibrium between the two states will be reached. This light-dependent equilibrium is called **photostationary state (PSS)**. If a photoswitch in PSS is left in the dark, the photoconversion stops and the mixture evolves to a different stationary state in which the most stable state will be the predominant species. This is called **thermal relaxation** of the photoswitch.

Photoswitches have several general properties critical to their photochromic behavior, including **quantum yield** (the rate of photoconversion per amount of photons absorbed per unit of time), **PSS composition, resistance to fatigue** (i.e. loss of reversibility of the photoconversion process over time and/or cycles of usage) and **solubility** in the solvents of choice for the intended application (aqueous for biological applications). To this general properties of interest two more can be added that are critical for the biological scope of this work: the

wavelengths promoting the photoconversion and the **reactivity and stability** of the photoswitch in life-compatible conditions.

A reversible transformation that comes with a change in absorption properties in response to light is sufficient to consider a molecule a photoswitch, but not to make it a useful photoswitch for engineered photocontrol of biomolecules. Further **changes in the physicochemical properties** are needed. These changes have to be such that they can induce in turn changes in the biomolecular system of interest that alter its normal behavior. In other words, the photoswitch must have a **built-in transduction mechanism** so its light sensitivity is transferred to a property of the target system. The transduction mechanisms can be large changes in geometry, rigidity, solubility or similar properties of the molecule that can be exploited to **affect the interactions and activities of biological molecules**. Because of this limitation, application of photoswitches to biological systems is only recent. There are several chemical groups that have properties useful for bio-photocontrol:

1.2.1. Azobenzene

Azobenzene is the synthetic photoswitch that has been most widely used with biomolecules. The term azobenzene describes two phenyl rings linked by a N=N double bond, but it is also applied, along with "**azocompound**", to the derivatives of that parent core that can be obtained by introducing substitutions in the phenyl rings. These substitutions can modify the photochromic and physicochemical properties of the parent azobenzene and in most cases the derivative is still a photoswitch. Thus, azobenzenes are an evolving family of chemical groups with different properties from which one can pick the most convenient member for the intended application.

The **photoswitching** of azobenzene consists of a photoisomerization of the N=N bond between the ***cis* and *trans* isomers**. A classical review on the chemistry of the photoisomerization of azobenzenes can be found in (Rau, 1989, 2003). Because of the size and rigidity of the phenyl rings, this photoisomerization results in a big **difference in end-to-end length** between the isomers (more than twice in the "extended" *trans*-isomer than in the "bent" *cis*-isomer of the parent azobenzene core). *trans*-azobenzene is symmetric and linear, so isomerization to cis also implies a **change in the dipolar moment** of the molecule.

Typically the *trans* isomer is the most stable in the dark and it is possible to have mixtures of *cis* and *trans* azobenzene thermally **relax in the dark** to virtually **100% *trans*-azobenzene**. This is called a “relaxed" or **"dark adapted" state**. The less stable *cis* isomer forms upon absorption of energy from light within a certain wavelength range. Under intense **360-380 nm** light, azobenzene can reach a PSS with more than **90% *cis*-azobenzene** (Beharry & Woolley, 2011). When applying azobenzene for the photocontrol of biological processes, it is important to take into account the remaining *trans*-azobenzene, as it will mean that a certain fraction of the photocontrolled biomolecule will remain unaffected in the PSS.

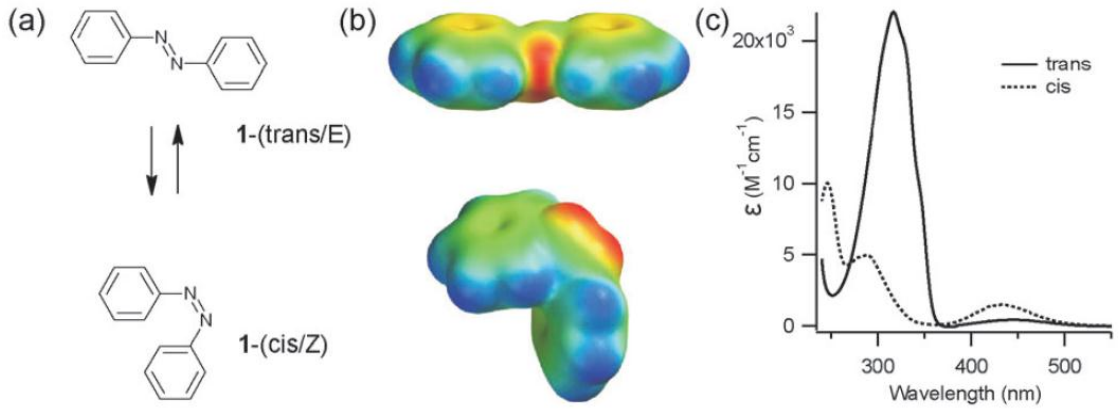

Figure 1 (a and b) Structures of trans and cis isomers of azobenzene. Space fill models are colored by electrostatic potential (red—negative to blue—positive). **c)** Electronic absorption spectra of the trans and cis isomers of azobenzene dissolved in ethanol. From (Beharry & Woolley, 2011).

Azobenzene has been used in the fields of organic chemistry and materials science (see (Merino & Ribagorda, 2012) for a review on uses of azobenzene in non-biological molecular machines). Focusing in **applications related to biology** and photocontrol, the most interesting property of azobenzene is its change in geometry upon photoisomerization. This has been applied to make **reversibly caged compounds**, also termed **photochromic ligands (PCLs)** such as neurotransmitter analogs BisQ (Bartels, Wassermann, & Erlanger, 1971), gluazo (Reiter, Skerra, Trauner, & Schiefner, 2013; Volgraf et al., 2007) and ATA-3 (Stawski, Sumser, & Trauner, 2012); **photoswitchable tethered ligands (PTLs)** for membrane receptor proteins and ion channels, such as QBr (Bartels et al., 1971), MAG (Volgraf et al., 2006) and MAL-AZO-QA (Banghart, Borges, Isacoff, Trauner, & Kramer, 2004); conformationally **photoswitchable nucleic acids** (Asanuma et al., 2007); conformationally **photoswitchable proteins** (Beharry et al., 2012; Browne et al., 2014; Schierling et al., 2010; Woolley et al., 2006); and conformationally **photoswitchable peptides and peptidomimetics** (Hoppmann

et al., 2009; Kuil, van Wandelen, de Mol, & Liskamp, 2009; Kumita, Smart, & Woolley, 2000; Parisot, Kurz, Hilbrig, & Freitag, 2009; Christian Renner & Moroder, 2006). When applied to peptides and proteins, azobenzene is commonly introduced as an **amino acid side chain-crosslinking bridge** (Flint, Kumita, Smart, & Woolley, 2002). In peptides it can also be introduced in the backbone or as a side chain by using it as **solid-phase synthesis building block** (Hoppmann, Schmieder, Heinrich, & Beyermann, 2011; C Renner, Kusebauch, Löweneck, Milbradt, & Moroder, 2005). It can also be introduced as side chain in proteins produced by cells via **stop-codon suppression** (Bose, Groff, Xie, Brustad, & Schultz, 2006; Hoppmann et al., 2014). The last strategy requires **genetic manipulation of the target living system**, as does targeting crosslinking and some PTLs to specific positions in proteins (Gorostiza & Isacoff, 2008a; Schierling et al., 2010).This wide application of azobenzenes owes to their **versatility**. Simple water-soluble azobenzene crosslinkers can be readily prepared at any standard organic chemistry laboratory and most biochemistry laboratories (Burns, Zhang, & Woolley, 2007). Azobenzene photochemical properties such as **absorption spectrum** (Chi, Sadovski, & Woolley, 2006; Kienzler et al., 2013; Sadovski, Beharry, Zhang, & Woolley, 2009), **stability of the *cis* state** (Poloni, Szymański, Hou, Browne, & Feringa, 2014; Pozhidaeva, Cormier, Chaudhari, & Woolley, 2004) or **two-photon photoswitching** (Izquierdo-Serra et al., 2014) can be **rationally tuned** by introduction of substitutions in the aromatic rings. The **length, rigidity and reactivity** of azobenzene crosslinkers can also be adjusted (Beharry & Woolley, 2011; Samanta & Woolley, 2011; Fuzhong Zhang, Sadovski, & Woolley, 2008).

1.2.2. Other switches

Among other synthetic photoswitches, only **spiropyrans and diarylethenes** have shown applicability to biological systems as described above. Spiropyran is a molecule containing multiple rings. Upon absorption of light in the 250-380 nm band, it photoisomerizes in a ring-opening process into **merocyanine**. Merocyanine can photoisomerize back into spiropyran upon absorption of visible light with a **relatively low energy barrier**. The isomerization of spiropyran and merocyanine can also be **induced thermally** (Fujimoto, Amano, Horibe, & Inouye, 2006; Guglielmetti, 2003). The ring opening gives merocyanine more **rotational freedom** over spiropyran and this can be exploited much like in the case of azobenzene to introduce **photoregulated conformational constraints**

in biomolecules (Fujimoto et al., 2006). Spiropyran has also a higher tendency to self-association than merocyanine that can be used to bias molecular conformations in polymers sporting multiple spiropyran side chains (Angelini, Corrias, Fissi, Pieroni, & Lenci, 1998). Despite these interesting properties, there are few examples of application of spiropyrans in biology, the most notable being using spiropyran-containing peptides as **fluorescent lysosomal trackers** (Chen, Wu, Schmuck, & Tian, 2014).

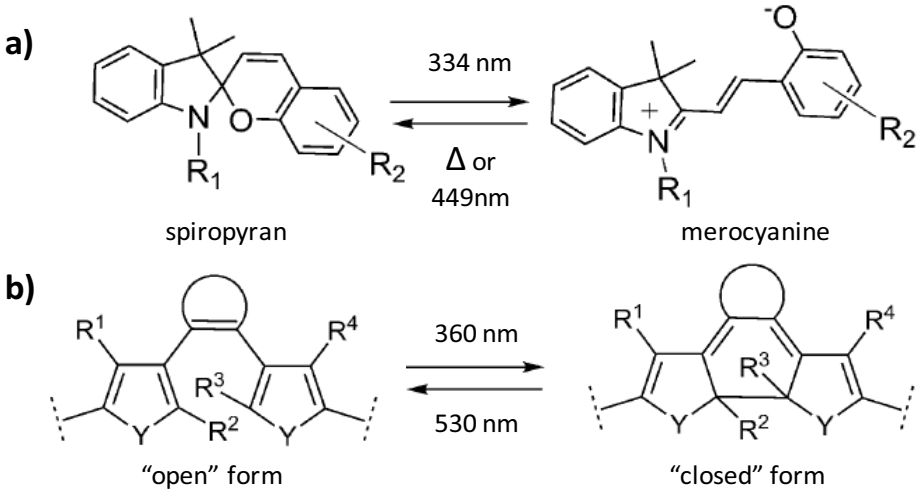

Figure 2 Spiropyran and diarylethene. a) Photochromism of spiropyran. From (Shiraishi, Itoh, & Hirai, 2010). **b)** Photochromism of diarylethene. From (Babii et al., 2014).

Diarylethenes, like spiropyrans, are ring systems that undergo photoisomerization in a ring opening process resulting in an important difference in flexibility between the isomers. In the case of diarylethene, the ring opens by absorption of light around 360 nm and closes with light around 530 nm. A notable feature of diarylethene is that **both isomers have a high thermal stability**, so virtually they only interconvert into each other by photoisomerization (Irie, 2000; Laarhoven, 2003). As with spiropyrans, there are only few, if recent and promising for the photocontrol of biological activities, reports of application to biological molecules. Like azobenzene, diarylethene has been introduced in the **backbone of peptides** (Babii et al., 2014), as a **side chain intramolecular crosslinker** in alpha helical peptides (Fujimoto, Kajino, Sakaguchi, & Inouye, 2012) and as an **intramolecular crosslinker** in a protein (Reisinger et al., 2014) to control their conformation and activity. It has also been used to control enzymatic activity in **cell-free preparations** via a photoswitchable small molecule enzyme inhibitor, a strategy analogous to PCLs (Vomasta, Högner, Branda, & König, 2008).

1.3. **Peptide inhibitors of protein-protein interactions**

PPIs are essential in almost every biological process. Recently, PPIs have emerged as **therapeutic targets of interest** (Ivanov, Khuri, & Fu, 2013; Mullard, 2012), and ligands directed to interactions mediated by **α-helices** (Azzarito, Long, Murphy, & Wilson, 2013; Bullock, Jochim, & Arora, 2011) **and β-sheets** have been systematically developed, which has driven the appearance of **peptidomimetics** imitating those structures (Becerril & Hamilton, 2007; Edwards & Wilson, 2011; Robinson, 2008). Since peptides themselves have been used as drugs and drug shuttles (Bellmann-Sickert & Beck-Sickinger, 2010) the application of **peptide molecules as inhibitors of PPI**, even directly derived from the interacting protein sequences, is an appealing possibility. Nevertheless, many **interesting target PPIs occur in the cytoplasm** of cells, and **peptide delivery can be an issue** in those cases. This problem can be overcome by application of **cell-penetrating peptide** sequences fused to the inhibitor sequence (Bechara & Sagan, 2013; Svensen, Walton, & Bradley, 2012). Actually, in some cases the inhibitor peptide sequence can constitute a cell-penetrating peptide on its own because of structural features and modifications, as in the case of α-helical and side chain intramolecularly bridged **stapled peptides** that have been reported to **inhibit intracellular cancer-related PPIs** (Grossmann et al., 2012; Moellering et al., 2009; Verdine & Hilinski, 2012; Walensky et al., 2004).

1.4. **Photoswitchable peptide inhibitors and proteins**

1.4.1. Regulation of secondary structure with chemical photoswitches

Introduction of **conformational constraints** in biopolymers with synthetic photoswitches can be combined with the **peptide and peptidomimetic drug discovery** trends described to obtain photoswitchable, peptide-based, inhibitors of PPIs (peptide PIPPIs). An intermediate step towards that goal is the development of **general strategies** to realize the potential of **transduction of photoswitching to the conformation** of broad classes of biomolecules. Defined three-dimensional folding motifs of biopolymer sequence (i.e. **secondary structures and folds**) are a natural ground for that strategy. The photoswitches described above have been used to control the secondary structure of peptides and proteins, with several reports of control **extending to the biological activity** of the target biomolecule or PPI.

Peptides

Synthetic photoswitches have been used to manipulate common secondary structures of peptides. To **photocontrol β-hairpins and β-sheets**, azobenzene has been inserted in the main chain of model peptides and peptides based on relevant proteins as a photoswitchable amino acid in solid-phase synthesis. This has enabled the structural control of a model sequence from the tryptophan zipper 2 β-hairpin (TrpZip2) (Schrader et al., 2007) and of a peptide mimicking the functionally relevant β-finger of neuronal nitric oxide synthase (nNOS) (Hoppmann et al., 2009). The strategy of inserting azobenzene in the polypeptide backbone has also been applied to attain conformational photocontrol of a γ-immunoreceptor tyrosine based activation motif (γ-ITAM) from the high affinity immunoglobulin E receptor FcεRI (Kuil, van Wandelen, de Mol, & Liskamp, 2008; Kuil et al., 2009).

The group of Woolley has dedicated many works to the **photocontrol of α-helical peptides** by azobenzene bridging between side chains and the development of azobenzene crosslinkers to that end. Besides studying **photocontrol of helicity** in model peptides of α-helix (Ihalainen et al., 2008; Kumita, Flint, Smart, & Woolley, 2002; Kumita et al., 2000), they have developed azobenzene variants with advantages for **specific applications**, such as **longer photoisomerization wavelengths** (Chi et al., 2006; Sadovski et al., 2009; Samanta et al., 2013), different **stabilities of the *cis* isomer** (Pozhidaeva et al., 2004), longer **crosslinker span and higher rigidity** (Fuzhong Zhang et al., 2008) and improved water solubility (Burns et al., 2007). Along with several reviews (Beharry & Woolley, 2011; Christian Renner & Moroder, 2006; Samanta & Woolley, 2011; Woolley, 2005) and application oriented studies (e.g. Janet R Kumita, Weston, Choo-Smith, Woolley, & Smart, 2003), these investigations provide a broad design toolbox and know-how that has contributed to popularize the strategy of azobenzene side chain bridging on alpha helical polypeptides to obtain conformational photoswitches. One report presents a similar use of the diarylethene photoswitch (Fujimoto et al., 2006).

Despite the relatively high number of publications on structural photocontrol of peptides, there is a smaller, if growing, number of reports of conformational **photocontrol extending to peptide activity** (e.g. interaction affinity) and/or function in living systems. Allemann and co-workers targeted an important cancer-related PPI and applied azobenzene crosslinking to BH3 domain peptides,

showing that both their helicity and their affinity for Bcl-XL were different before and after irradiation in vitro, but **without proof of thermal or light-dependent reversibility** of the photocontrol (Kneissl, Loveridge, Williams, Crump, & Allemann, 2008). Renner and co-workers achieved photocontrol of the assembly of collagen triple helices (Kusebauch, Cadamuro, Musiol, Moroder, & Renner, 2007) but, as in the previous example, **without showing photocontrolled effects in cells or *in vivo***. Similarly, the strategy of azobenzene in the backbone of β-hairpins has produced a report of photocontrolled binding of a nNOS-related peptide to syntrophin only in cell-free preparations (Hoppmann et al., 2009). These reports have then to be regarded as examples of **higher order structural photocontrol** and milestones towards the goal of functional photocontrol of PPIs, but still far from it. Conversely, a recent report by Woolley and co-workers demonstrates structural photocontrol of reporter fluorescent peptides microinjected into zebrafish embryos (Samanta et al., 2013) with the approach of bridging peptide helices with azobenzene. While this study reaches the *in vivo* level, it does not show photocontrol of biological functions and constitutes just a proof of **feasibility of *in vivo* photocontrol** of exogenous peptides inside model organisms.

While the previous reports rely on the solid design of **targeting strong common secondary structures**, mostly α-helices and with azobenzene crosslinking, some examples deviating from that design have gone further in photocontrol of biological activities with photoswitchable peptides. The antibacterial ion channel cyclic peptide **gramicidin** has been made photoswitchable by introduction of the infrequent **hemithioindigo** photoswitch in its backbone (Lougheed, Borisenko, Hennig, Ruck-Braun, & Woolley, 2004). In this case a **change in the polarity** of the photoswitch was exploited to alter the ion conductivity of the channel peptide. A very recent study resorts to **structural photocontrol**, this time with **diarylethene** to modulate the function of gramicidin and show **light-patterned anti-bacterial activity** (Babii et al., 2014). Gramicidin does not act on a PPI and acts extracellularly so these studies, although having strong photocontrolled biological activity, add little to the development of peptide PIPPIs. A study included in this thesis presents **photomodulation of clathrin-mediated endocytosis (CME)** in **mammalian cells** with weakly helical, flexible peptides derived from **β-arrestin** and side-chain bridged with azobenzene (Nevola et al., 2013), showing that azobenzene crosslinking can be applied **beyond the strong structure** paradigm (particularly beyond strong helices) and parallels peptide

stapling, resulting in **increased cell permeability**. Recently, a technique to evolve and select peptides for azobenzene crosslinking and significant photoswitching of affinity has been successfully implemented to evolve ligands for streptavidin as a model binder (Bellotto, Chen, Rentero Rebollo, Wegner, & Heinis, 2014). Taken together, the last two works open the way to application of the azobenzene crosslinked peptide technology to **virtually any target PPI** through convergence of the approaches of **rational design** and blind **evolution-selection** they represent.

Proteins

Another approach that has been taken to photocontrol biological activities is the **structural photocontrol** of functionally important **proteins** to affect their interactions or intrinsic activities. This approach actually precedes in time the reports of photoswitchable peptides, as it includes the PTLs (reviewed above) applied to obtain light-responsive ion channels applied in neuroscience. PTLs, along with the advent of **optogenetics** (see below), have promoted the concept of **optical manipulation** that is now expanding to other fields of cell and molecular biology. There are also other instances of direct photocontrol of proteins, including **direct gating**(as opposed to ligand-mediated gating) of ion channels with an azobenzene photoswitch (Lemoine et al., 2013), regulation of **metabolic and restriction enzymes** with diarylethene and azobenzene (Reisinger et al., 2014; Schierling et al., 2010) and **photocontrolled DNA-binding domains and transcription factors** (Kumita, Flint, Woolley, & Smart, 2003; Morgan, Al-Abdul-Wahid, & Woolley, 2010; Woolley et al., 2006). Notably, optogenetics, many PTL-photocontrolled channels and receptors and direct structural control of proteins share the technical requirement of **heterologous (gene-engineered) protein expression** in the target biological systems, not needed for photoswitchable peptide-mediated photocontrol of biological activities.

1.4.2. Genetically encoded photoswitches

Optogenetics defines the expression of exogenous natural light-sensitive proteins (ion channels, pumps or GPCRs) in cells to manipulate their functions with light and the research field that emerges from their application (Miller, 2006). It has been widely **applied in neuroscience to control membrane potentials**, becoming synonyms with that application, where it overcomes the diffusion limitation that caged compound have and where optogenetics has the advantage that light control can be **targeted to specific cell types** by genetic manipulation.

Optogenetic tools derive from **microbial opsins** including light-gated ion channels (**channelrhodopsins, ChR**) and light-driven pumps (**bacteriorhodopsins and halorhodopsin**). Opsins are transmembrane proteins associated with the co-factor **all-trans retinal**, the light sensitive switch in the system. This chromophore is **naturally synthesized** in all vertebrate tissues and, thus there is no need to supplement the experimental system with the compound. The first microbial opsins, Channelrhodopsins, were introduced in cells in the early 2000s (Boyden, Zhang, Bamberg, Nagel, & Deisseroth, 2005; Nagel et al., 2002, 2003). Optogenetic use of halorhodopsin (NpHR) was introduced later that decade (Feng Zhang et al., 2007). The optogenetic use of these molecules in neuroscience has fueled an extensive development of new photocontrolled microbial pumps and channels and mutant variants of the existing opsins with tuned biophysical and photochemical properties. Put together, these opsins make a**broad array of optogenetic tools** (Lin, 2011). Optogenetics has been applied to investigate neuronal circuits (Mao et al., 2011; Packer et al., 2012; Petreanu, Mao, Sternson, & Svoboda, 2009) and also to manipulate **behavior in animal models,** including primates (Fenno, Yizhar, & Deisseroth, 2011).

Despite having emerged in the context of neurosciences, **optogenetics are extending to other fields** and producing similar applications as protein modification with synthetic photoswitches and perturbation of biological functions with photoswitchable peptides. A notable instance is the use **of light-oxygen-voltage-sensing (LOV) domains** to make photoswitchable chimeric proteins. These domains come from **phototropins**, natural photoswitchable kinase enzymes involved in the phototropism of plants and algae carrying **flavin chromophores** that play a similar role as retinal in opsins. The **AsLOV2** domain has been optimized for its use as **gene-encoded photoswitch**(D Strickland, Yao, & Gawlak, 2010). LOV domain-containing, chimeric, modular proteins miniproteins have been applied to rearrange PPIs in yeast, and termed **tunable, light-controlled interacting protein tags (TULIPs)** in a strategy that resembles the one underlying PIPPIs: to control the availability of a competing ligand for an PPI with light. In the case of TULIPs, the photoresponse of the LOV domain is used to **expose or mask an interacting protein domain**(Devin Strickland et al., 2012). Recently, a similar strategy with an added **membrane anchoring modular domain** has been used to produce **lumitoxins**, protein constructs that are functionally analog to PTLs (Schmidt, Tillberg, Chen, & Boyden, 2014). Along with the protein modification with synthetic photoswitches strategies described

above, these branches of optogenetics complete a **continuous landscape of tools** for the optical manipulation of biomolecular functions that ranges **from all-synthetic pharmacology to fully genetically encoded optogenetics**, potentially covering any devisable application.

1.5. Clathrin-mediated endocytosis and the endocytic interactome

1.5.1. Clathrin-Mediated Endocytosis

Clathrin-mediated endocytosis (CME) is one of the major mechanisms present in mammalian cells to incorporate integral membrane proteins and their ligands to the cell interior. CME uses energy to incorporate large and polar molecules that won't passively cross the plasma membrane. This process is mediated by the structural protein clathrin and a plethora of associated protein molecular machinery that performs several functions, such as:

I. **Concentration** of specific membrane proteins (receptors) and their ligands, collectively known as "**cargo**" at specific points in the membrane. This function is carried out by transmembrane receptors and the intracellular primary adaptors and secondary or alternative adaptors, known as **clathrin-associated sorting proteins (CLASPs)**, which recognize them and drive them to the concentration point in the membrane.

II. **Induction of membrane curvature** and invagination by assembling as a lattice in the intracellular side of the membrane. This function is performed by **clathrin** and curvature-inducing CLASPs, as epsin and the coat protein complexes I and II (COPI and COPII), that supply the conformational energy required for the bending and produce the active patches of membrane for CME: the **clathrin-coated pits (CCPs)**.

III. Transformation of CCPs into **clathrin-coated vesicles (CCVs)** by inducing further curvature and scission of nascent vesicles into the cytoplasm. This function is orchestrated by BAR domain-containing proteins that sense the membrane curvature of CCPs and recruit **dynamin**, a GTPase that uses the energy provided by its catalytic

activity to pinch the neck of the nascent vesicle and excise it into the cytoplasm.

IV. Determination of the destination of the formed vesicles in the intracellular stage of the endocytic pathway and removal of clathrin coat.

Recent reviews on CME and the regulation of its molecular machinery can be found in (Canagarajah, Ren, Bonifacino, & Hurley, 2013; Doherty & McMahon, 2009; Traub, 2009)

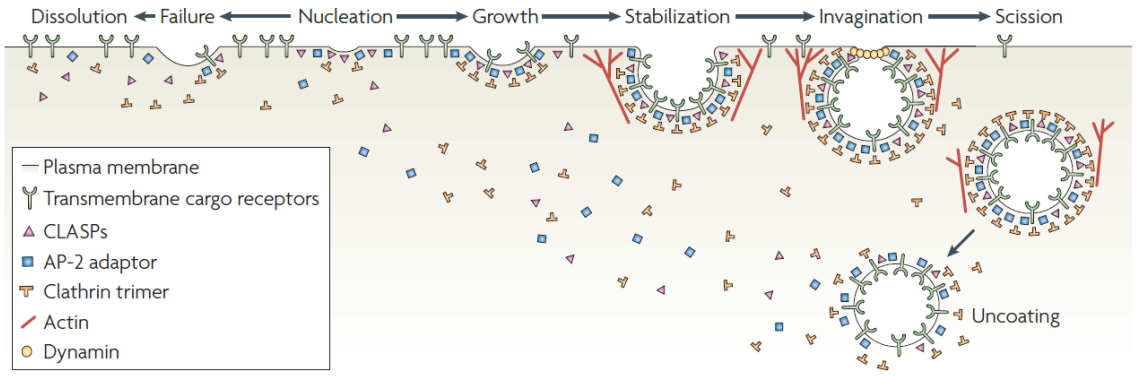

Figure 3 Formation of CCVs. From(Traub, 2009).

1.5.2. Adaptor proteins in CME: AP-2, β- adaptin 2 and β-arrestin

CLASPs, among other functions, allow the cells to use the same core mechanism and molecule (clathrin) to specifically incorporate a host of different molecules by combining different adaptors and receptors to produce many **specific internalization and sorting processes**. The scaffolding protein clathrin interacts with adaptors and simultaneously they interact with cargo or secondary adaptors that interact with cargo. In this way **cargo and receptors are physically linked to clathrin assemblies** and sorted into nascent CCVs. Classical primary adaptors are termed **adaptor protein complexes (APs)**. There are 6 kinds of APs (AP-1 to AP-5, plus the subcomplex COPI-F) depending on the protein subunits that compose them and determine their functions(Canagarajah et al., 2013). Only AP-1 through AP-3 are involved in CME. APs are tetrameric complexes with **five structural domains** that don't correspond exactly to the subunits. These structural domains are **one core domain** (also termed "trunk" in AP-1 and AP-2) that interacts with the cell membrane**, 2 appendage domains** that bind to secondary adaptors and activated receptors and **2 hinge domains** that link the trunk with each of the appendages, acting as flexible tethers that

allow the appendage domains to probe a large space around the trunk for interactions. The hinge domains also bind to coat proteins, so the AP complexes ensure the spatial convergence of the structural elements of a CCV. All APs are conformed by **two large subunits and two small subunits**. Each large subunit forms part of the core, one of the two hinges and one of the two appendages, while the small subunits are only part of the core. One of the large subunits is always of the β class (β, β1, β2, β3, β4 or β5) while the other may be α, γ, δ, ε or ζ. Of the small subunits, one belongs to the set (μ1, μ2, μ3, μ4, μ5 or δ) while the other belongs to the set (σ1, σ2, σ3, σ4, σ5 or ζ). The main and **canonical AP is AP-2**, composed of subunits α, β2, δ and μ2. The β2 subunit is also known **as β-adaptin 2** and its appendage C-terminal domain is also known as **β-appendage**.

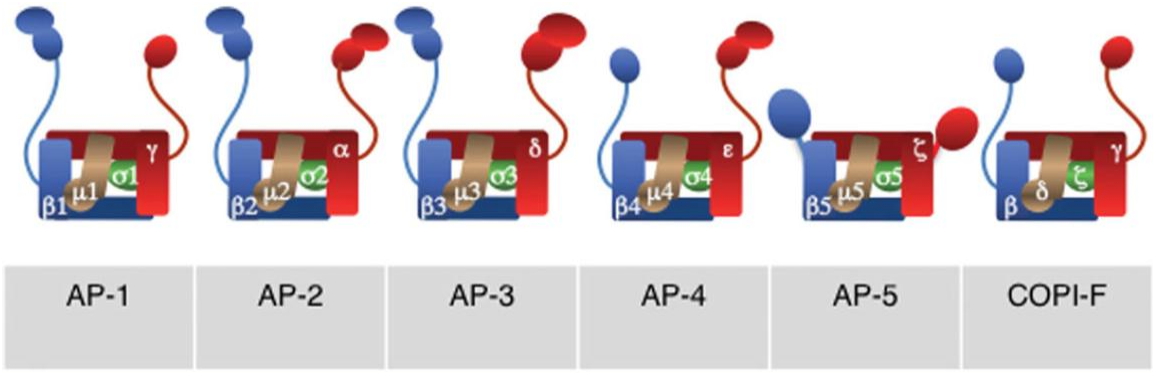

Figure 4 Structure and subunits of AP complexes. The four general subunits are depicted in different colors and the names of the subunits are displayed for every kind of classical adaptor complex. Adapted from (Canagarajah, Ren, Bonifacino, & Hurley, 2013).

β-appendage has different possible binding partners, and one of them is a protein named **β-arrestin**-arrestin binds to the intracellular domain of ligand-activated **seven membrane-spanning helix receptors (7MSR),** also known as G-protein coupled receptors **(GPCRs)**, arresting their response to ligand stimulation. This process has been reported to drive CME of the canonical GPCR **β_2-adrenergic receptor**, after which β-arrestin is named. This receptor's canonical agonist is **epinephrine**. Epinephrine binding mediates the **"fight or flight"** response in higher vertebrates (a complex multi-organic state in which the alertness level of the organism is increased and the availability of energy and oxygen to skeletal muscle is reinforced by diminishing the activity of non-critical organs and functions and increasing the catabolic side of metabolism). This response can only be sustained for short periods of time and has evolved to be a quick reaction system to potential danger, so it requires a mechanism to prevent a noxious overstimulation. This mechanism is **desensitization**: the reduction of the

response of an already activated system to further activation. When epinephrine or another agonist binds to the β_2-adrenergic receptor, it produces a conformational change that provokes the dissociation of the G-protein associated to the receptor and the propagation of the conformational change to associated calcium channels. These events result in a **branched signaling cascade** that also evokes the desensitization response via activation of the **G-protein coupled receptor kinase 2 (GRK2)**. GRK2 phosphorylates serine and threonine residues in the intracellular domain of the β_2-adrenergic receptor, facilitating its binding to β-arrestin. With β-arrestin bound, the receptor is not available for G-protein coupling, so an agonist-responsive receptor complex cannot be armed again (Johnson, 2006; R. J. Lefkowitz & Whalen, 2004). Furthermore, β-arrestin links the receptor to the CME machinery, promoting its internalization upon prolonged activation so it's not available to respond in the cell surface even if an agonist is present. β-arrestin, GRK 2 and other GRK proteins also act as signaling molecules mediating response to receptor activation themselves (R. Lefkowitz, 2007). After the decline of the response, the receptors will be dephosphorylated and recycled back to the membrane by **exocytosis**, where they will be available for interaction with associated calcium channels and inactivated G protein to arm an inactive receptor complex, thereby resensitizing the cell towards adrenergic agonists (R. J. Lefkowitz & Whalen, 2004; Vasudevan, Mohan, Goswami, & Prasad, 2011). A detail of the molecular mechanism of the β_2-adrenergic receptor/β-arrestin/CME coupling is the basis for the molecules developed in this thesis.

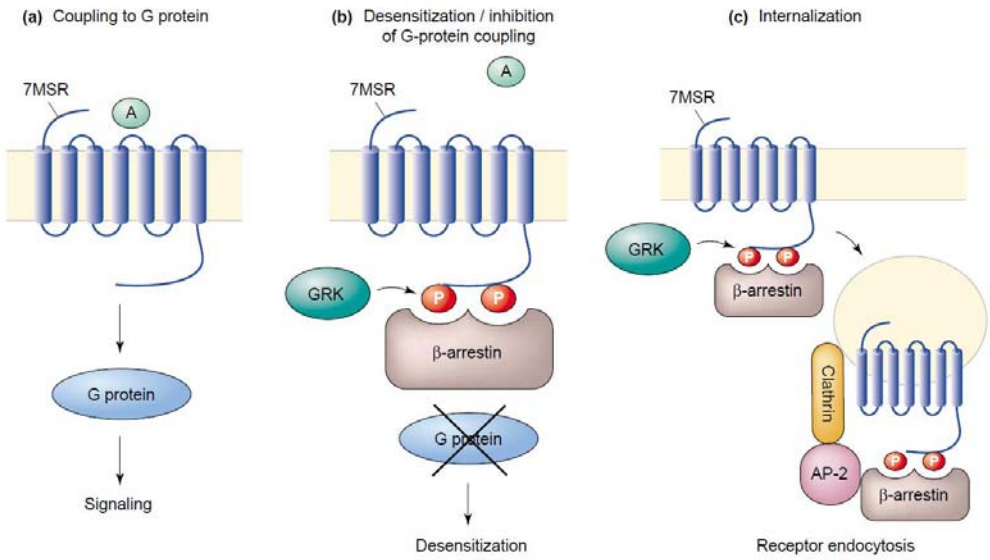

Figure 5 Receptor desensitization. Classical model of (a) 7MSR activation and signaling, (b) GRK-mediated receptor phosphorylation and b-arrestin mediated desensitization, and (c) β-arrestin-mediated clathrin/AP-2 dependent receptor endocytosis. From (R. J. Lefkowitz& Whalen, 2004).

1.5.3. β-arrestin peptide-long

β-adaptin 2 will engage β-arrestin only if it exposes a **binding motif** on its C-terminal region that is normally packed against the core of the protein, but that is **released by a conformational change** of β-arrestin upon binding to an activated GPCR (Edeling et al., 2006; Schmid et al., 2006). This peptide motif, corresponding to the sequence DDDIVFEDFARQRLKGMKDD and termed **"β-arrestin P-long" (BAP-long)** has been reported to adopt an α-helical conformation when it binds to β-adaptin 2. Furthermore, it has been observed to bind the β-adaptin 2 appendage domain even when separated from the rest of the β-arrestin sequence in cell-free preparations. In these conditions, it also adopts a helical conformation only when bound to β-adaptin 2.Taken together, these observations suggest that BAP-long holds potential for the competitive inhibition of the β-arrestin/ β-adaptin 2 PPI and that such inhibition could affect clathrin dynamics and CME. Moreover, the binding-driven helical structure of BAP-long suggests a **high flexibility and weak intrinsic helicity** of BAP-long, potentially amenable to structural photocontrol through photoswitch crosslinking as described above.

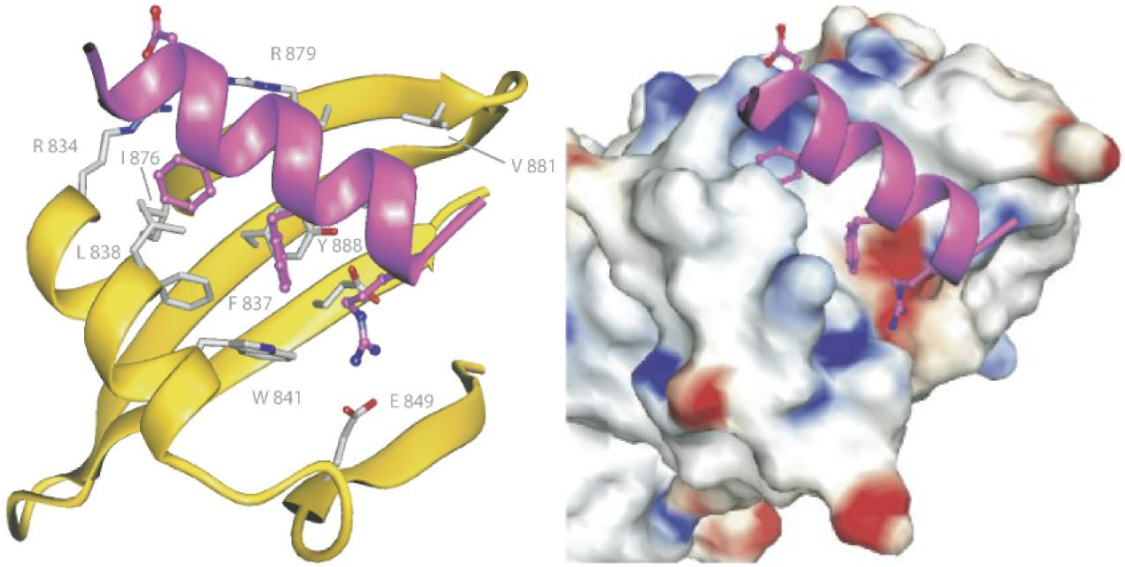

Figure 6 BAP-long bound to β-adaptin 2 in ribbon (left) and space fill (right) view. Interacting residues are labeled in the ribbon view and residue charge (red = negative, blue = positive) is color-coded in the space fill view. From (Schmid et al., 2006).

1.6. **Objectives of the thesis**

Based on the reviewed literature, we hypothesize that **it is possible to put under optical control the cellular activities in which PPIs are involved by means of delivery of structurally photoswitchable peptides derived from the interaction surface to target cells and appropriate illumination conditions**. In order to test this main hypothesis, we have set the following objectives for this thesis:

- To establish a strategy to explore PPIs and obtain candidate sequences for photoswitch derivatization.
- To find molecular design features for photoswitch crosslinking to the candidate sequences that facilitate the obtention of peptides with both photocontrolled structure and photocontrolled target affinity.
- To seek simple means of delivery of the obtained molecules to the cytoplasm of cells in order to facilitate application of the developed technology.
- To verify if the biological processes in which the target PPI is involved are affected by the peptides assayed with the same dependence of light established for structure and affinity.
- To pursue all the previous objectives in the model system of the β-arrestin/β-adaptin 2 interaction and its functional context, clathrin-mediated endocytosis.

2. Design of photoswitchable inhibitors of the interaction of β-adaptin 2 with β-arrestin

2.1. Contributions

Several parts of this section have been carried out in collaboration. Andrés Martín performed synthesis of BSBCA, peptide crosslinking and purification, absorption measurements and fluorescence polarization measurements, as well as processing and interpretation of all data from these techniques and development of the photoswitchable interaction model. Kay Eckelt collaborated in the peptide purification. Laura Nevola synthesized fluorescent peptide for fluorescence polarization, participated in the measurements and performed NMR measurements of the composition of the PSS of BSBCA. Sergio Madurga performed and interpreted all molecular dynamics simulations.

2.2. Introduction

PPIs are crucial for biological function and they constitute therapeutic targets of interest. Many PPIs are mediated by a short linear peptide, often an α-helix. Rigid molecules mimicking these peptides have been used to inhibit the PPIs that they mediate. However, photoswitchable peptides without a strong common secondary structure also hold potential as inhibitors and as photoswitchable molecules. Here we used a panel of 14 azobenzene-crosslinked peptides derived from the β-arrestin BAP-long sequence to assess the relevance of secondary structure and flexibility in their interaction with β-adaptin 2 and to identify the requirements for the design of photoswitchable inhibitors of protein-protein interaction (PIPPIs). We assayed several crosslinking positions and distances and tested two kinds of non-proteinogenic amino acids as design tools. Our results show that flexible structures show greater inhibitory capacity over the observed PPI and enhanced ability to photoswitch than rigid structures. Therefore, flexibility is identified as an additional criterion to consider for the selection of PIPPI candidates. Our findings expand the field of potential peptide inhibitors and target complexes beyond the well-defined α-helices and into flexible peptides without a pronounced secondary structure.

In the last decade, PPIs have emerged as key determinants in biological processes, thus prompting their recognition as highly promising therapeutic targets (Arkin & Wells, 2004; Mullard, 2012). Although large-scale interactomics projects have greatly contributed to our understanding of intracellular and extracellular PPI networks, they often do not consider two key aspects, namely the subcellular localization of the protein partners involved and their temporal dynamics (Mackay, Sunde, Lowry, Crossley, & Matthews, 2007; Tompa & Fuxreiter, 2008). The development of cell-permeable PIPPIs would pave the way to manipulating a specific PPI locally and in a time-controlled manner using light patterns.

Careful inspection of protein-protein interfaces reveals two main categories of PPIs, namely those mediated by domain-domain interactions and those mediated by peptide-domain interactions. Up to 40% of all PPIs can be classified in the latter group, where one of the partner proteins 'offers' the other a short linear peptide binding motif, often in an α-helical conformation (Neduva et al., 2005; Petsalaki & Russell, 2008). Not surprisingly, relatively rigid helical peptides or peptidomimetics have proven to be highly efficient inhibitors of several peptide-mediated PPIs (Moellering et al., 2009; Verdine & Hilinski, 2012; Walensky et al., 2004).

Flexibility is emerging as a key factor in molecular recognition at protein surfaces. An increasing number of so-called intrinsically disordered proteins are recognized as crucial interacting molecules in protein-protein networks, especially in highly evolved eukaryotes (Tompa & Fuxreiter, 2008). Here we studied the relationships between the structure of peptide PIPPIs and their capacity to bind β-adaptin in a photo-regulated way. We also address the relevance of peptide flexibility in this molecular recognition. Finally, we propose a series of features that could facilitate the design of PIPPI peptides as well as other compounds able to modulate PPIs in a reversible way, thus enabling the distinction between PPI photoswitches and PPI inhibitors or triggers.

2.3. **Results and discussion**

2.3.1. Design, crosslinking, and photoswitching of PIPPI peptides

We designed a panel of 14 peptides (Figure 7) based on the sequence of the BAP-long 20-mer peptide, known to interact with the binding partner of β-arrestin,

β-adaptin 2 (Edeling et al., 2006; Schmid et al., 2006). These 14 peptides were cyclized by crosslinking of cysteine side chains with 3,3'-bis(sulfonato)-4,4'-bis(chloroacetamido)azobenzene (BSBCA). In response to light at different wavelengths, this water-soluble crosslinker is known to undergo a considerable reversible change in end to end distance, which affects the structure of crosslinked peptides (Burns et al., 2007; Rau, 1989; Woolley, 2005). The panel included design elements, such as various crosslinking positions in the peptide sequence (avoiding insertion of azobenzene in the interacting surface of the helical peptide), different crosslinking distances, and the presence of the non-proteinogenic amino acids α-aminoisobutyric acid (Aib), 1-naphtylalanine (1-Nal) or 2-naphtylalanine (2-Nal). These elements have been recognized to be useful in the design of α-helix mimetics (Becerril & Hamilton, 2007; Edwards & Wilson, 2011), stapled cell-penetrating peptides (Moellering et al., 2009; Verdine & Hilinski, 2012; Walensky et al., 2004), structurally photoswitchable α-helical peptides (Kumita et al., 2002, 2000; Kumita, Weston, et al., 2003; Woolley, 2005), and photo-triggered peptide inhibitors (Kneissl et al., 2008). Briefly, BSBCA was synthesized and coupled to the peptide, which were then purified and obtainment of the expected molecules was verified by mass spectrometry (Figure 8 and Figure 9).

a

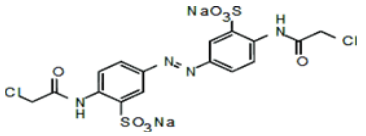

b

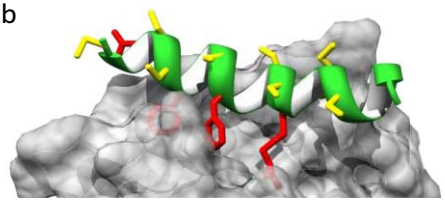

c

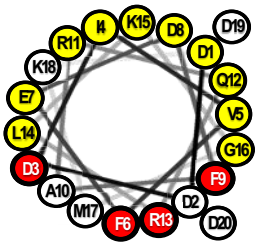

d

Peptides	sequence
BAP short	H_2N-DD**D**IV**F**ED**F**ARQ**R**-COOH
BAP long	H_2N-DD**D**IV**F**ED**F**ARQ**R**LKGMKDD-COOH
1	H_2N-DD**D**CV**F**EC**F**ARQ**R**LKGMKDD-COOH
2	H_2N-DD**D**IV**F**EC**F**ARC**R**LKGMKDD-COOH
3	H_2N-DD**D**IV**F**ED**F**ACQ**R**LCGMKDD-COOH
4	Succ-CD**D**VB**F**EC**F**ARQ**R**LKGMKDD-NH_2
5	H_2N-DD**D**CV**F**ED**F**ACQ**R**LKGMKDD-COOH
6	Succ-DD**D**CV**F**VB**F**ACQ**R**LKGMKDD-NH_2
7	H_2N-DD**D**IC**F**ED**F**ARC**R**LKGMKDD-COOH
8	H_2N-DD**D**IC**F**ED**$**ARC**R**LKGMKDD-COOH
9	H_2N-DD**D**IC**F**ED**€**ARC**R**LKGMKDD-COOH
10	Succ-DD**D**IV**F**CD**F**VBQ**R**CKGMKDD-NH_2
11	H_2N-DD**D**IV**F**EC**F**ARQ**R**LCGMKDD-COOH
12	H_2N-DD**D**IV**F**EC**F**AVB**R**LCGMKDD-COOH
13	Succ-DD**D**CV**F**ED**F**ARQ**R**LCGMKDD-NH_2
14	Succ-DD**D**IC**F**EDFARQ**R**LKCMKDD-NH_2

Figure 7 PIPPI peptide design a) Structure of the photoswitchable crosslinker BSBCA. b) Cartoon of the interaction between BAP-long and β-adaptin (from PDB 2IV8). Conserved residues critical for the interaction are shown in red(Edeling et al., 2006; Schmid et al., 2006). Crosslinking positions are depicted as yellow cysteine side chains. c) Helical wheel representation of BAP-long with the same color code. d) Summary table of the peptides assayed. Critical residues are shown in bold, the azobenzene bridge is represented by a line below the sequence. B = α-aminoisobutyric acid, $ = 1-naphtylalanine and € = 2-naphtylalanine. Succ- = succinyl N-terminal capping.

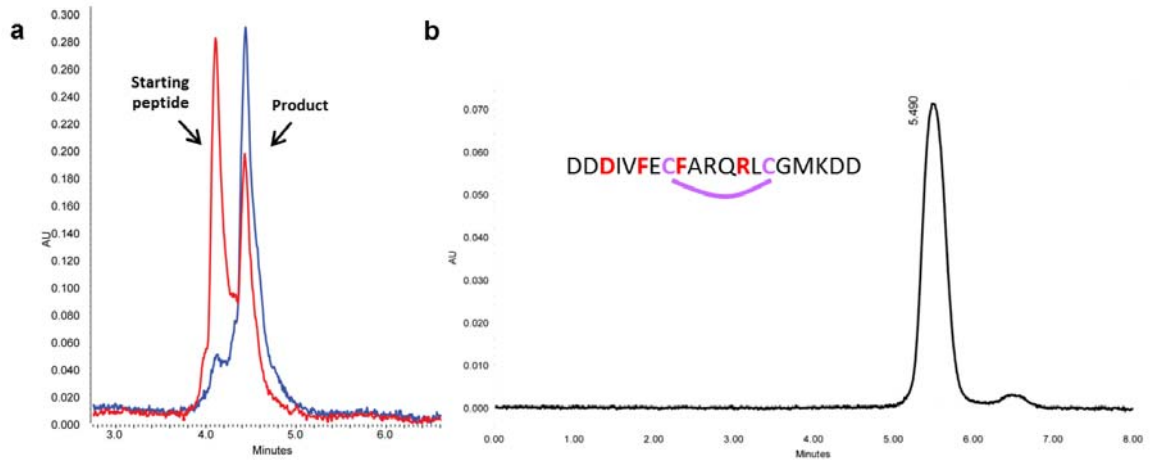

Figure 8 HPLC analysis of crosslinking reaction of peptide 11. a) Time monitoring of crosslinking reaction; red chromatogram = reaction mixture after 3 h; blue chromatogram = reaction mixture after 24 h. b) Chromatogram after purification.

Peptide	Exact Mass (calc.)	Exact Mass (found)	Elemental composition
1	2843.66	2842.06	$C_{115}H_{167}N_{33}O_{42}S_5$
2	2828.71	2827.08	$C_{116}H_{170}N_{32}O_{41}S_5$
3	2787.56	2785.97	$C_{113}H_{159}N_{29}O_{44}S_5$
4	2912.79	2912.09	$C_{119}H_{174}N_{34}O_{42}S_5$
5	2802.57	2800.99	$C_{113}H_{160}N_{30}O_{44}S_5$
6	2841.71	2841.08	$C_{117}H_{170}N_{31}O_{42}S_5$
7	2844.66	2843.05	$C_{115}H_{166}N_{32}O_{43}S_5$
8	2894.72	2893.06	$C_{119}H_{168}N_{32}O_{43}S_5$
9	2894.72	2893.06	$C_{119}H_{168}N_{32}O_{43}S_5$
10	2885.72	2884.07	$C_{118}H_{169}N_{31}O_{44}S_5$
11	2828.66	2827.05	$C_{115}H_{166}N_{32}O_{42}S_5$
12	2728.59	2727.02	$C_{113}H_{162}N_{28}O_{41}S_5$
13	2929.67	2928.04	$C_{117}H_{165}N_{33}O_{46}S_5$
14	3014.82	3013.13	$C_{122}H_{176}N_{34}O_{46}S_5$

Figure 9 Crosslinked peptide exact mass analysis. Purified peptides samples were introduced by direct infusion (Automated Nanoelectrospray) through the nano ESI Chip towards the LTQ-FT Ultra mass spectrometer (Thermo Scientific). Spray voltage was 1.70 kV and delivery pressure was 0.50 psi. Data was acquired with Xcalibur software, vs.2.0SR2 (Thermo Scientific). Ion deconvolution to zero charged monoisotopic masses was performed using Xtract algorithm in Xcalibur software and elemental compositions from experimental exact mass monoisotopic values were obtained with a dedicated algorithm integrated in Xcalibur. Analysis performed at the proteomics platform of the Barcelona science park (PCB).

For every peptide, thermal *cis* to *trans* relaxation of azobenzene, circular dichroism spectra under 365nm light and in the dark-adapted state, and displacement of fluorescently labeled BAP-long from the β-adaptin 2 binding site under 365 nm light and in the dark-adapted state were measured. Below are presented, from left to right: recovery over time of the absorption at 363 nm after 3 min of irradiation with 365 nm light, circular dichroism spectra in the dark and after 3 min irradiation with 365 nm light and competitive fluorescence polarization curves showing displacement of a carboxyfluorescein labeled BAP-long peptide from the β-adaptin 2 binding site by the assayed peptides, both in the dark (teal) and under 365 nm light (purple). Error bars are S.E.M. Figure 24 summarizes these results by collecting the obtained exponential decay mean lifetimes (τ) of cis to trans relaxation, ellipticity at 222 nm (indicative of helical conformation) and BAP-long/β-adaptin 2 interaction inhibition constants.

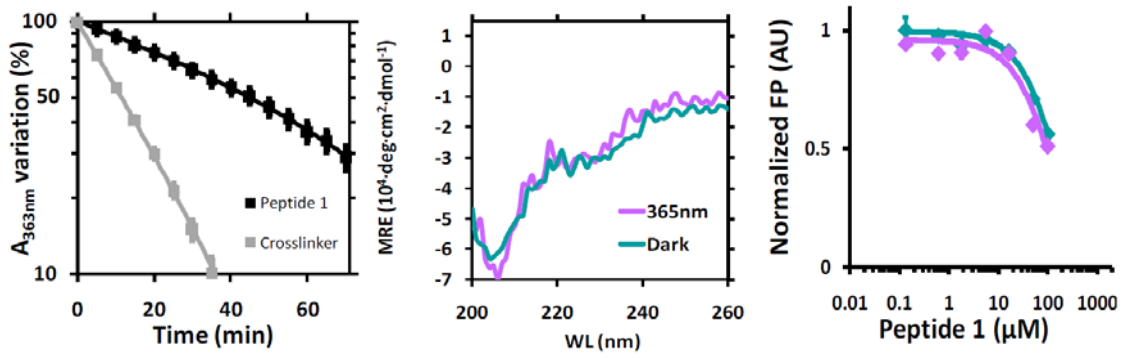

Figure 10 Peptide 1.

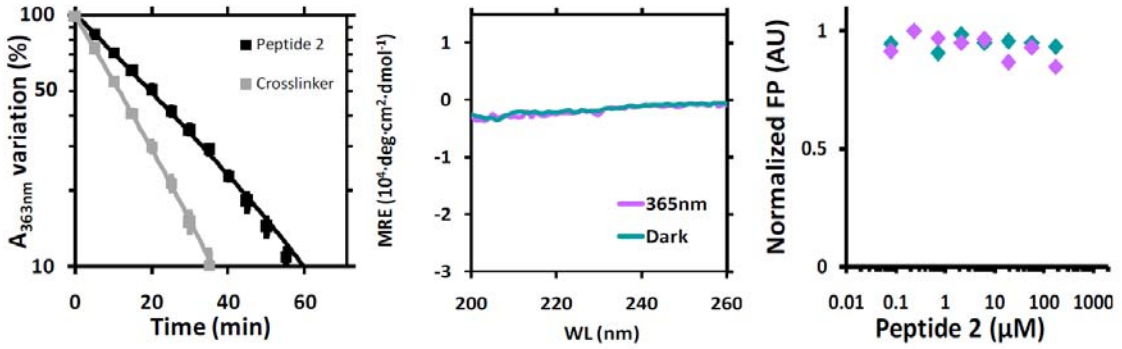

Figure 11 Peptide 2.

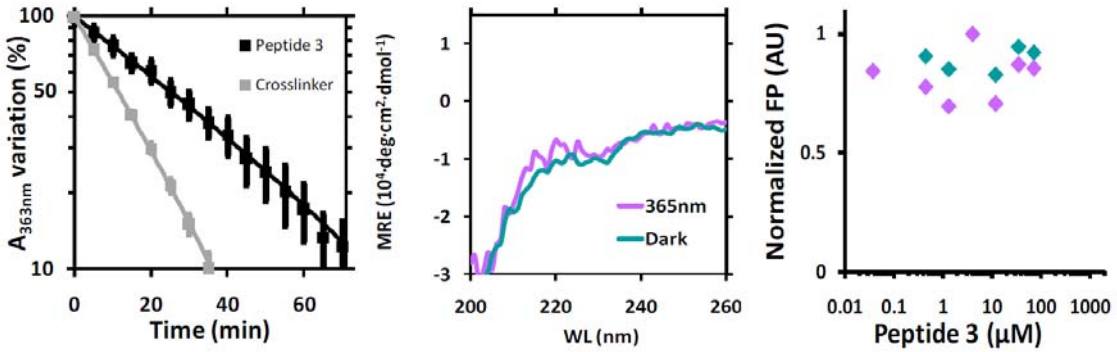

Figure 12 Peptide 3.

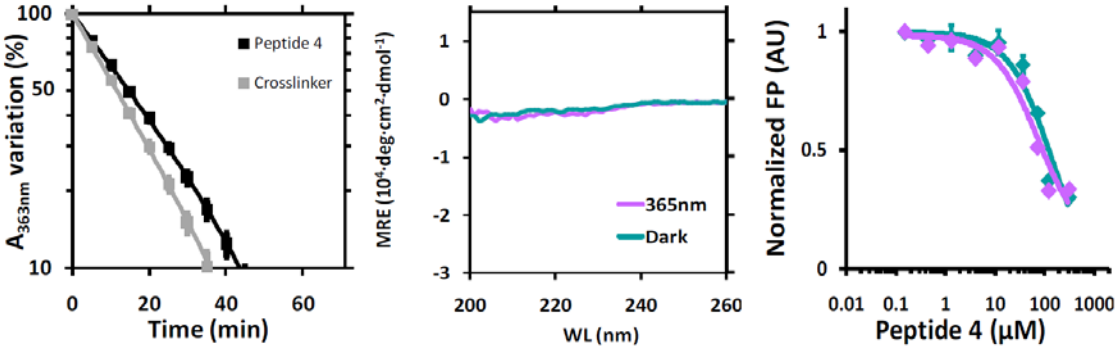

Figure 13 Peptide 4.

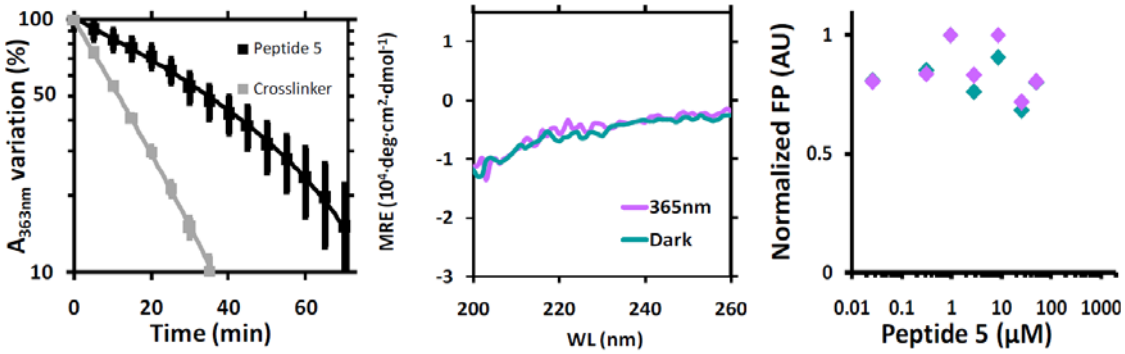

Figure 14 Peptide 5.

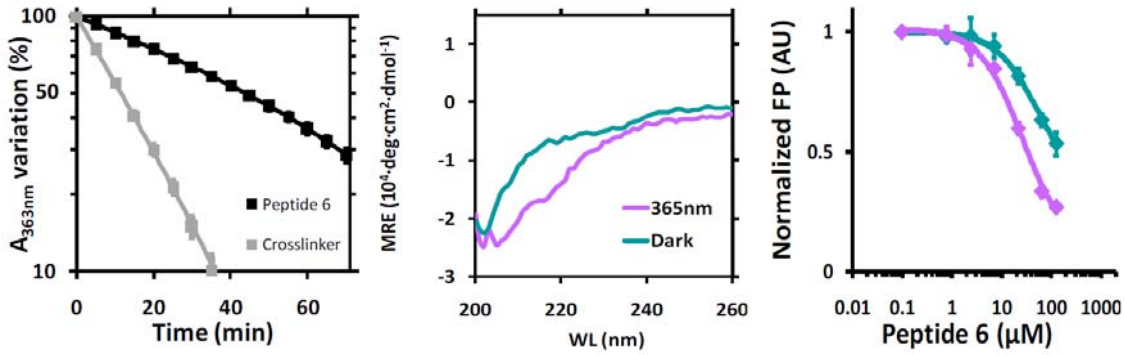

Figure 15 Peptide 6.

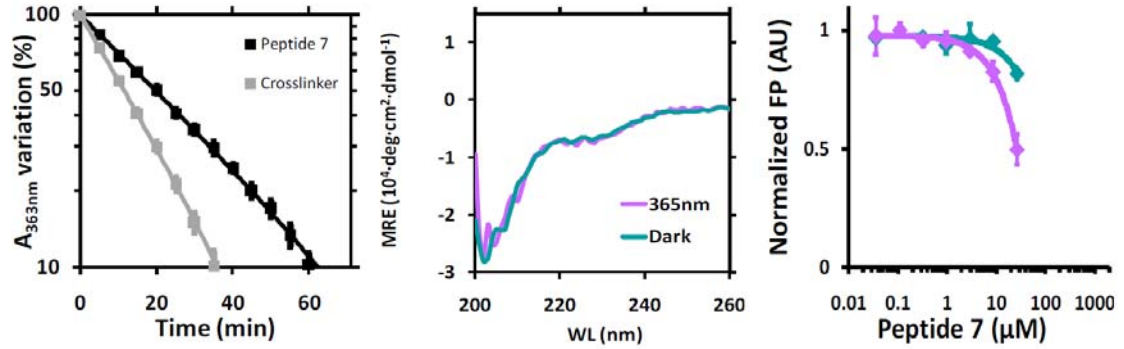

Figure 16 Peptide 7.

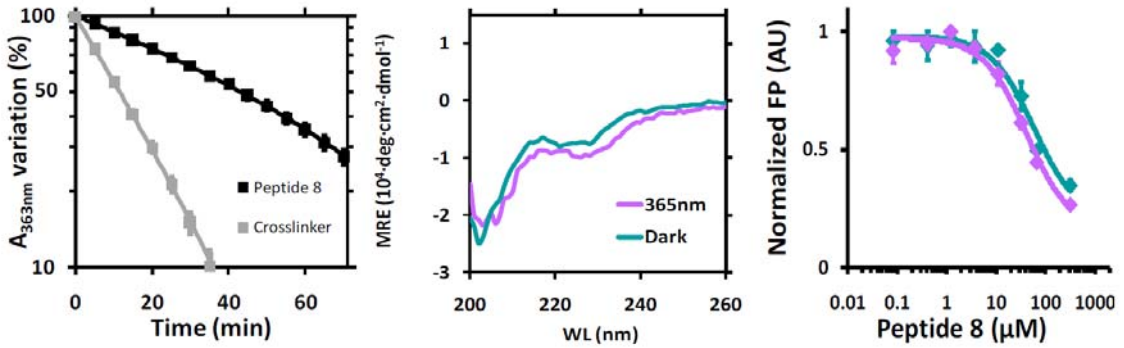

Figure 17 Peptide 8.

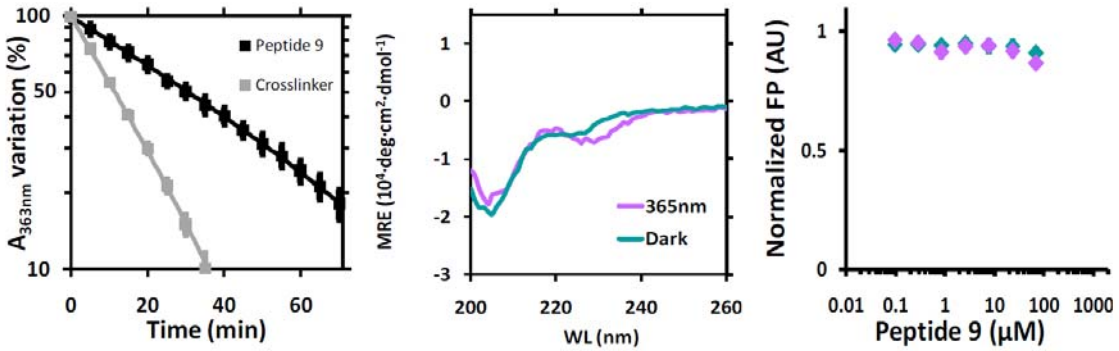

Figure 18 Peptide 9.

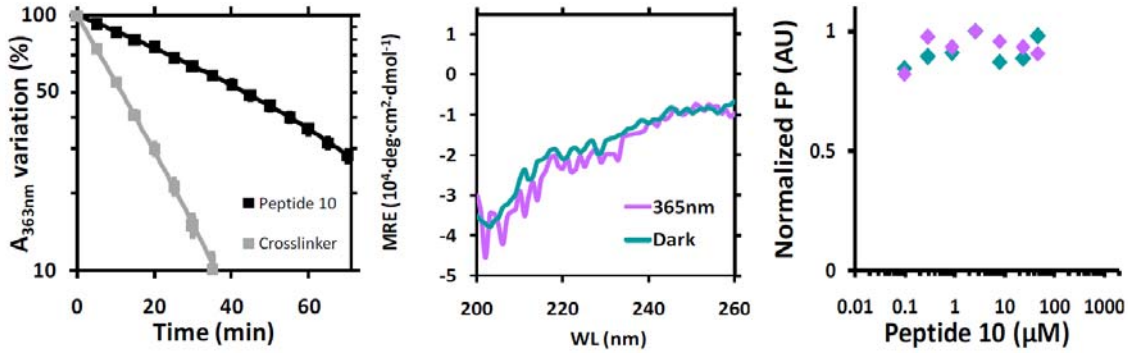

Figure 19 Peptide 10.

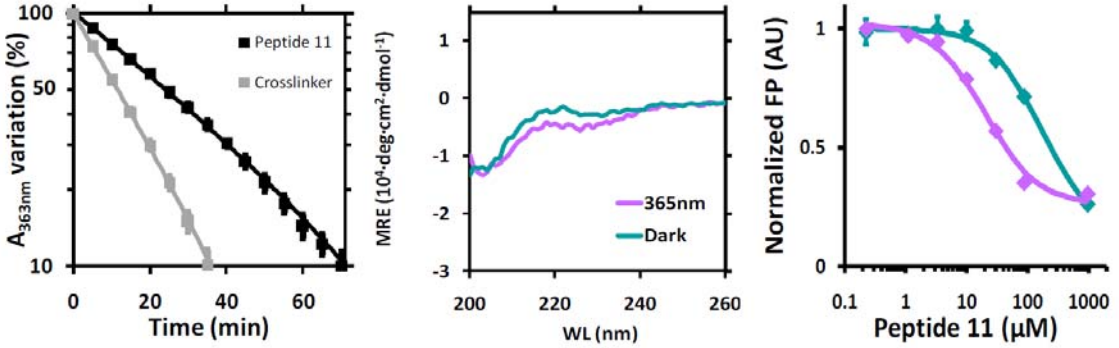

Figure 20 Peptide 11.

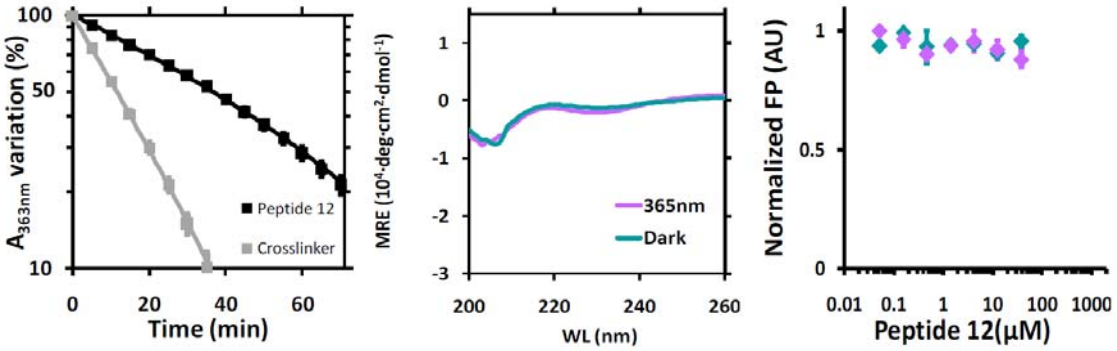

Figure 21 Peptide 12.

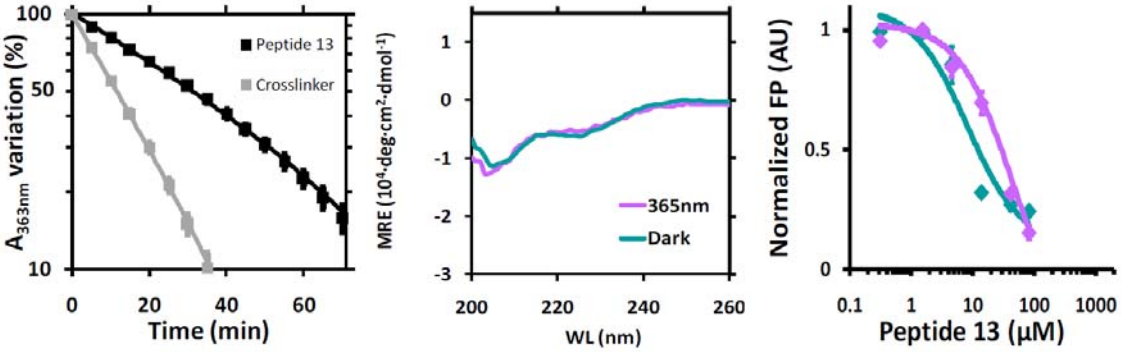

Figure 22 Peptide 13.

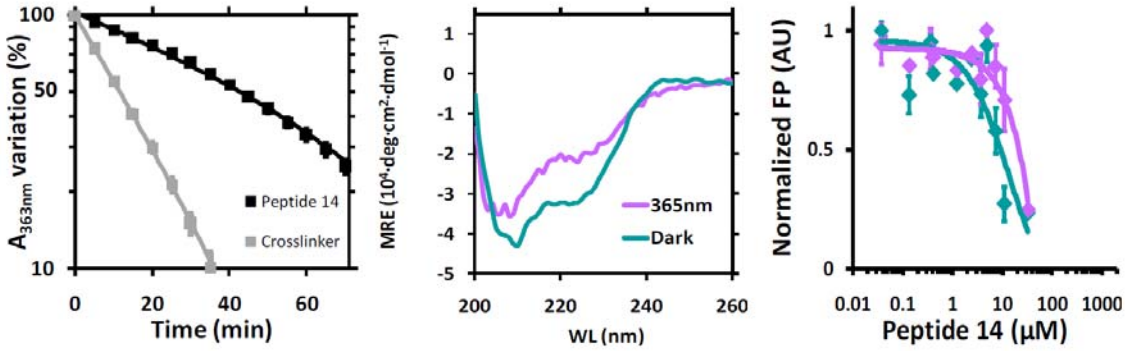

Figure 23 Peptide 14.

Peptide	Azobenzene cis to trans τ (min)	MRE_{222nm} dark-adapted (Kdeg·cm²·dmol⁻¹)	MRE_{222nm} UV light (Kdeg·cm²·dmol⁻¹)	K_I dark-adapted (μM)	K_I UV light (μM)	Change factor	Color code
1	120±40	-32±0.5	-33±5	NB	NB		
2	29±1	-1.9±0.9	-2.4±0.9	NB	NB		
3	39±7	-11±1.2	-8±1.2	NB	NB		
4	23±1	-2.1±0.2	-2.9±0.2	130±6	62.0±0.1	2.10	
5	90±10	-6±2	-3±2	NB	NB		
6	110±10	-6.2±0.3	-11.6±0.3	59±4	24±2	2.46	
7	30±2	-4±0.5	-5±0.5	1500±7000*	700±1700*	2.14	
8	100±10	-7.8±0.8	-8.8±0.8	60±10	39±6	1.54	
9	50±7	-5.8±0.8	-5.9±0.8	NB	NB		
10	100±10	-19±5	-24±5	NB	NB		
11	37±2	-1.4±0.6	-5±0.6	240±150	19.0±0.3	12.63	
12	69±6	-0.8±0.06	-1.5±0.1	NB	NB		
13	53±4	-6.2±0.4	-5.4±0.4	8±1	31±3	3.88	
14	100±10	-33±3	-21±3	NB	NB		

Figure 24 Parameters determined for each assayed peptide: *cis*-azobenzene mean lifetime τ (calculated from fitting data to an exponential decay model) as an indicator of structural rigidity, MRE_{222nm} as an indicator of tendency to adopt helical structure, and calculated inhibition constants as probe for affinity photocontrol. Error values are s.e.m. for at least two replicates. Peptides have been color-coded to show the relative change of their inhibition constants in response to 365 nm illumination. * Variation of affinity in this peptide is evident from the displacement curve, although lack of displacement saturation introduces great dispersion in the calculated constant.

The photoswitching of crosslinked peptides was characterized by their *cis*-isomer mean lifetime (τ) from absorption measurements and their circular dichroism (CD) spectra in the dark-adapted state and after exposure to a light source of 365 nm. The value of τ is readily obtained by spectrophotometric measurements and reflects the stability of the *cis* isomer (stable conformations are associated with longer τ). Thus, this parameter is a useful indirect indicator of structure and stability for the initial stages of photoswitchable peptide design. Most CD spectra of the peptide panel indicated little secondary structure both in the dark-adapted state and after illumination at 365 nm.

After recording the light-induced change in molar ellipticity by CD (Figure 25a-c), we conducted replica-exchange molecular dynamics (REMD) simulations in order to gain structural insight into this spectroscopic behavior. These simulations resulted in highly flexible conformational ensembles of reduced helicity but that were clearly different for the *cis* and *trans* states of the crosslinker, in agreement with the CD observations (Figure 25d-i).

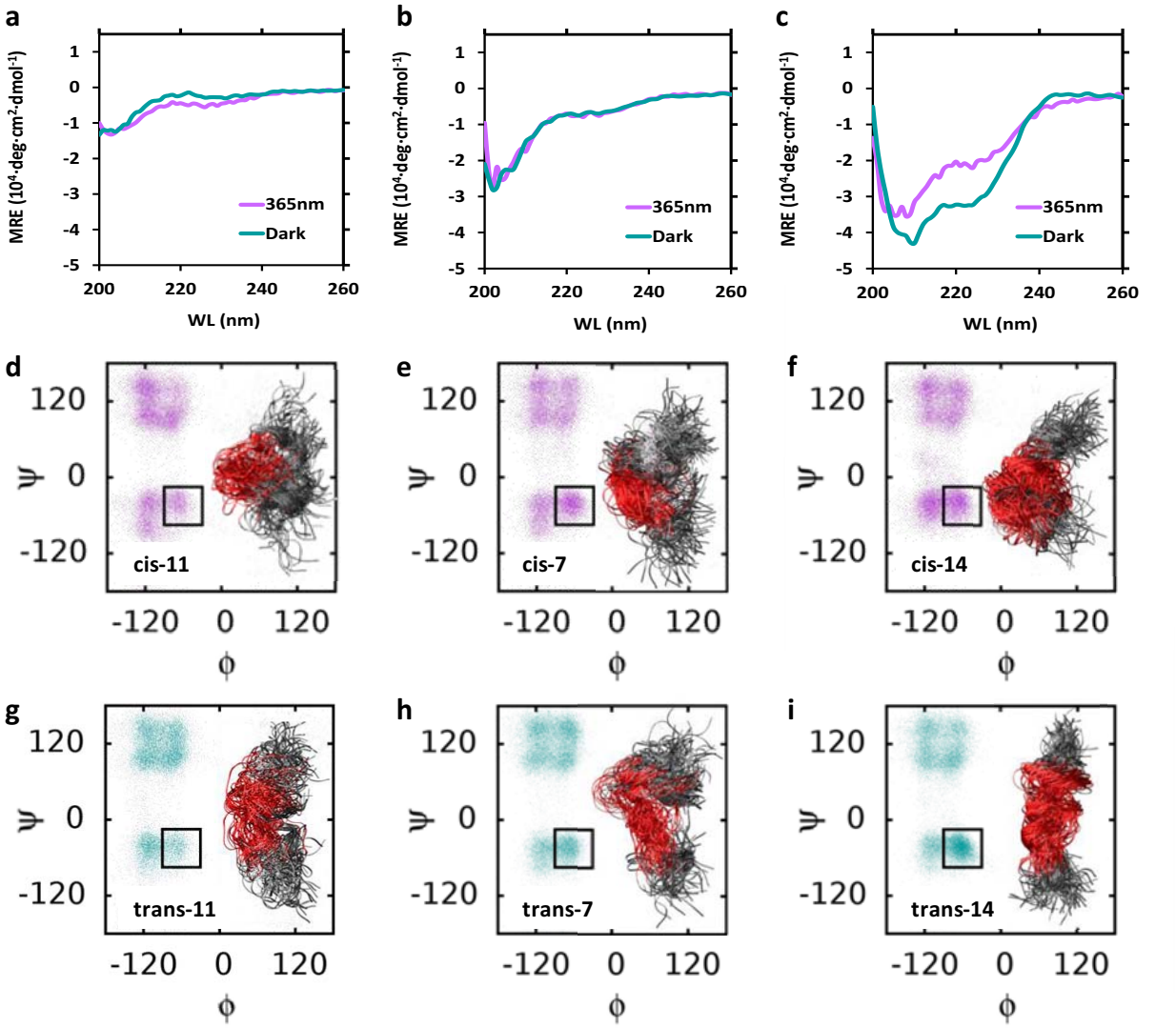

Figure 25 Secondary structure of PIPPI peptides in solution. (a-c) Circular dichroism spectra of azobenzene-crosslinked 11 (a), 7 (b) and 14 (c) in solution showing the conformational change of PIPPI peptides in response to illumination; purple lines correspond to the spectrum after irradiation with 380 nm light and teal lines to the spectrum in the dark or after irradiation with 500 nm light. (d-i) Representation of the backbone of an ensemble of 100 conformations for the 80-ns REMD simulations corresponding to the 300 K and Ramachandran plots of *cis*-11 (d), *trans*-11 (g), *cis*-7 (e), *trans*-7 (h), *cis*-14 (f) and *trans*-14 (i). Backbone of residues that fall within the region between cysteine residues are shown in red and outside that region in grey. Ramachandran plots show the Φ and Ψ dihedral angles of all residues of the peptides every 50 ps. Purple and teal correspond to *cis*- and *trans*-isomers, respectively. REMD simulations performed by Sergio Madurga.

2.3.2. Interaction with β-adaptin.

In order to assess the performance of PIPPI peptides, we used a fluorescence polarization (FP) assay to test their ability to displace a fluorescently labeled BAP-long from its interaction with β-adaptin 2, as a function of illumination (Figures 2-6 to 2-20 in the additional information section below). Comparison of FP data with the structural results reveals that, for this panel, peptides with relatively high helicity show no binding to β-adaptin 2, whereas stronger binders show little helicity (Figure 26). Interestingly, both the higher affinity peptides and the peptides showing greater changes in affinity in response to light also show flexible structures in REMD simulations.

Regarding crosslinking distance, bridging one α-helix turn (peptide residues i, i+4) or two helix turns (residues i, i+7) should result in peptides that are more helical (and hence active) under light of 365 nm, while bridging three helix turns (residues i, i+11) should render peptides that are more helical (and active) in the dark (Woolley, 2005). In this collection, all but one peptide that bound β-adaptin 2 represented i, i+7 crosslinking. No i, i+4 peptides and only one i, i+11 peptide displayed measurable binding. On the basis of these results, we propose that under both states of the photoswitch the i, i+4 crosslinking distance imposes a strong structural constraint that eliminates the flexibility of the peptide required for interaction with β-adaptin 2. As for the i, i+11 crosslinking, it offers only 3 positions in 20-mer peptides, leaving little space for improving binding or photoswitching by scanning the sequence with the crosslinker. Nevertheless, our panel included 2 out of the 3 possibilities and one peptide displayed photoswitchable binding. These results favor the use of i, i+7 crosslinking when developing PIPPIs for interactions that require flexible ligands.

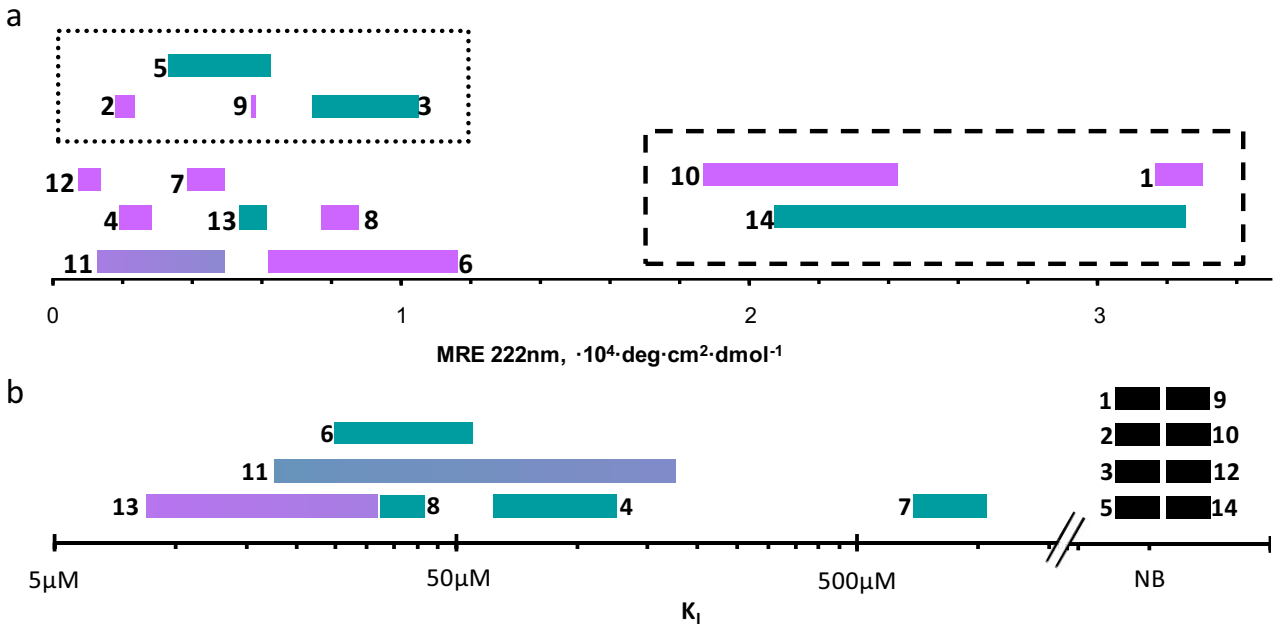

Figure 26 Structure and affinity switches. a) Range diagram of peptide circular dichroism at 222 nm (indicator of helical conformation of peptides). The color of the boxes shows the light corresponding to each extreme of the range (purple = 380 nm, teal = dark or 500 nm). For convenience, the scale is represented as absolute value of mean molar per residue ellipticity (MRE_{222nm}), all the raw values being negative. Black boxes enclose the peptide sequences unable to bind β-adaptin 2 in the competition assay (dotted = i, i+4 crosslinked peptides and dashed = high MRE peptides). b) Range diagram of peptide affinity change in response to light, with the same color code. Peptides with no binding (NB) to β-adaptin 2 in the competition assay are shown in black to the right of the axis.

2.3.3. Effect of non-proteinogenic amino acids.

In weak interactions characterized by flexibility (e.g. interactions with intrinsically disordered proteins), relatively small structural changes in one of the interacting molecules can greatly influence binding. In these cases, the substitution of residues with non-proteinogenic amino acids can be used to tune the binding strength of the resulting peptides. This study includes two instances of such use. The non-proteinogenic amino acid Aib is a strong 3–10 helix inducer in peptide chains. It imposes a limitation on the dihedral angles of its peptide bonds. Thus, the introduction of Aib in a peptide sequence has two effects: rigidifying its local environment and introducing 1/3 of a 3–10 helix turn. Aib has also been reported to prevent fibril formation and thereby improve peptide solubility in water (Kumita, Weston, et al., 2003). Aib was included in several peptides in our collection in order to assess its effects on peptide performance as photoswitchable inhibitors. Diverse results were obtained (Figure 28 and Figure 29). On the one hand, the presence of Aib in peptide **11**, which displays photoswitchable inhibitor properties,

resulted in the non-interacting peptide **12**. On the other hand, the introduction of Aib in the non-interacting peptide **5** resulted in peptide **6**, which displayed photoresponsive interaction capacity. The lack of binding of peptide **12** could be related to the nearly two-fold increase in the di-azo bond isomerization relaxation time (Figure2-20). Peptides **11** and **12** showed low helicity by CD, although REMD simulations suggest that a local increase in helicity at residue 7 is deleterious for binding both *trans*-**11** and the two *cis/trans* isomers of **12 (**Figure 27**)**. The rescue of the binding capacity of peptide **5** via the introduction of Aib at position 8 is harder to interpret on the basis of the conformational information available. Taken together, these results reveal that Aib can be a useful resource for the design of PIPPIs; however, it must be used with caution when working on PPIs characterized by flexibility of the interacting molecule mimicked.

Naphtylalanine (Nal) was the second non-proteinogenic amino acid introduced into our design. It can be used as a more hydrophobic substitute of phenylalanine to enhance hydrophobic interactions. We generated peptides **8** and **9** by replacing the second phenylalanine residue in the DxxFxxFxxxR motif of peptide **7** with 1- and 2-Nal respectively. In binding assays, peptide **8** displayed greater affinity than 7 whereas 9 did not bind to β-adaptin (Figure 29b). Longer τ values of **8** and **9** evidenced that the phenylalanine to naphtylalanine substitution stabilizes the cis-isomer of azobenzene (Figure 24). This binding behavior suggests a better fit of 1-Nal (in red in Figure 29c) within the structure of the β-adaptin binding pocket (Schmid et al., 2006). However, the enhancement in affinity achieved with **8** was accompanied by loss of ability to reversibly photoswitch the interaction.

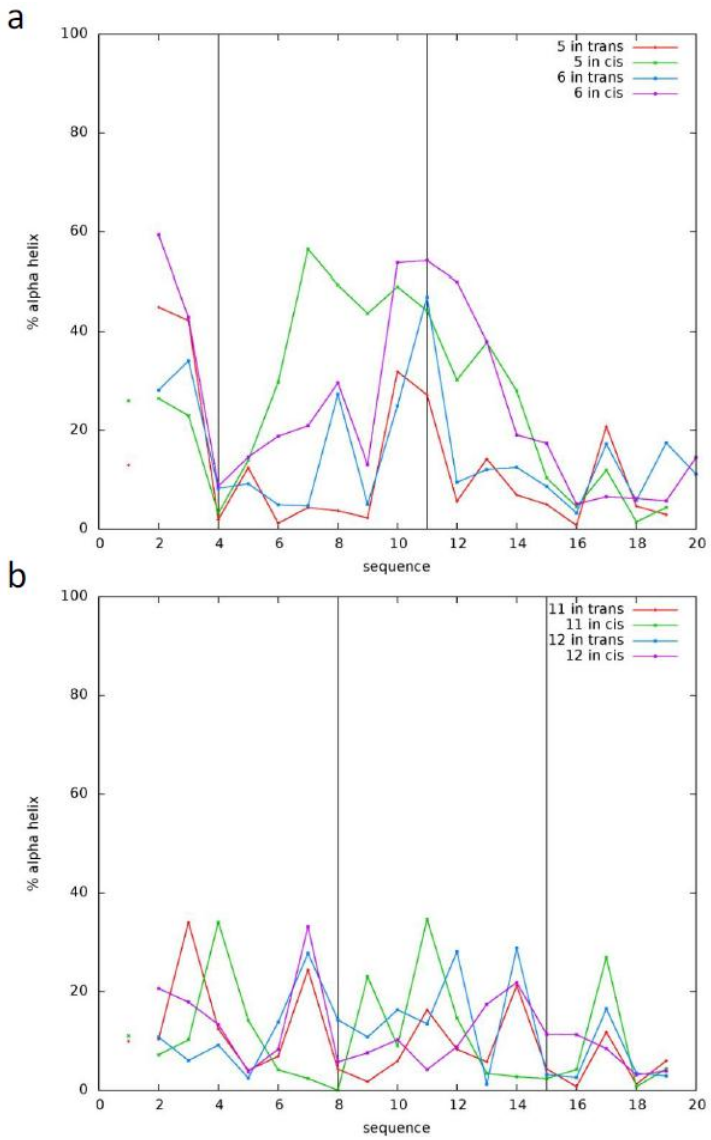

Figure 27 Effect of Aib on helicity in REMD simulations. Comparison of the relative frequency of α-helical conformation in the sampled ensemble of structures for every amino acid position between Aib-containing and Aib-free peptides. Imposition of both *cis* and *trans* conformations of the azobenzene in the simulation is shown. a) Peptide 5 vs. peptide 6. Aib is residue 8 of peptide 6. b) Peptide 11 vs. peptide 12. Aib is residue 12 of peptide 12. Conformational analysis performed with GROMACS. A residue is considered α-helical if its predicted dihedral angles are $\Phi \in [-90°, -30°]$ and $\Psi \in [-75°, -15°]$. Simulations by Sergio Madurga.

Peptide	Sequence	K_I dark-adapted (μM)	K_I UV light (μM)	MRE_{222nm} ($deg \cdot cm^2 \cdot dmol^{-1}$)	τ (min)
4	CDDVBFECFARQRLKGMKDD	62±0.1	130±6	2900±200	23±1
10	DDDIVFCDFVBQRCKGMKDD	NB	NB	24000±500	100±10
5	DDDCVFEDFACQRLKGMKDD	NB	NB	6000±200	90±10
6	DDDCVFVBFACQRLKGMKDD	24±2	59±4	11600±300	110±10
11	DDDIVFECFARQRLCGMKDD	19±0.3	240±150	5000±600	37±2
12	DDDIVFECFAVBRLCGMKDD	NB	NB	1500±100	69±6

Figure 28 Comparative of the Aib-containing peptides and their Aib-free analogs. Residues interacting with β-adaptin 2 are shown in red. The azobenzene bridge is represented by a line below the sequence. B represents Aib in the sequences. Values of MRE_{222nm} correspond to the absolute value of the most helical conformation for each peptide.

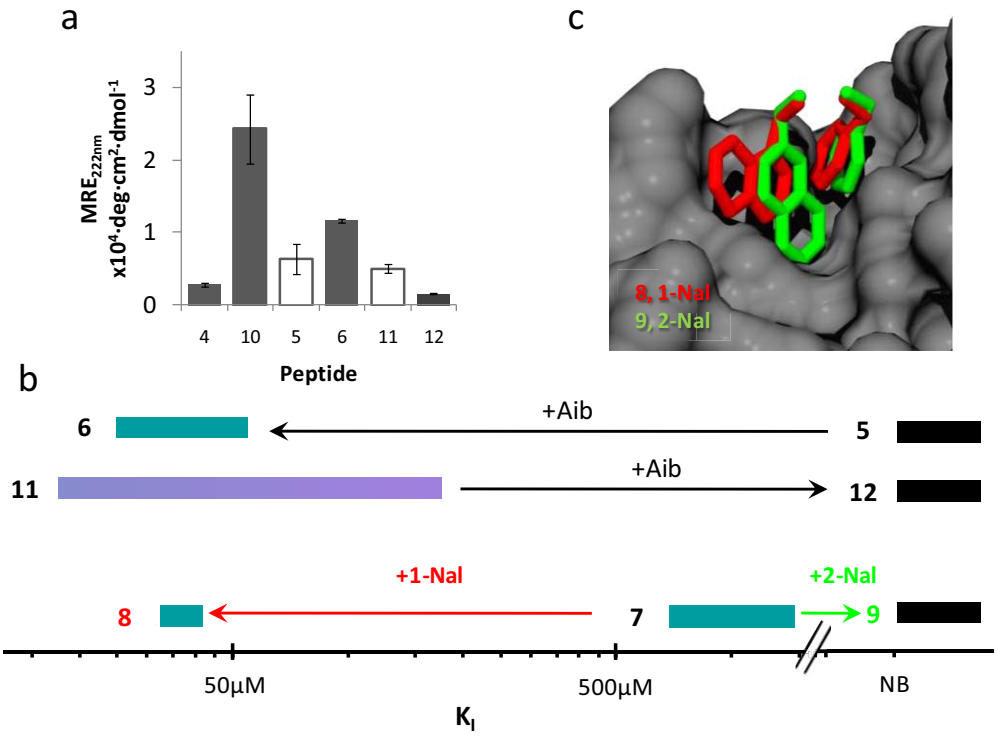

Figure 29 Use of non-proteinogenic amino acids. a) Ellipticity at 222 nm (absolute value) for TL peptides. Grey bars indicate peptides containing Aib. White bars indicate Aib-free versions of 6 and 12. b) Affinity switching ranges for sequences containing non-proteinogenic amino acid and the corresponding all-natural amino acid sequences. NB indicates that no binding or switching was detected in the FP competition assay. c) Cartoon representation of the side chains of residues 6 and 9 of peptides 8 (red) and 9 (green) inside the binding pocket of β-adaptin 2.

2.3.4. Photoswitchable ligand binding model

An ideal PIPPI should display two states of highly distinct affinity for its binding target and interconvert between them in response to light. When using photochromic crosslinkers such as BSBCA, two main factors come into play. First,

under light of 365 nm, a photostationary state that contains a certain proportion of the two states will be reached. Second, each state will have an intrinsic affinity. The effect observed in binding assays can be seen as a result of the combination of these two factors. Thus the calculated interaction or inhibition constants under 365 nm do not equal the intrinsic inhibition constant of the corresponding state (active for *i, i+7* peptides or inactive for *i, i+11* peptides) but are apparent inhibition constants corresponding to a mixture of active and inactive molecules.

In terms of PIPPI design two parameters require optimization: the composition of the photostationary state and the difference in intrinsic binding affinities of each of the states. It must be noted that in the photoswitching of interactions, these parameters play different roles depending on the kind of photoswitching involved (PSS active or PSS inactive). To inform design and optimization efforts, we applied a simplified interaction model, detailed below, reflecting this view of photoswitchable ligands. The predictions of this model match our experimental observations for peptides **11** and **13**, which are cases of PSS active and PSS inactive inhibitors respectively. Two main conclusions can be drawn from the model: first, for PSS active inhibitors, such as **11**, the photocontrol of binding will improve when the difference between intrinsic affinities of the active and inactive states is increased and not when the photostationary state is enriched in active inhibitor (Figure 2-36). Second, and conversely, for PSS inactivated inhibitors, such as peptide **13**, the photocontrol of binding will be better when the composition of the photostationary state is enriched in inactive molecule than when the intrinsic affinity of the inactive state is further reduced (Figure 2-37).

In this scenario, optimizing the composition of the photostationary state means tuning the photochemistry of the azobenzene crosslinker (e.g. by introducing substituents in the azobenzene rings). On the other hand, increasing the difference between active and inactive states implies altering the structure of the peptide and/or the interacting amino acid side chains (e.g. by introducing phenylalanine to naphtylalanine mutations) in order to obtain, when crosslinked and photoswitched, conformational ensembles that are structurally more different and/or have increased or decreased affinity for their target. However, it is difficult to introduce peptide modifications that will affect only one of the states. Regarding the photostationary state, the caveat lies in the effect of target binding, which can in some cases stabilize the active state of the inhibitor, effectively rendering it a phototrigger and not a photoswitch (Woolley, 2005).

Description of the model

When a protein P is mixed with a photoswitchable ligand with two states (active or folded L^F and inactive or unfolded L^U) in a certain photostationary state, several photoswitching and binding equilibria co-exist. In an homogeneous assay, such as our FP experiments, the active and inactive ligands are indistinguishable and only the fraction of probe bound to the protein is known. A simplified description of the binding and switching equilibria (Figure 30) was used to model this situation in terms of the classical dissociation equilibrium constant for a ligand-protein interaction (K_D).

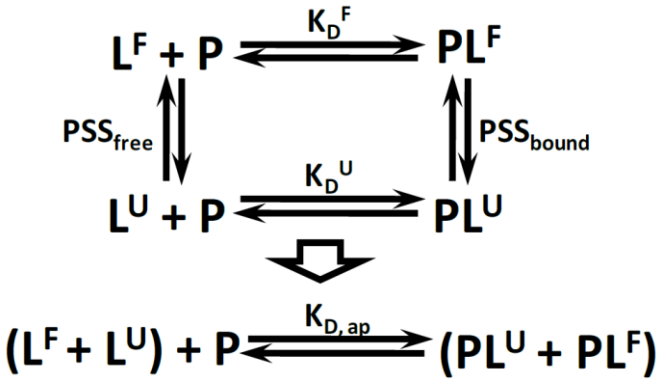

Figure 30 Photoswitchable ligand binding model. The binding equilibria of the folded and unfolded photoswitchable ligand are in turn in equilibrium with the photoswitching equilibria (photostationary state, PSS) of the bound and free ligand. When the folded and unfolded conformations cannot be distinguished, all four equilibria appear as a single apparent equilibrium.

This simplification assumes that a certain composition can be imposed upon the mixture of free active and inactive ligand and this composition is maintained constant (i.e. a photostationary state is reached and maintained, unaffected by the binding equilibrium). Thus the equilibria can be considered as the binding of two different molecules to the same protein, each one with its own dissociation equilibrium constant, expressed as

(1)
$$K_D^U = \frac{[L^U]\cdot[P]}{[PL^U]}$$

for the binding constant of the unfolded (U) peptide, and

(2)
$$K_D^F = \frac{[L^F]\cdot[P]}{[PL^F]}$$

for the binding constant of the folded (F) peptide. Since L^U and L^F appear in the assay as a single ligand L_T (total ligand) and a fixed composition is imposed by the photostationary state, the following expressions also hold:

(3) $$[L_T] = [L^F] + [L^U]$$

(4) $$[PL_T] = [PL^F] + [PL^U]$$

(5) $$[L^F] = \alpha \cdot [L_T]$$

where *α* is the fraction of total ligand in active form in the photostationary state.

The bound forms of the ligand also appear as a single species in the assay and thus an apparent dissociation equilibrium is observed with

(6) $$K_{D,ap} = \frac{[L_T]\cdot[P]}{[PL_T]}$$

This apparent dissociation constant can be related to the dissociation equilibrium constants of the active and inactive form and to *α* as follows:

$$K_{D,ap} = \frac{[L_T]\cdot[P]}{[PL_T]} \overset{(4)}{\Rightarrow} K_{D,ap} = \frac{[L_T]\cdot[P]}{[PL^F]+[PL^U]} \overset{(1),(2)}{\Longrightarrow}$$

$$\overset{(1),(2)}{\Longrightarrow} K_{D,ap} = \frac{[L_T]\cdot[P]}{\frac{[L^F]\cdot[P]}{K_D^F}+\frac{[L^U]\cdot[P]}{K_D^U}} = \frac{[L_T]}{\frac{[L^F]}{K_D^F}+\frac{[L^U]}{K_D^U}} \overset{\times K_D^F\cdot K_D^U}{\Longrightarrow}$$

$$\overset{\times K_D^F\cdot K_D^U}{\Longrightarrow} K_{D,ap} = \frac{[L_T]\cdot K_D^F\cdot K_D^U}{[L^F]\cdot K_D^U+[L^U]\cdot K_D^F} \overset{(3),(5)}{\Longrightarrow}$$

$$\overset{(3),(5)}{\Longrightarrow} K_{D,ap} = \frac{[L_T]\cdot K_D^F\cdot K_D^U}{\alpha\cdot[L_T]\cdot K_D^U+(1-\alpha)\cdot[L_T]\cdot K_D^F}$$

which simplifying yields:

(7) $$K_{D,ap} = \frac{K_D^F\cdot K_D^U}{\alpha\cdot K_D^U+(1-\alpha)\cdot K_D^F}$$

and rearranging:

(8) $$K_D^U = \frac{1-\alpha}{\frac{1}{K_{D,ap}}-\frac{\alpha}{K_D^F}}$$

(9) $$K_D^F = \frac{\alpha}{\frac{1}{K_{D,ap}}-\frac{1-\alpha}{K_D^U}}$$

With these expressions it is possible to calculate the intrinsic dissociation equilibrium constants of the *cis* isomer of azobenzene crosslinked peptides (K_D^U or K_D^F depending on the crosslinking distance) even when the photostationary state contains a certain fraction of *trans* isomer. The constants for the dark-adapted state and the photostationary state and the fraction of *trans* isomer in the

photostationary state are required for the calculation. The fraction of *trans* isomer can be determined from peak integration of NMR spectra of the azobenzene-crosslinked peptides and was found to be 32% for the peptides and conditions used in this study.

The expression for the apparent constant is useful when determining which properties of the photoswitchable ligands have to be improved for a certain application and which properties will have little effect on the operation of the system. This has been applied to the cases of peptide **11** and peptide **13** as examples of PSS active and PSS inactive ligands respectively (Figure 32 and Figure 33).

The expression (8) is used to calculate K_D^U for a PSS inactivated peptide. This expression is a hyperbola with a vertical asymptote and will be negative beyond $\boldsymbol{\alpha = \frac{K_D^F}{K_{D,ap}}}$. This can be interpreted as theoretical null binding of the inactive state. In those cases, if a $K_{D,ap}$ can be observed (i.e. there is an appreciable binding in the inactive state), it must be assumed that all the binding corresponds to residual active peptide (Figure 31).

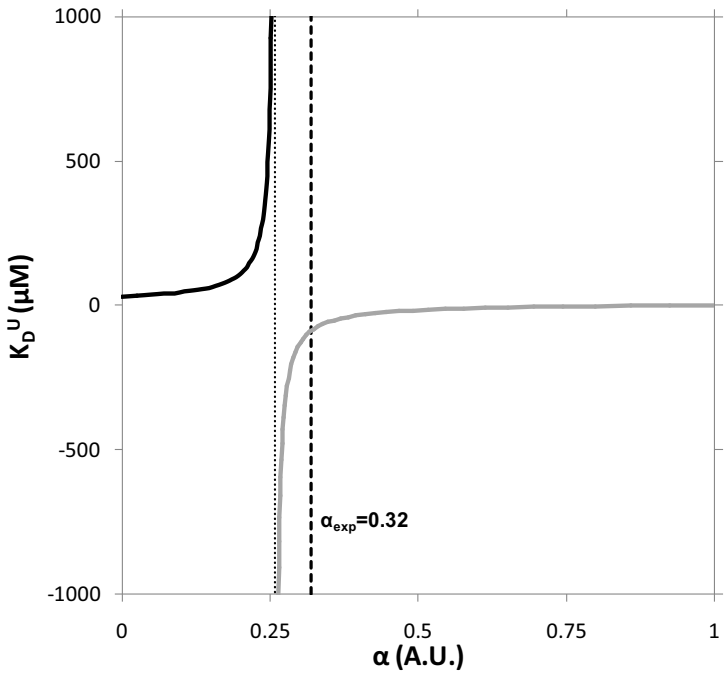

Figure 31 Binding constant of the inactive state (K_D^U) as a function of the cis-fraction (α) for *cis*-active inhibitors. Plot of expression (8) for the case of peptide 13 ($K_{D,ap}$ = 31±3 μM, K_D^F = 8±1 μM). Dotted line is the vertical asymptote representing the *trans* content of the photostationary state (α) beyond which negligible binding of the inactive form is assumed. The part of the function without physical meaning is drawn in grey. Dashed line represents the experimental value of α.

The case of an absolutely inactive form of the ligand would represent an ideal photoswitch. In that case, the apparent dissociation constant can be estimated as

(10) $$\lim_{K_D^U \to \infty} K_{D,ap} = \frac{K_D^F \cdot K_D^U}{\alpha \cdot K_D^U + (1-\alpha) \cdot K_D^F} = \lim_{K_D^U \to \infty} \frac{K_D^F \cdot K_D^U}{\alpha \cdot K_D^U} = \lim_{K_D^U \to \infty} \frac{K_D^F}{\alpha} = \frac{K_D^F}{\alpha}$$

Peptide **13** fits into this description. Its $K_{D,ap}$ and K_D^F were observed as 31±3 μM and 8±1 μM respectively. With the estimated *α* of 0.32, expression (8) yields a negative result for **13** so a negligible contribution of *cis*-**13** to the total binding was assumed. Using expression (10), $K_{D,ap}$ was estimated as 25±3 μM. This is very close to the observed $K_{D,ap}$ showing that this simplified model has predictive capacity (Figure 33).

The design tips drawn from the model are that (1) great changes in intrinsic affinity should be the main feature sought when designing cis-active azobenzene-based photoswitchable inhibitors, and (2) high content of cis isomer in the photostationary state should be the target feature when designing trans-active inhibitors.

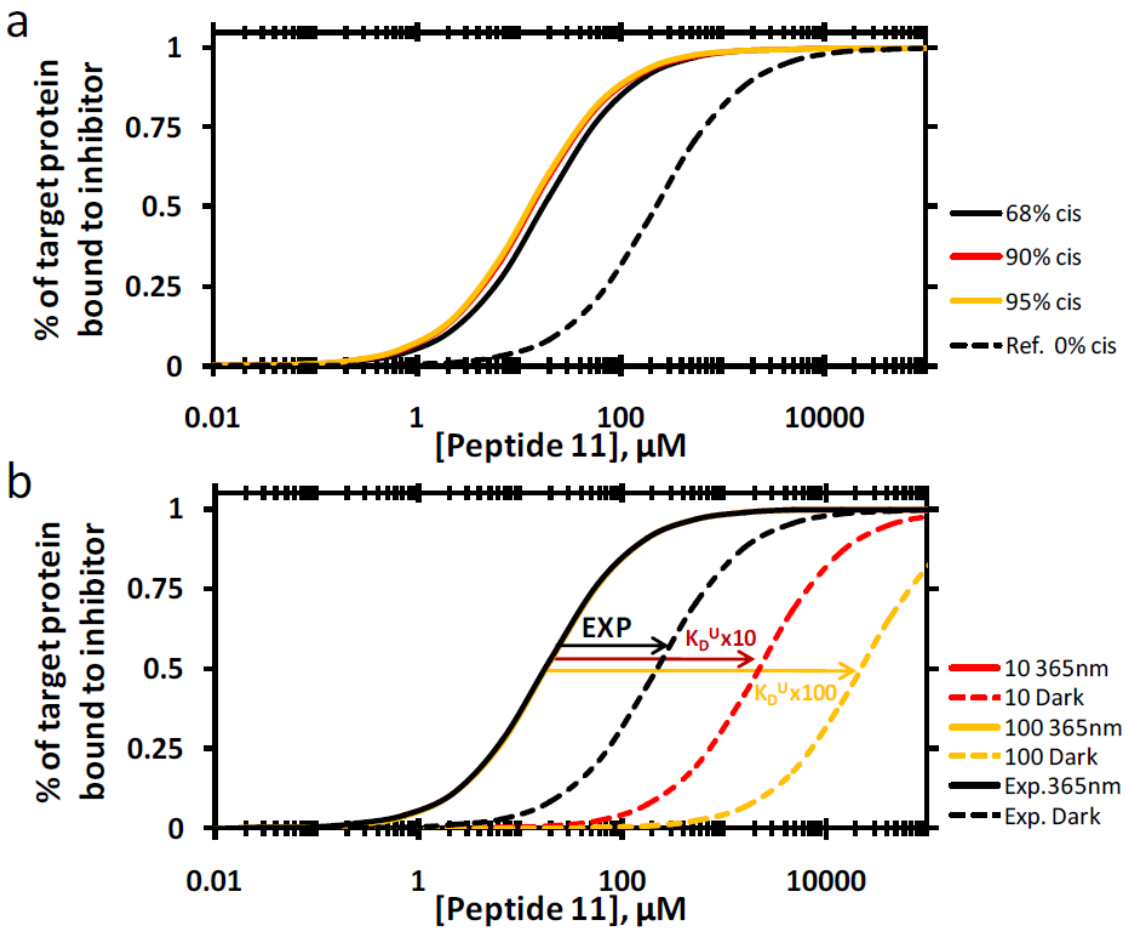

Figure 32 Model predictions for a PSS active ligand. Comparison between the predictions of the model for the experimentally observed situation for peptide 11 (68% *cis* and 32% residual *trans* ligand under 365 nm illumination) and hypothetical peptides with enhanced properties: (a) 90% and 95% *cis* ligand in the photostationary state (azobenzene tuning) or (b) 10- or 100-fold increase of the K_D for the unfolded conformation (affinity tuning). Photoswitching is predicted to improve with affinity tuning and not with azobenzene tuning.

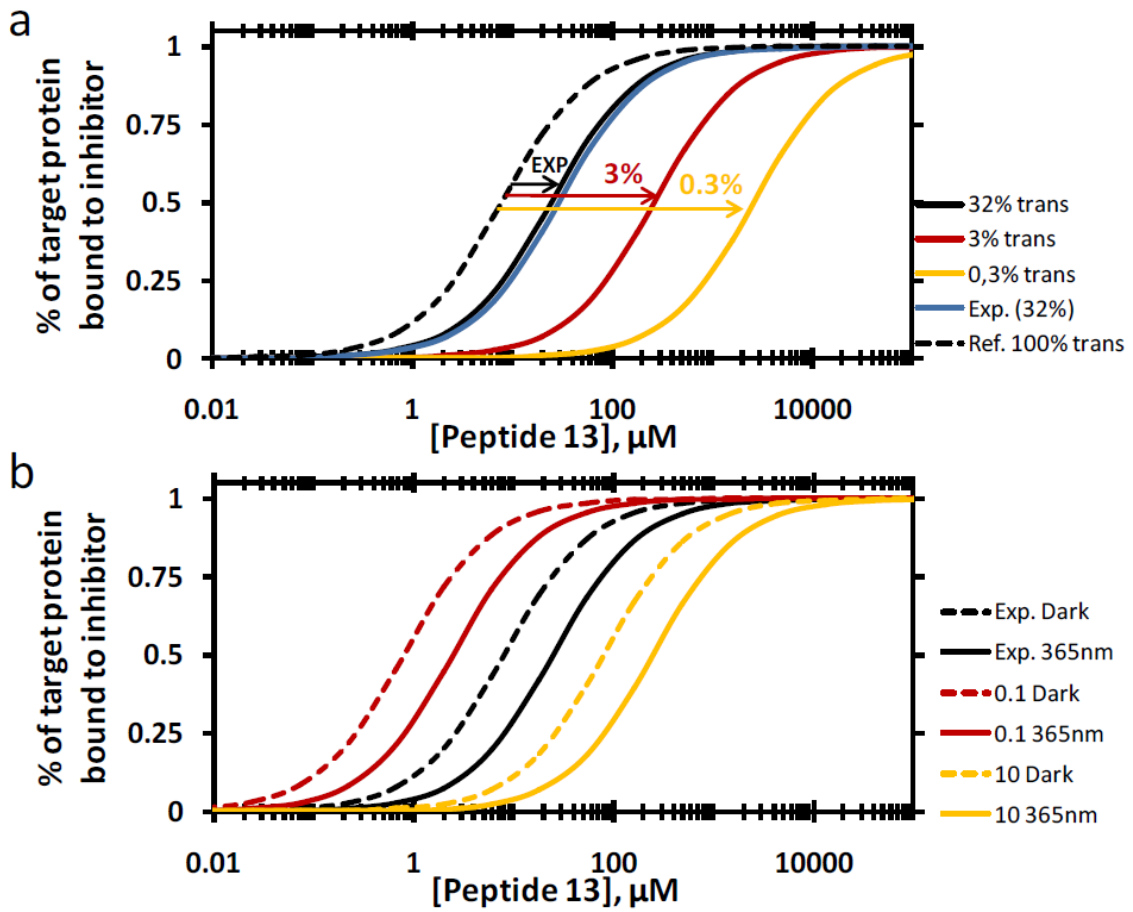

Figure 33 Model predictions for a Dark-active ligand. Comparison between the predictions of the model for the experimentally observed situation for peptide 13 (68% *cis* and 32% residual *trans* ligand under 365 nm illumination) and hypothetical peptides with enhanced properties: (a) 10- and 100-fold reductions of residual *trans* ligand (azobenzene tuning) or (b) 10-fold increase or decrease of the K_D of the folded conformation (affinity tuning). Photoswitching is predicted to improve with azobenzene tuning. Blue curve in a) represents the experimentally observed apparent K_D in a case of predicted $K_D^U \rightarrow \infty$ as a comparison with the one predicted by the model (black solid curve).

2.4. Conclusion

In order to understand the key engineering features leading to functional PIPPIs for CME, here we generated a panel of 14 peptides crosslinked with azobenzene and with different characteristics. In particular, we examined the best positions in the 20-mer peptide in which to insert the crosslinker attachment sites, and we manipulated the peptide affinity and structural constraints to investigate their performance as light-regulated inhibitors. Based on the ensemble of our results, we have developed a mathematical model of photoswitchable binding and proposed a set of design recommendations. These include the choice of 3 optimal positions within an "actuation surface" of 7 residues that lies opposite to the "interaction surface" of the peptide; the preference mainly of *i, i+7* and *i, i+11*

crosslinking distances over *i, i+4* (Figure 34); the impact of introducing peptide-rigidifying modifications; and the possibilities of enhancing the photocontrol of binding by increasing peptide affinity and altering the photostationary state. The peptides with the best performance had a low tendency to form helices in solution and a mild stability of the cis-azobenzene form. These observations indicate that flexible structures (from both points of view of peptide backbone and di-azo bond isomerization) are easily amenable to photoregulation and constitute stronger inhibitors of the β-arrestin/β-adaptin 2 PPI. These findings expand the field of potential α-helical inhibitors of PPIs to the wide group of flexible peptides characterized by a weak or absent secondary structure and discourage the consideration of secondary structure as the sole criterion to use when selecting PIPPI candidates.

Four peptides forming a design sub-family with opposite binding photocontrol properties have been identified as candidates for photocontrol of cellular activities and tested in cellular assays as shown in next s. These peptides have been dubbed traffic lights (TLs) for their potential role as controllers of membrane traffic by means of light. They are peptides **13**, **11**, **12** and **3** (TL-1, TL-2, TL-3 and TL-4 respectively).

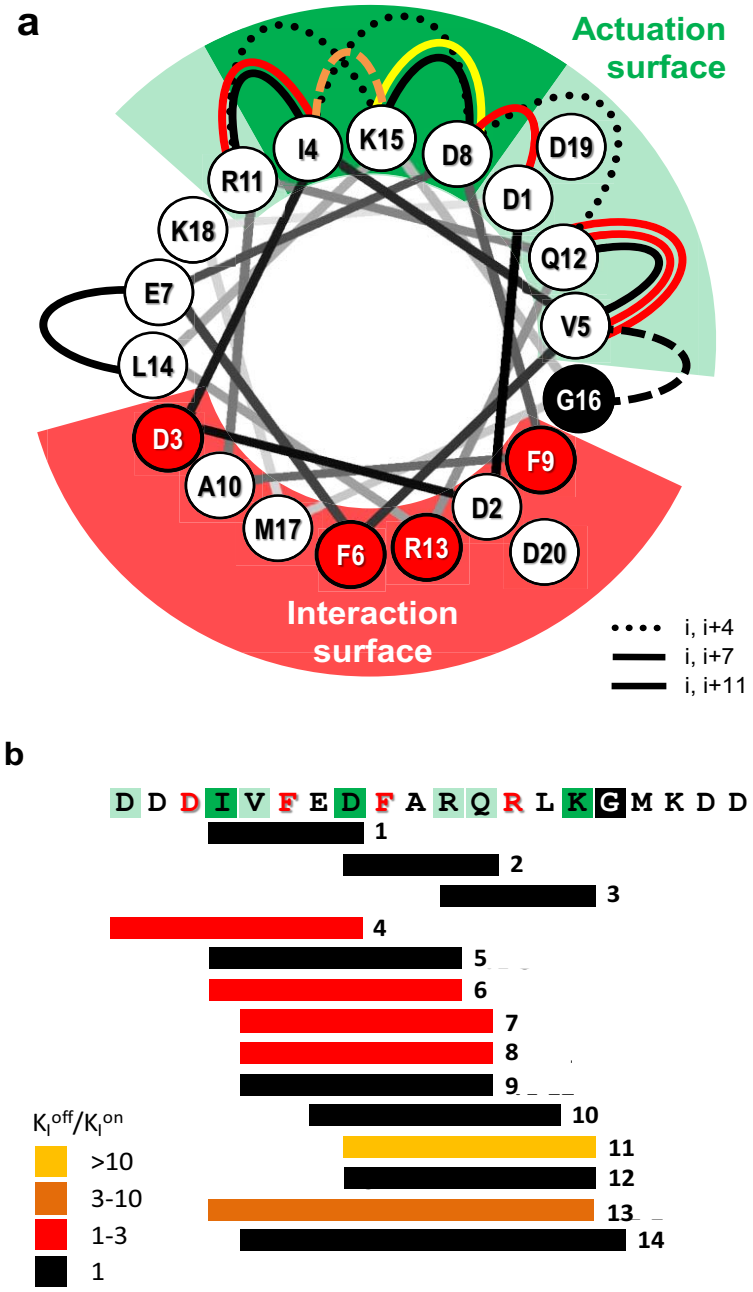

Figure 34Summary of crosslinking design results. a) Helical wheel representation of an alpha-helical β-arrestin 2 peptide-long. Critical, conserved, β-adaptin 2 interacting residues and the interaction surface they define in the helix are highlighted in red. G16 is highlighted in black as its alteration or deletion has been found to abolish interaction capacity of peptides(Schmid et al., 2006). Loops represent the mutation to cysteine and azobenzene crosslinking positions included in the peptide panel. The kind of line of the arches indicates the crosslinking distance in the sequence, while its color codes for the observed affinity switch ratio. The region containing the most successful binding and switching peptides is highlighted in green. b) Representation of the crosslinking positions and range over the peptide sequence. The name of each peptide is displayed for convenience.

3. Control of clathrin-mediated endocytosis using light

3.1. Contributions

Several parts of this section have been carried out in collaboration. Andrés Martín performed synthesis of BSBCA, peptide crosslinking and purification, absorption measurements, fluorescence polarization measurements, cell culture, confocal microscopy and cytometry uptake assays as well as processing and interpretation of data from all the techniques included in the section. Kay Eckelt collaborated in the peptide purification. Laura Nevola synthesized fluorescent peptides for fluorescence polarization and uptake assays, in which she also took part, recorded TIRF and confocal microscopy images, performed toxicity and uptake assays and participated in the processing and interpretation of the data.

3.2. Introduction

Since PPIs are precisely orchestrated in cells, it would be useful to complement the pharmacological selectivity of peptide inhibitors with a means of controlling their kinetics and site of action. In this regard, one option would be to regulate the activity of PPI inhibitors with light, thus controlling their effects with spatiotemporal patterns of illumination (Gorostiza & Isacoff, 2008b). Photosensitive crosslinkers have been introduced in peptides or small proteins to regulate their structure (Kumita et al., 2000; Christian Renner & Moroder, 2006) and binding properties (Guerrero et al., 2005; Kneissl et al., 2008; Schierling et al., 2010; Fuzhong Zhang, Timm, Arndt, & Woolley, 2010). Here we apply the strategy to obtain photoswitchable inhibitors of protein–protein interactions (PIPPIs) described in the previous section to photoregulate clathrin-mediated endocytosis (CME) in living cells, focusing on photocontrol of helicity and comparing four crosslinked peptides.

CME is a key process in all eukaryotic cells. It supports a wide range of functions, including the regulation of surface expression of proteins, the uptake of nutrients, the control of cell signaling, and the turnover of membrane components (McMahon & Boucrot, 2011). CME encompasses a complex network of PPIs

involving many and diverse protein families. The main adaptor protein of this machinery is the AP-2 complex, which mediates the binding of clathrin to the membrane or to cargo receptors, with or without the help of accessory proteins (such as β-arrestin, AP180, and epsin). In addition to the small-RNA interference strategy (Boucrot, Saffarian, Zhang, & Kirchhausen, 2010; Motley et al., 2006), the screening of small-molecule libraries has led to the identification of new CME inhibitors that target clathrin (von Kleist et al., 2011) and dynamin (Joshi et al., 2010; Lee et al., 2010; Macia et al., 2006). These inhibitors are membrane-permeable, can be applied directly to cells, and dramatically perturb clathrin-coated pit (CCP) dynamics in minutes; however, their action cannot be localized and is reversible only after a long washing time (1–2 h). One way to tackle this limitation would be to selectively target specific PPIs to turn CME on and off in designated cell populations or subcellular regions. Here we apply PIPPIs targeted to AP-2, the best characterized hub of the CME interactome. These inhibitors, which we call traffic light (TL) peptides, are cell-permeable photoregulators of CME that enable “stop” and “go” signals to control membrane endocytosis, thus allowing the spatiotemporal patterning of membrane receptor internalization in living cells.

3.3. **Results and discussion**

3.3.1. Peptide design summary

Our design strategy (Figure 35) was based on the structure of the BAP-long peptide bound to β-adaptin 2 (Edeling et al., 2006; Schmid et al., 2006). This peptide binds to β-adaptin 2 with an α-helical structure, in which four conserved residues of the DxxFxxFxxxR motif (red in Figure 35 and Figure 36) are aligned along the helix side facing the binding pocket. We reasoned that it should be feasible to reversibly regulate peptide biological activity by using the techniques described in previous sections to photocontrol their secondary structure (Beharry & Woolley, 2011; Kumita et al., 2000; C Renner et al., 2005; Christian Renner & Moroder, 2006) and affinity.

We tested this idea by conjugating the photoisomerizable crosslinker BSBCA (Burns et al., 2007) between pairs of cysteines introduced in the BAP-long sequence (yellow residues in Figure 36) in order to reversibly change the stability of the interactive conformation by using 380 nm and 500 nm light (wavelengths that favor the *cis* and *trans* isomers, respectively, indicated in purple and blue-

green in Figure 35). The peptides used in this study, form a design subgroup among the panel presented in the previous section. Two criteria were used for the choice of cysteine substitution sites in TL amino acid sequence. First, we applied the reported design rules to photocontrol the helix propensity of the peptide alone (Beharry & Woolley, 2011). We then considered the structure of the peptide bound to β-adaptin (Edeling et al., 2006; Schmid et al., 2006) to select sites that could drive large conformational changes of the interactive residues upon photoisomerization, while minimizing steric clash of the azobenzene crosslinker with the adaptin binding domain. The selected sequences had one of the cysteines at a fixed position, replacing the lysine K15, and the other cysteine at the11th, 7th, or 4th position to the left (sequences indicated in Figure 36 by TL-1, TL-2 and TL-4 respectively). Thus, cysteine pairs were separated by approximately three, two, or one helix turns, respectively and lay on the same side of the helix, opposite the interacting face. This set of peptide mutants was completed with TL-3, in which an additional structural constraint, α-aminoisobutyric acid, was introduced.

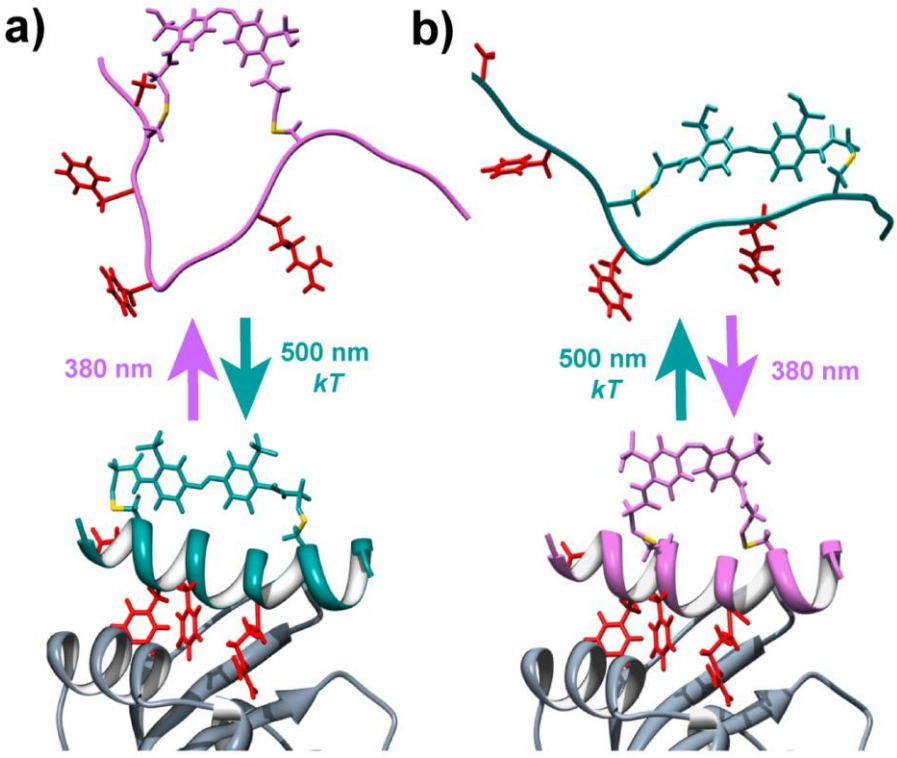

Figure 35 Representation of the AP2 β-appendage (gray) and photoswitchable peptide inhibitors displaying key interacting residues in red(modified from (Schmid et al., 2006), PDB ID 2V8): a) when the azobenzene crosslinker is conjugated at cysteine residues (yellow) at positions *i* and *i+11*, the binding would be favored in trans configuration; b) the case would be the opposite by conjugating the crosslinker at positions *i* and *i+7*.

According to the separation between the cysteine pairs of the photocontrolled peptides, we predicted that TL-1 would be able to adopt an interactive structure more easily when azobenzene was in the *trans* configuration (in the dark-adapted state or under 500 nm light), than in the *cis* configuration (under 380 nm light). Conversely, TL-2, TL-3, and TL-4 would have better interaction in the *cis* configuration than in *trans*. TL-1 could therefore be an active inhibitor under visible light and should be inactivated by UV light (Figure 35a). In contrast, TL-2, TL-3, TL-4 could behave as inhibitors under UV light and should be inactive in the dark or under visible light (Figure 35b). We synthesized the dithiol linear peptides by classical solid-phase peptide synthesis. The intramolecular crosslinking with BSBCA was performed by following reported procedures (Burns et al., 2007). All completed TL peptides were purified and their photoisomerization properties (absorption spectra and relaxation kinetics) were verified by UV/Vis spectroscopy (Figure 37).

Peptide	sequence	design	K_D µM	K_I µM (500 nm)	K_I µM (380 nm)
BAP long*	DDDIVFEDFARQRLKGMKDD	-	2.1	-	-
BAP short*	DDDIVFEDFARQR	-	NB	-	-
ARH*	LDDGLDEAFSRLAQSRTNPQ	-	4.7	-	-
TL-1	DDDCVFEDFARQRLCGMKDD	*trans*-bound	-	8 ± 1	31 ± 3
TL-2	DDDIVFECFARQRLCGMKDD	*cis*-bound	-	240 ± 150	19 ± 0.3
TL-3	DDDIVFECFAV@RLCGMKDD	*cis*-bound	-	NB	NB
TL-4	DDDIVFEDFACQRLCGMKDD	*cis*-bound	-	NB	NB

Figure 36 Sequences and binding constants of unmodified (*) peptides (Schmid et al., 2006) and designed TL peptides. In red, interaction sequence motif. In yellow, cysteine pairs introduced for crosslinking. Shadowed in grey, amino acids between crosslinking points. @ = α-aminoisobutyric acid. K_I values of TL peptides were obtained from a FP competition assay.

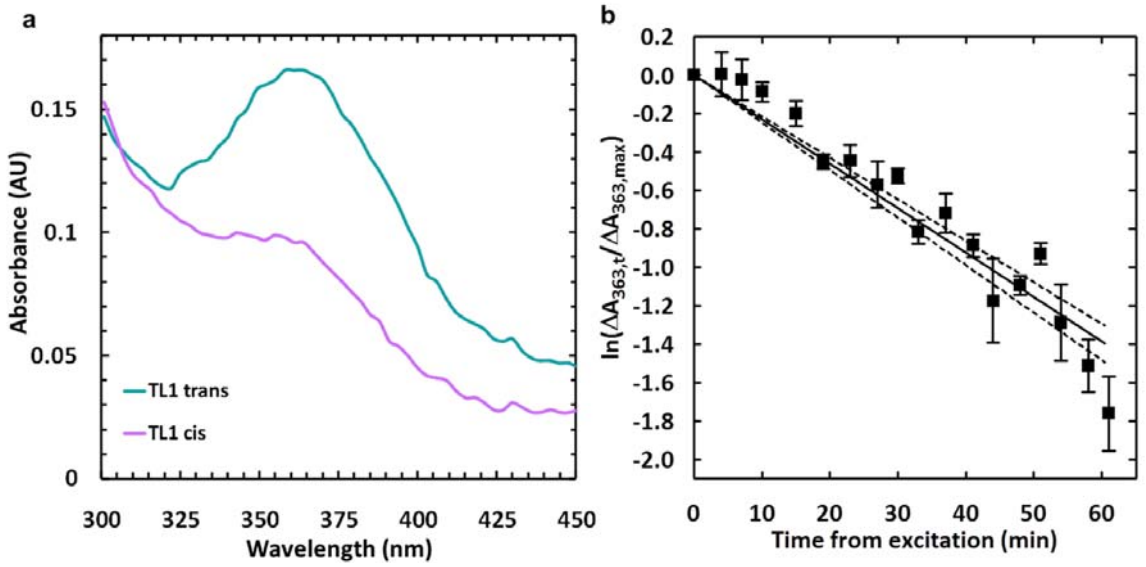

Figure 37 Thermal relaxation of TLs. a) Absorption spectra of TL-1 around the 360 nm region, corresponding to *trans*-azobenzene absorption maximum, before (*trans*) and after (*cis*) 5 min irradiation with 380nm UV light. The spectra were recorded at room temperature in full DMEM cell culture medium at a TL-1 concentration of 30 μM to match the conditions of experiments in living cells. The *trans* to *cis* transition of azobenzene is present in the crosslinked peptide. b) Thermal *cis* to *trans* relaxation of TL-1 at room temperature, followed as evolution of absorption at 363 nm, linearized and adjusted to an exponential decay model. The calculated half-life time is 30 min.

3.3.2. Photocontrolled inhibition of BAP-long/β-adaptin 2 interaction

To assess peptide capacity to bind to β-adaptin2 and light-regulated binding, we used the FP competition assay described in sections 1 and 2 (Guerrero et al., 2005; Schierling et al., 2010; Yin et al., 2005). The assay was also used it to assess reversibility of the light-regulation as detailed below. This test was validated with unlabeled BAP-long and a non-interacting sequence, BAP-short, both of which showed binding strengths comparable to reported results (Schmid et al., 2006)(Ki=5.51 μM and no binding, respectively; see Figure 38).

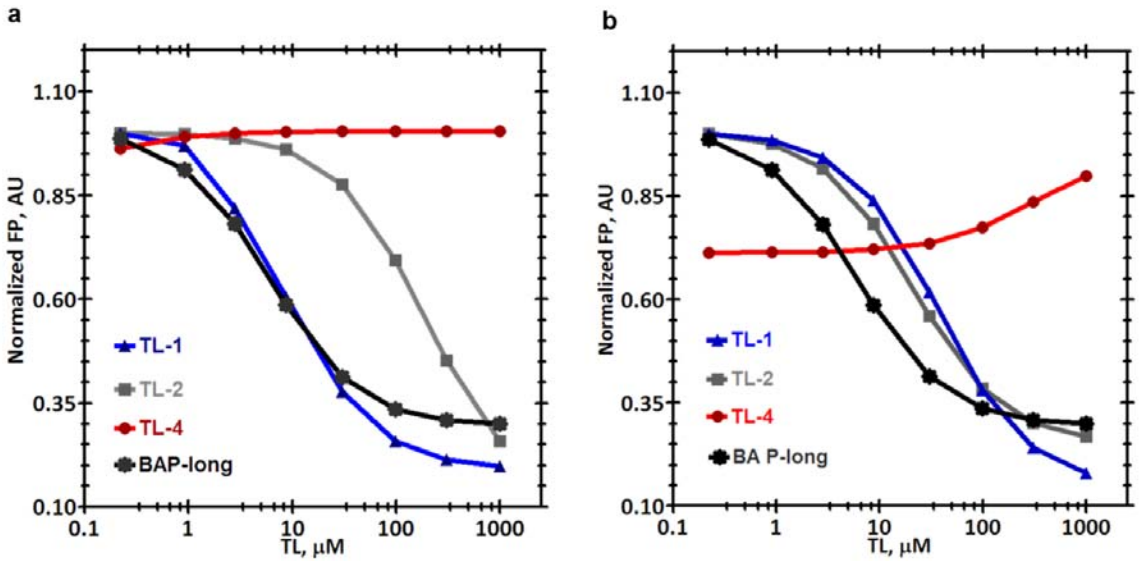

Figure 38 Comparison of titration curves of TLs with BAP-long a) in the dark-adapted state and b) under 380 nm irradiation.

TL peptides were assayed by recording FP signals both in the dark and after a 3 min exposure to 380 nm and 500 nm light. TL-1 showed satisfactory binding in the *trans* state and lost binding strength in response to 380 nm (Figure 35c,d and Figure 38). TL-2 bound weakly in *trans* and more tightly in *cis* configuration (Figure 35c,f and Figure 38). In general, the results for TL-1 and TL-2 are consistent with the scheme shown in Figure 35a,b. However, TL-3 and TL-4 did not bind β-adaptin 2 in any of the conditions assayed. We further tested the reversibility of TL-1 and TL-2 binding by measuring K_I in cycles of illumination at 380 nm and 500 nm. Switching of the wavelengths led to an almost complete recovery of the K_I values of each peptide under the same light conditions (Figure 39 and Figure 40).

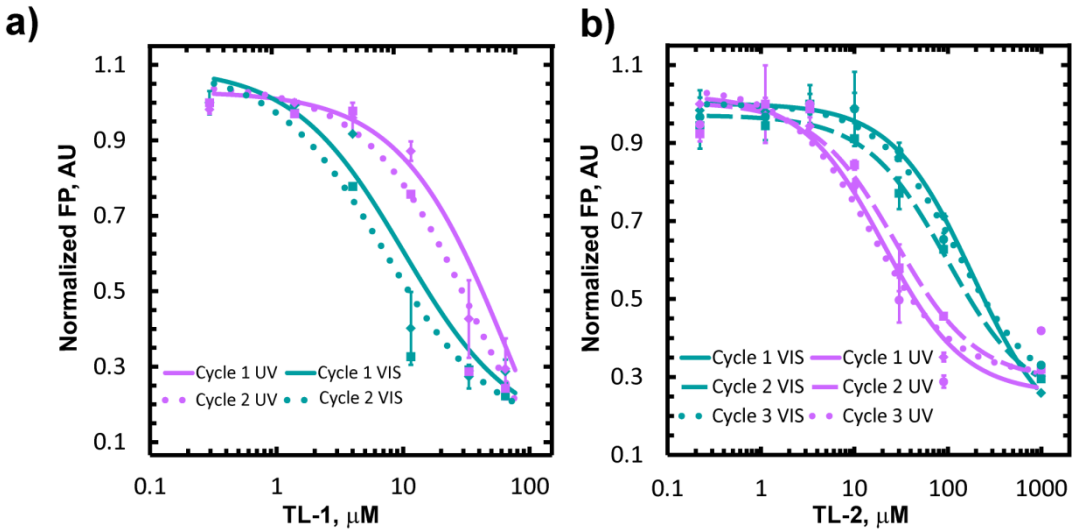

Figure 39 Reversible, light-controlled displacement of BAP-long from the binding domain of β-appendage by TL-1 (a) and TL-2 (b) over various light cycles as described in the legend.

Although azobenzene-crosslinked homologue peptides had displayed a limited photocontrol of the helical structure by itself as determined by circular dichroism, FP experiments confirmed our assumptions and allowed the identification of active PIPPIs, as well as the characterization of their optopharmacological performance in vitro. It has been proposed that TL peptides adopt an α-helical structure upon binding to the β-appendage, as shown by BAP-long (Edeling et al., 2006; Schmid et al., 2006), suggesting an “induced-fit” process (Bosshard, 2001). In this case, the crucial point of photocontrol is the ability of the crosslinker to allow or not the formation of helical structures in the presence of the target protein, rather than the amount of helicity that it can induce in the peptide alone.

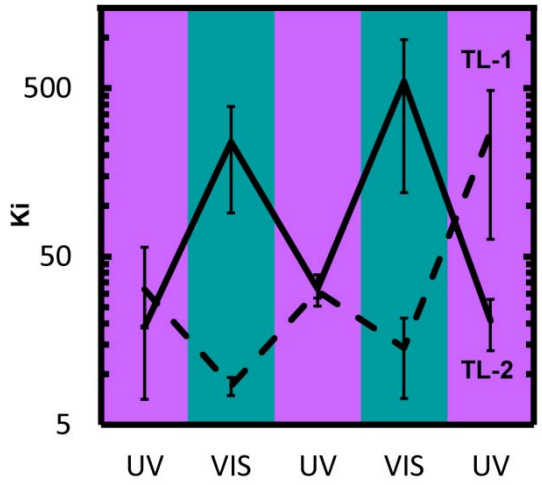

Figure 40 Reversible photocontrol of binding constants. Plot of K_I in μM obtained from FP assays during the illumination cycles performed on TL-1 (dashed line) and TL-2 (solid line). FP experiments were performed in duplicate, and error bars represent the standard deviation (S.D.).

3.3.3. Spontaneous uptake of TL peptides by cells

We tested the two TL peptides with in vitro activity against β-adaptin and opposed photocontrol (TL-1 and TL-2) in living cells. Since all the PPIs involved in CME are cytosolic, TLs must be targeted intracellularly. Cultured HEK293 cells were incubated for 30 min at 37 °C with fluorescently labeled TL-1 and TL-2. Surprisingly, the spontaneous uptake of these two peptides was observed by using flow cytometry and confocal microscopy imaging in living cells. TL-1 and TL-2 internalized in a dose-dependent manner (Figure 41a,b), the latter showing stronger cell-penetrating peptide ability (Figure 41c). Membrane permeability was enhanced by the presence of the crosslinker, but the conformation switching did not influence the uptake (Figure 41d). Confocal microscopy imaging performed in the same cell line and under the same conditions confirmed the cytometry results (Figure 41e). The permeability of the TL peptides was observed in several cell lines (Figure 41f–h) and with distinct fluorescent dyes (Figure 41h). Treatment with the TL peptides did not affect cell viability in our experimental conditions, and low cytotoxicity was observed after 24 h of exposure.

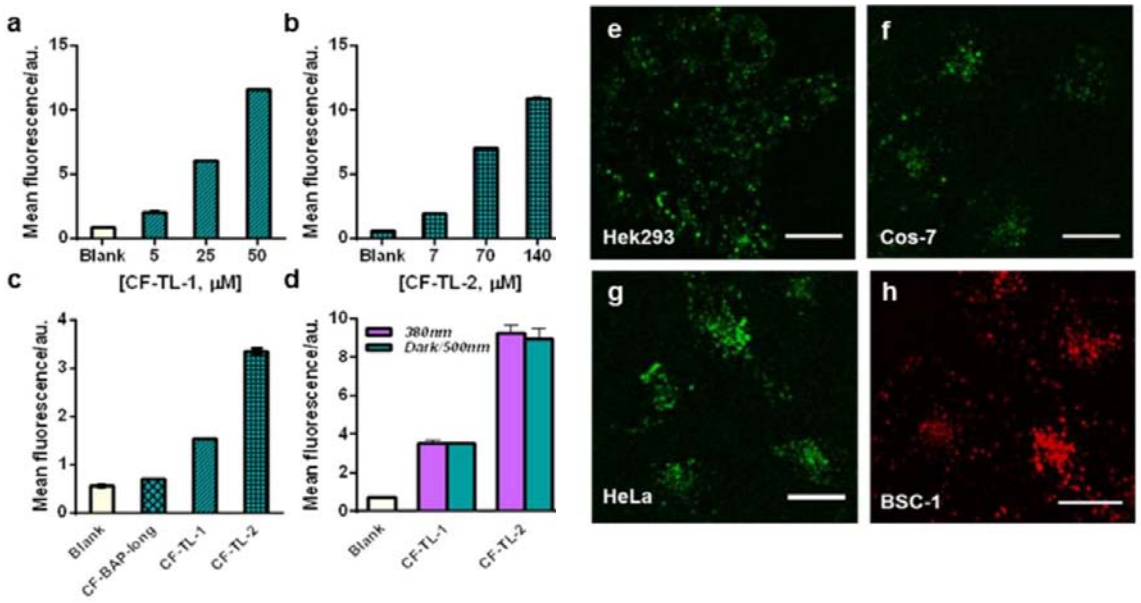

Figure 41 Dose-dependent internalization of fluorescein-labeled TL-1 (a) and TL-2 (b) quantified by flow cytometry in HEK293 cells. c) Uptake of fluorescein-labeled BAP-long and TLs compared at the same concentration (17μM). d) Uptake of TL-1 and TL-2 under dark/500 nm and 380 nm. Internalization was verified by confocal microscopy: e) living HEK293 cells incubated with carboxyfluorescein-TL-1 (80μM); f) living COS7 cells incubated with carboxyfluorescein-TL-2 (50μM); g) living HeLa cells incubated with carboxyfluorescein-TL-1 (80μM); h) living COS7 cells incubated with Rhodamine-TL-2 (30μM). All cells were incubated at 37°C for 30 min. Scale bars: 20 μm. Assays performed by Laura Nevola.

3.3.4. Photocontrolled inhibition of transferrin receptor endocytosis

Since PIPPIs are targeted intracellularly after incubation, photocontrol of endocytosis can be tested directly by using a CME assay. The transferrin receptor (TfR) is one of the best characterized cell-surface transmembrane proteins that undergo CME. TfR is constitutively expressed in many cell types and is overexpressed in cancer cells (Ponka & Lok, 1999). To evaluate the capacity of the TL peptides to inhibit CME, we used confocal microscopy to observe TfR uptake in living cells. In the absence of CME inhibitors, cells internalized fluorescent transferrin (Figure 42a). Cells that had been pre-incubated with TL-1 in the dark accumulated transferrin on the membrane, thereby indicating CME inhibition (Figure 42b). The same result was observed in a time-lapse confocal microscopy experiment.

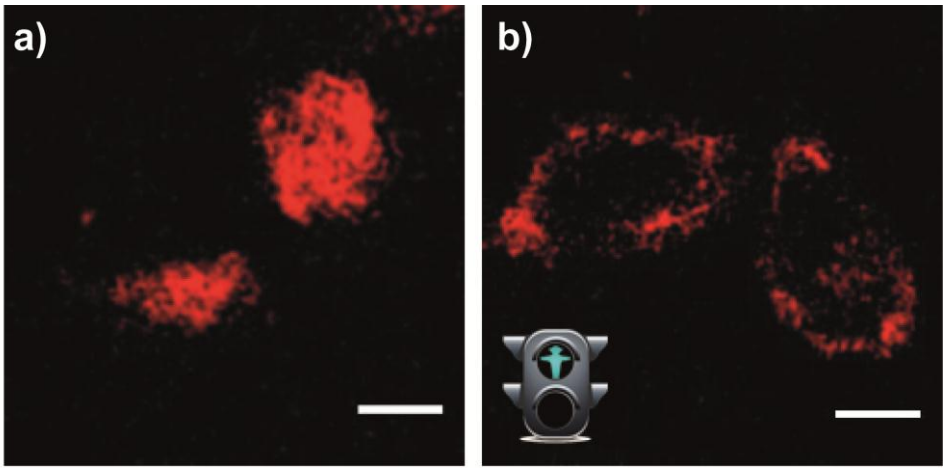

Figure 42 Transferrin uptake assay by confocal microscopy. After incubation, internalization, and final acid-wash, Alexa647–transferrin is diffused in untreated HeLa cells (a), whereas it is accumulated at the membrane of cells incubated with TL-1 in the dark (b); scale bars, 10 μm.

After having shown that TL peptides inhibit CME, we addressed whether the peptide activity could also be photocontrolled in living cells, as suggested by the in vitro results. For this purpose, we set up a cytometry-based quantitative TfR uptake assay adapting the conditions previously used in the fluorescence imaging of TfR uptake (Macia et al., 2006). By using this method, we verified that TL-1 in the dark reduces the internalization of Alexa647–transferrin in various cell lines constitutively expressing TfR (HeLa, HEK293, and MCF7, see Figure 43 and Appendix I).We compared HeLa cells incubated with TL-1 or TL-2 at 37°C, both in the dark and under 380 nm light (2 min every 15 min to revert thermal relaxation). After removing the solution containing the inhibitor, cells were exposed to Alexa647–transferrin and then analyzed by cytometry. While TL-1 in the dark inhibited TfR uptake, a reduction of TL-1 inhibitory capacity was observed under UV illumination (Figure 43). In contrast, TL-2 did not alter TfR uptake in the dark, but strongly inhibited this process after irradiation at 380 nm.

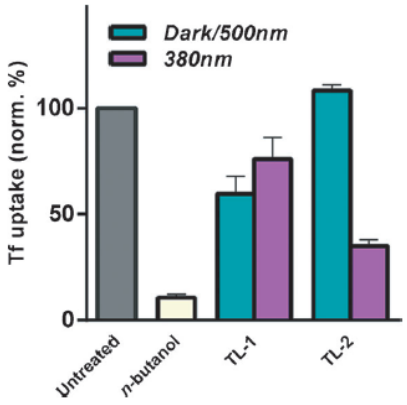

Figure 43 TL peptides inhibit CME in a light-dependent manner, as shown by flow cytometry quantification of transferrin uptake in HeLa cells after incubation with TL-1 and TL-2 under 380 nm and 500 nm light. The results correspond to the average of three independent experiments and are normalized to the fluorescence signal of untreated cells (100% uptake).

These effects confirmed what was previously shown by confocal microscopy imaging and are in agreement with the in vitro results, indicating that TL peptides allow photocontrol of the inhibition of CME in living cells. Thus, TL-1 and TL-2 can be envisaged as traffic lights that direct one pathway of cellular communication with the exterior. TL-1 slows down membrane traffic ("stop" signal) in the dark or under 500 nm light, while it slightly interferes with this process ("go" signal) under 380 nm light. In contrast, TL-2 does not alter traffic in the dark or at 500 nm (go), and strongly reduces membrane internalization at 380 nm (stop).

3.3.5. Effects of TLs on clathrin-coated pit dynamics

To further characterize the inhibition of CME by TL peptides in living cells, we monitored the dynamics of CCPs at high resolution by using total internal reflection fluorescence microscopy (TIRFM) (Ehrlich et al., 2004; Merrifield, Feldman, Wan, & Almers, 2002). Individual HeLa cells transfected with a plasmid encoding clathrin light chain fused with mRFP and displaying a homogeneous footprint were observed at 37 °C for 15 min and compared to cells preincubated with TL-1 for 30 min in the dark. Changes in the morphology and dynamics of the CCPs are shown in Figure 44. Quantification by image analysis yielded a larger average size of CCPs in the presence of TL-1 (Figure 45).

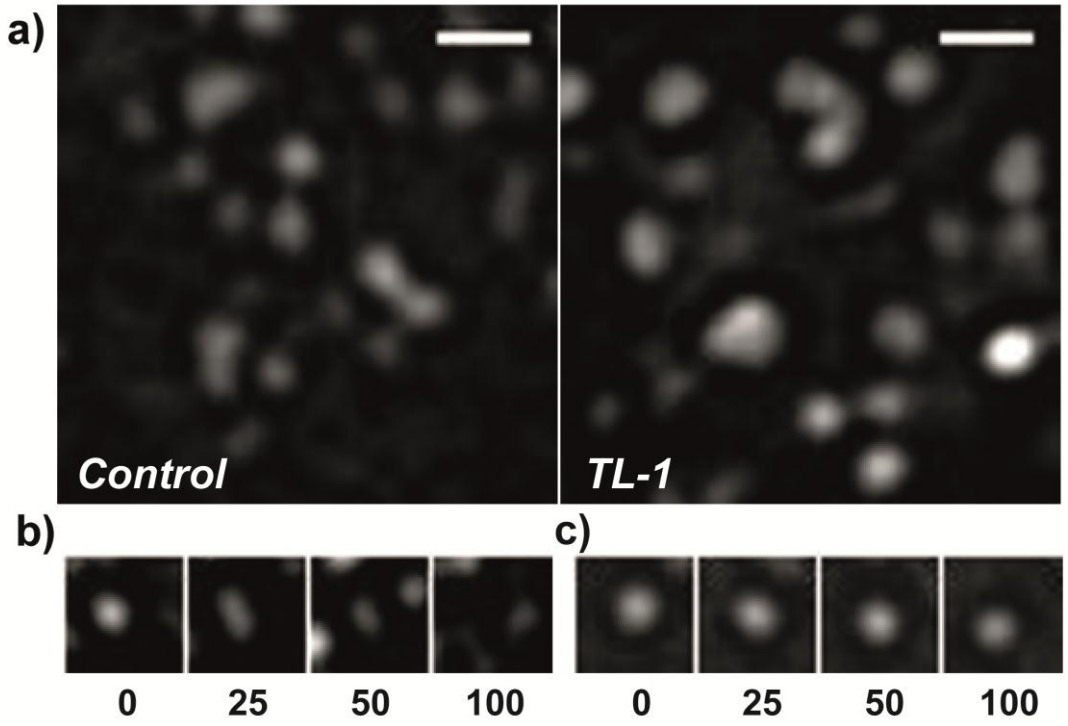

Figure 44 Magnified TIRFM images at 37°C of living HeLa cells transfected with a plasmid encoding clathrin light chain fused with monomeric red fluorescent protein (LCa–mRFP). The cells shown are untreated (left) and incubated for 30 min with TL-1 in the dark (right). Scale bar, 1 μm. Time-lapse TIRFM sequences of these regions are presented for untreated cells (d) and after incubation with TL-1 (e). The time in seconds is indicated under each frame. Micrograph by Laura Nevola.

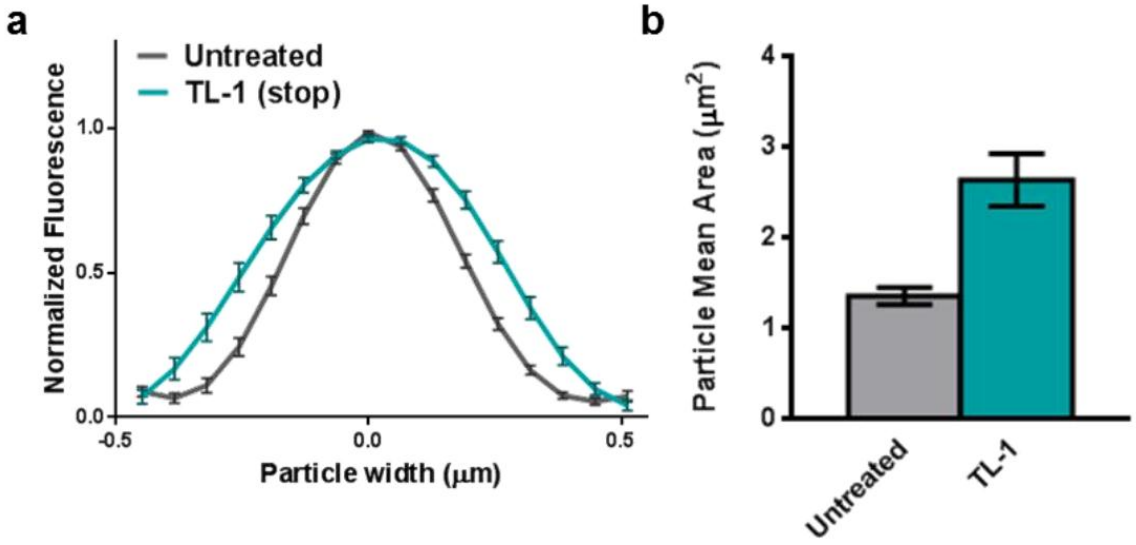

Figure 45 The size of CCPs is altered by TL-1. a) Averaged plot profile of single CCPs of untreated cells (gray) and of cells treated with dark-adapted TL-1 (teal). b) Averaged mean area in TIRFM images of particles observed in untreated cells (gray) and in cells treated with dark-adapted-TL-1 (teal). Error bars are S.E.M. N = 30 particles analyzed.

To visualize how TL peptides switch CME on and off in living cells, we monitored CCP dynamics by TIRFM in the presence of TL-1 or TL-2, during illumination at 380 nm or 500 nm for 2.5 min. By using a customized particle tracking software (see below) we studied how the number of detected CCPs, their average speed and lifetime distribution changed with the illumination conditions (dark, 380 nm, and 500 nm). In the case of cells treated with TL-1, exposure to 380 nm released the inhibited CME, and individual cells showed an increase in the number of CCPs (Figure 46a). This increment was accompanied by an increase in their average speed (Figure 47) and a decrease in their lifetime, measured over three cells (Figure 48). Illumination at 500 nm partially reversed these effects (Figure 46b, Figure 47 and Figure 48). Correspondingly, TL-2 released CME from inhibition at 500 nm, which increased the number of events detected (Figure 46c), increased their speed (Figure 49), and decreased their lifetime (Figure 50). These effects were partially reversed at 380 nm (Figure 46d, Figure 49and Figure 50). It should be noted that in untreated cells the distribution of speed averages of the tracks detected was consistent with reported results (Merrifield et al., 2002) while in the presence of TL peptides it changed significantly depending on light: CCPs globally slowed down during inhibition conditions (stop signals), and the regular rates were almost completely recovered upon release of the inhibition (go signals). Changes in the lifetime distribution with illumination were less pronounced but in complete agreement with the photocontrol of CME inhibition induced by TL-1 and TL-2.

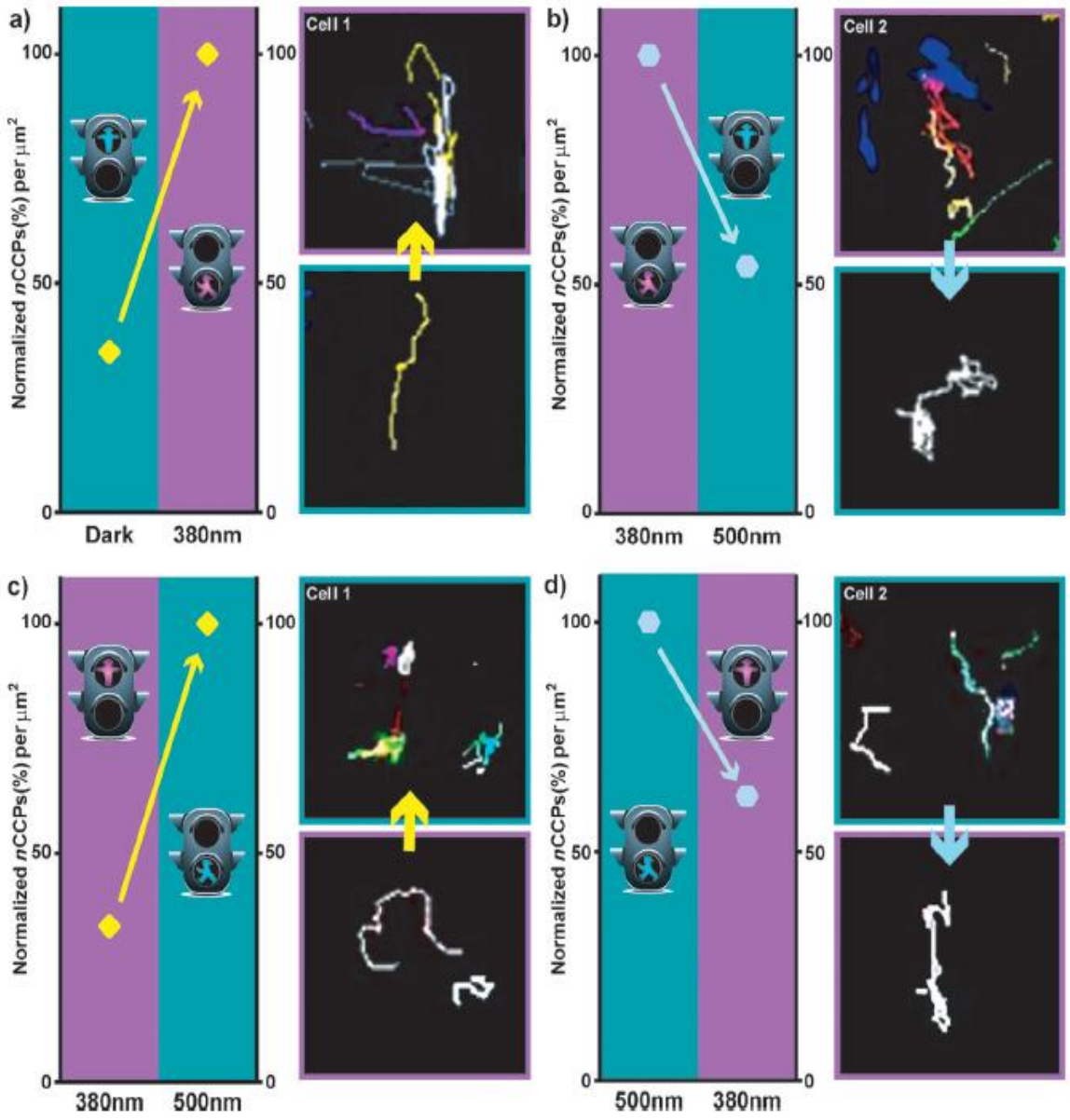

Figure 46 TL peptides provide stop and go signals to CME. Processed TIRFM of clathrin dynamics. Plots show the number of CCP events per square micron on the cell membrane surface. For each data point under visible and UV light, representative CCP tracks detected with a particle-tracking software are presented in the magnified cell images with lines of different colors. a) Using TL-1, the go signal is given by 380 nm light, which increases the number of CCPs per square micron. b) CCP events are reduced with the stop signal (500 nm). c) Using TL-2, the go signal (500 nm light) produces an increase in the number of CCP events and d) the stop signal (380 nm) correspondingly reduces them. The results are representative of three independent experiments.

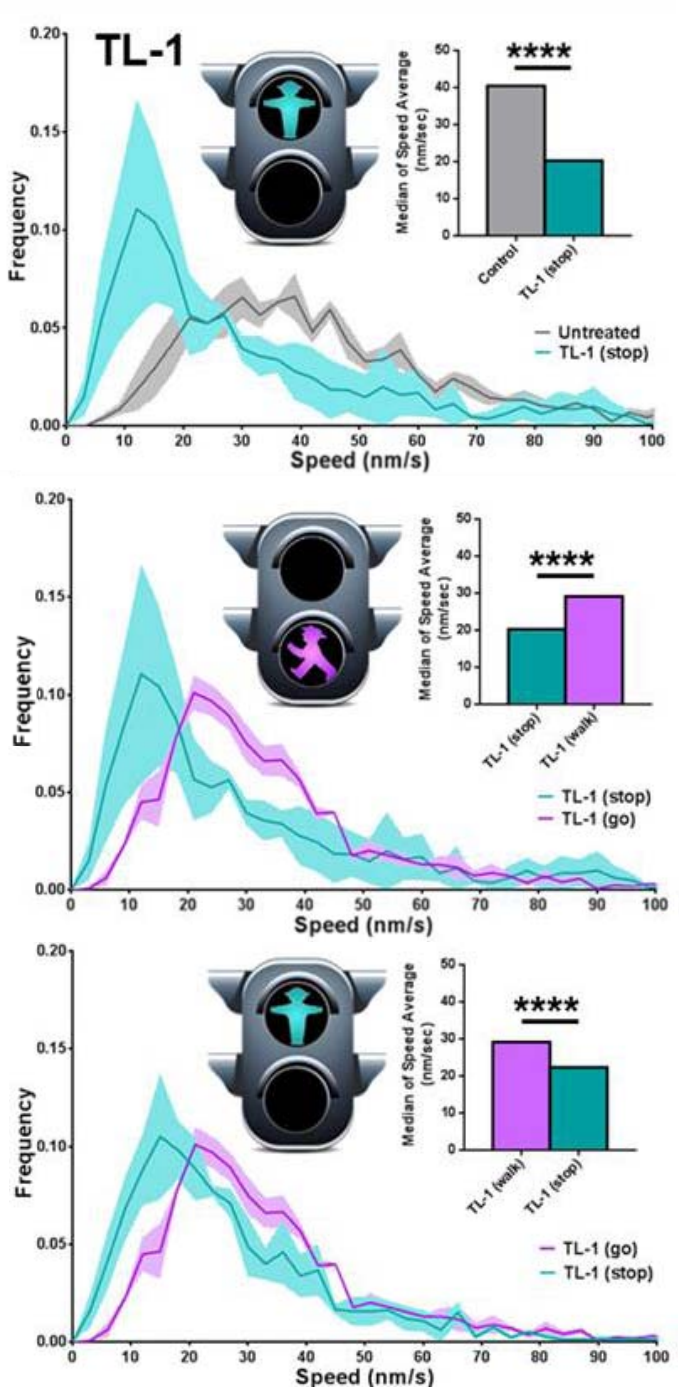

Figure 47 Effect of TL-1 on CCP lateral movement speed. Average speed distributions of detected tracks. From top to bottom: untreated HeLa cells vs. HeLa cells treated with dark-adapted TL-1; HeLa cells treated with dark-adapted TL-1 vs. HeLa cells treated with TL-1 irradiated at 380nm; HeLa cells treated with TL-1 irradiated at 380nm vs. HeLa cells treated with TL-1 irradiated at 380nm and then at 500nm. Data represent the distribution of events of 3 cells; bars represent the median of the individual speed average. The Mann-Whitney U-test evaluates the difference between distributions as statistically different (****p<0.0001).

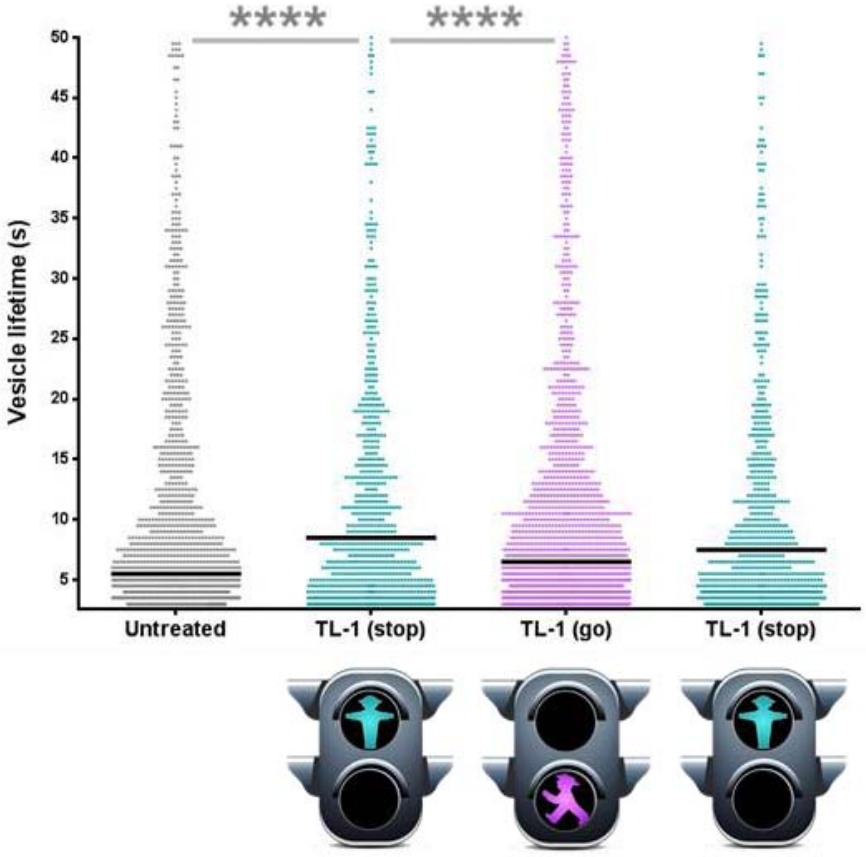

Figure 48 Effect of TL-1 on CCP lifetime. Scatter plot of detected CCP track lifetimes in HeLa cells (from left to right: untreated, treated with dark-adapted TL-1, treated with 380 nm-irradiated TL-1, treated with TL-1 after irradiation at 380 nm and then at 500 nm). Data represent all detected particles in 3 cells with lifetime>3 s. Bars represent the distribution median (****p<0.0001).

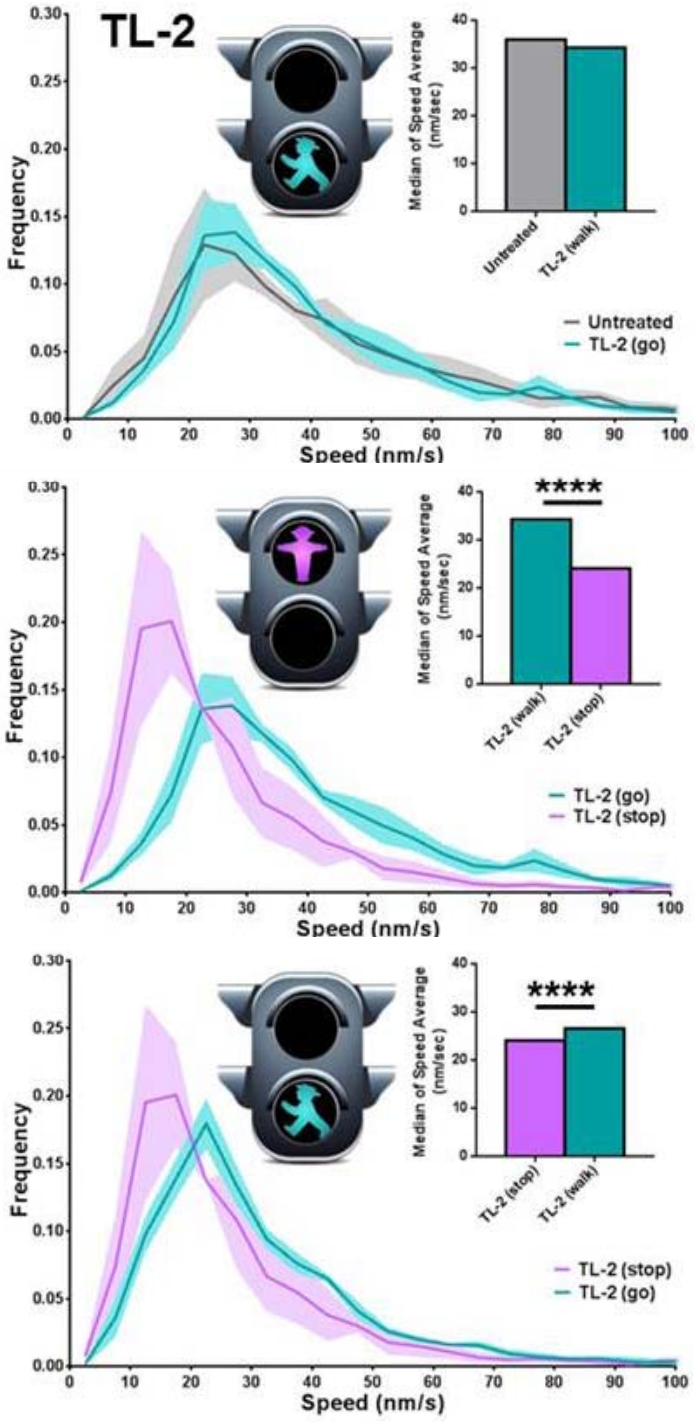

Figure 49 Effect of TL-2 on CCP lateral movement speed. Average speed distributions of detected tracks. From top to bottom untreated HeLa cells vs. HeLa cells treated with dark-adapted TL-2; HeLa cells treated with dark-adapted TL-2 vs. HeLa cells treated with TL-2 irradiated at 380nm; HeLa cells treated with TL-2 irradiated at 380nm vs. HeLa cells treated with TL-2 irradiated at 380nm and then at 500nm. Data represent the distribution of events of 3 cells; bars represent the median of the individual speed average. The Mann-Whitney U-test evaluates the difference between distributions as statistically different (****p<0.0001).

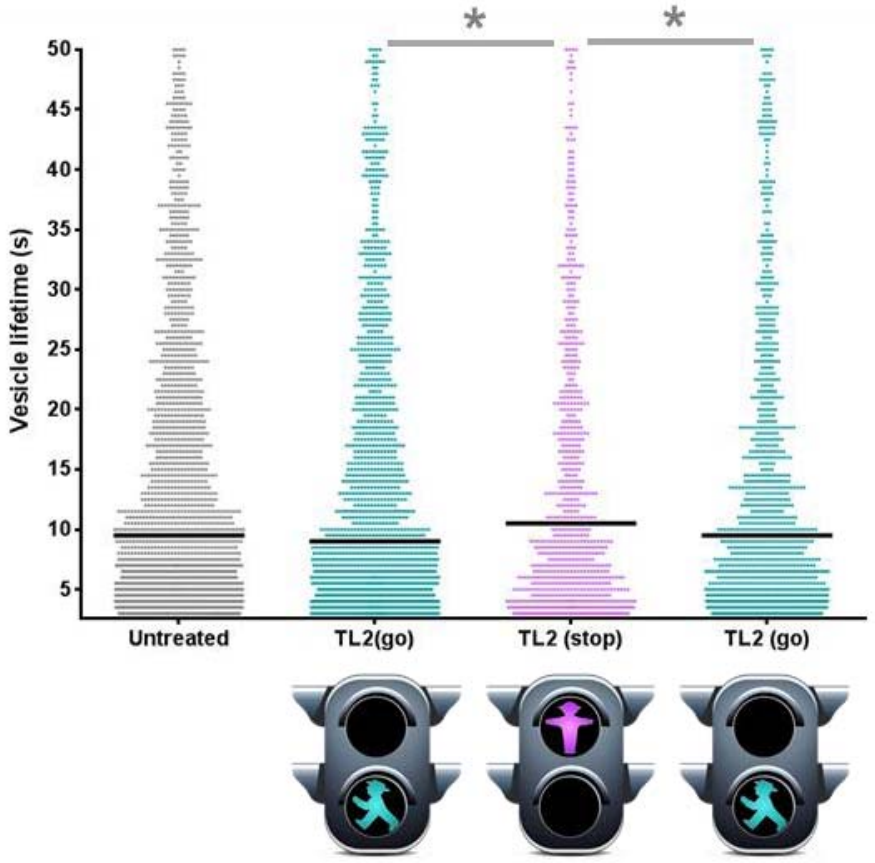

Figure 50 Effect of TL-2 on CCP lifetime. Scatter plot of detected CCP track lifetimes in HeLa cells (from left to right: untreated, treated with dark-adapted TL-2, treated with 380 nm-irradiated TL-2, treated with TL-2 after irradiation at 380 nm and then at 500 nm). Data represent all detected particles in 3 cells with lifetime > 3 s. Bars represent the distribution median (*p<0.02).

Image processing and data analysis

Detection of CCPs (i.e. discrete round structures of 0.3-0.8 µm width, with x/y and z mobility) and quantification of their parameters (average speed, lifetimes and number of events) was performed on TIRFM images with a section area of 100 μm^2. Images were processed using the ImageJ software (Ferreira & Rasband, 2012; Schindelin et al., 2012). To enhance the spots and reduce the background, level the movies were preprocessed by a 2D Laplacian filter (radius around half the typical radius of the vesicles), followed by a pass of rolling ball algorithm (morphological top-hat opening). Detection and tracking of the spots was done with the help of the "Particle tracker" ImageJ plugin implementing the algorithm described by (Sbalzarini & Koumoutsakos, 2005). This plugin is well adapted to track Gaussian spots of up to a few pixels in radius in intermediate signal-to-noise (SNR) conditions and for reasonably good temporal resolution. For each

class of image quality, the parameters of the algorithm were tweaked to ensure the best apparent tracking results: rejection of spurious detections, single hit for most apparent spots and robust track linking. The results were consistently satisfactory at the observed spot density and were cross-checked against a manual tracking performed on sample populations with the help of the MTrackJ ImageJ plugin (Meijering, Dzyubachyk, & Smal, 2012), which allows flexible recording of the tracks and straightforward extraction of the statistics under study. An ImageJ macro was written to automate the pre-filtering and the extraction of the statistics of interest from the results of the automatic tracking. These statistics include particle lifetime and their average speed over the candidate tracks, that is the tracks with a duration over a minimum threshold of 3 sec (6 frames), since shorter events were considered transient structures. The basic moments of the statistical distributions derived from the manual and automatic tracking were compared for each condition. The difference was found not to be relevant and in all cases negligible with respect to the differences observed between each condition, as shown in Figure 51 and Figure 52.

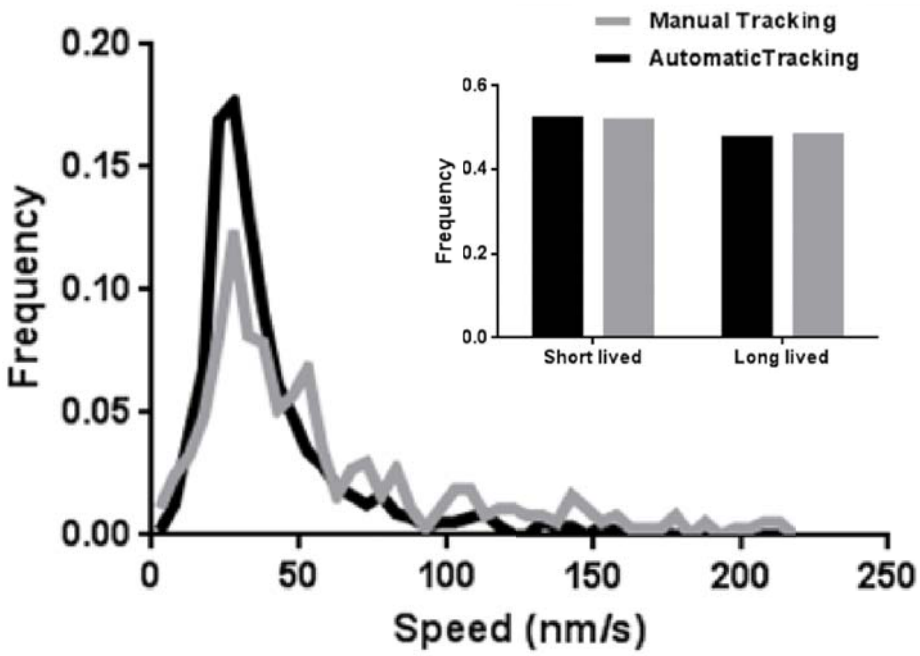

Figure 51 Comparison of manual and automated CCP tracking. Distribution of average speeds of detected CCPs. Despite higher noise in the manual tracking, due to a smaller amount of tracked CCPs, the distributions show the same result. The inset shows the almost identical proportion of short- and long-lived CCPs (<20 s and >20s respectively) found by both methods. The Mann-Whitney-Wilcoxon *U*-test evaluates the two distributions as not different with $p<0.02$.

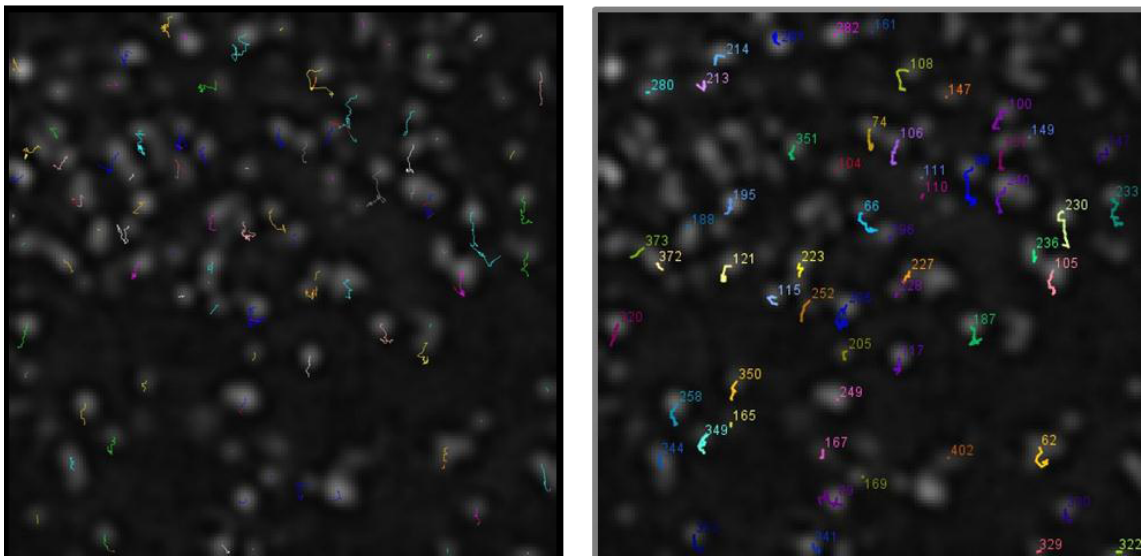

Figure 52 Comparison of manually and automatically found CCP tracks. Overlay of a time course TIRFM experiment with the detected tracks (in color). Tracks found by automated software (left) and by manual tracking (right) for the same image. Tracks correspond to the comparison of populations shown above and are largely similar between both methods even in the individual comparison.

The Mann-Whitney-Wilcoxon *U*-test was used to assess whether the variables followed by the particle tracking algorithm were affected in a different manner by TL-1 and TL-2 under 500 nm than under 380 nm. This test is based only on the rank of the data groups (i.e. a non-parametric test) and assesses whether one of two data groups tends to have larger values than the other, providing as a result the probability of one of the groups stochastically showing larger values (the p-value obtained).

3.4. **Conclusion**

Here we report two cell-permeable molecules, TL-1 and TL-2, which are able to disrupt a key PPI for CME in a photocontrolled manner. The evaluation of the strength of CME inhibition and of the capacity to turn this process on and off with light in living cells renders the TL peptides light-responding traffic regulators that allow CME control in spatiotemporally defined patterns. This chemical discovery, applied to a biological process of great interest such as endocytosis, is expected to have a significant impact in the scientific community devoted to cell biology. In addition the TL peptides provide an example of a direct optopharmacological strategy to manipulate the assembly and activity of endogenous protein complexes, without requiring chemical or genetic modification of the target, and can be extended to further applications for the inhibition of other protein–protein interactions.

4. General conclusions

The main conclusions drawn from this work are:

- It is possible to use azobenzene-crosslinked peptides with sequences from the interface of a PPI as photoswitchable inhibitors of that PPI.
- The structural photoswitching of azobenzene can be applied to photocontrol the affinity and biological activity of peptides without a strongly defined secondary structure.
- Azobenzene photoswitchable peptide inhibitors of the β-arrestin/β-adaptin 2 PPI perform better when they have higher conformational freedom. This can be extended to the photocontrolled inhibition of PPIs characterized by conformational adaptation between flexible surfaces.
- The natural sequence of a peptide from an interaction surface can bear a number of modifications in addition to the introduction of cysteines for side chain azobenzene crosslinking without losing its ability to interact with the target and function as an inhibitor, as long as the residues forming the interaction hotspot are conserved and free to reach the relative positions they occupy in the original interaction.
- In interactions mediated by a single side of a helical molecule, the residues on that side conform an interaction surface and have to be preserved while the residues on the opposite side, or actuation surface, are the ideal place for modifications (such as crosslinking and mutation of amino acids to enhance photoswitching).
- For peptides active in the photostationary state, molecular design should be applied to promote high differences in affinity between the active and inactive state.
- For peptides active in the dark, molecular design should be applied to promote the highest possible content of inactive peptide in the photostationary state.

- Non-proteinogenic amino acids as α-aminoisobutyric acid and naphtylalanine can be introduced in inhibitor peptides to enhance the photoswitching of their affinity, but their effect depends on the position and the particular interaction. Their use requires as much information on the molecular details of the target interaction as available.
- Intramolecular azobenzene crosslinking is a form of peptide stapling that promotes the cell-penetrating peptide behavior of the crosslinked peptide, enabling application in living cells.
- Disruption of the β-arrestin/β-adaptin 2 PPI with TL peptides in living cells produces an inhibition of clathrin-mediated endocytosis that can be reversibly photocontrolled with cellular and potentially subcellular resolution.
- TL peptides affect the size and dynamics of clathrin-containing supramolecular ensembles characterized as CCPs, probably acting on the AP-2 complex.
- TL peptides, when activated, induce the accumulation of stalled endocytic machinery, as shown by the formation of bigger and slower clathrin-containing structures.
- Photoswitchable peptides enable the photocontrol of cellular activities with high spatiotemporal resolution, with the specificity of biomolecular interactions and without the need for chemical or genetic modification of the target system.
- The potential optopharmacological use of structurally photoswitchable, azobenzene crosslinked peptides has been demonstrated for the first time and it should be possible to apply it to many other biological systems.

5. Resumen en castellano

5.1. Introducción

Las interacciones proteína-proteína (Arkin & Wells, 2004) son procesos fundamentales para la mayoría de las funciones biológicas. Su estudio mediante técnicas bioquímicas, biofísicas y bioinformáticas ha dado lugar a los campos de la proteómica y la interactómica, así como a la identificación importantes dianas farmacológicas (Mullard, 2012). Para trazar mapas de los interactomas se han empleado con frecuencia técnicas de los doble híbrido, que permite identificar interacciones binarias de una en una. Sin embargo, los estudios masivos con estas técnicas incluyen falsos positivos en la forma de interacciones entre proteínas que no se expresan en el mismo lugar o momento y por tanto no tienen lugar en la función biológica normal. Además, los resultados deben ser complementados con purificación por afinidad seguida de análisis por espectrometría de masas de los complejos proteicos encontrados.

Para validar y caracterizar interacciones funcionales individuales in vivo se necesitan nuevos métodos de manipulación molecular que actúen en los niveles celular y subcelular con selectividad farmacológica y también espacio-temporal, permitiendo considerar la polarización y compartimentación de las interacciones entre proteínas dentro de las células. La luz resulta particularmente útil para ello, ya que puede enfocarse con gran resolución y su aplicación puede controlarse en periodos de tiempo muy cortos mediantes sistemas electrónicos. La luz por sí misma es relativamente poco invasiva cuando se la compara con otros medios para obtener acceso al interior de las células, como la electrofisiología, la transfección, la microinyección o la disrupción celular directa.

Disponer de inhibidores de la interacción entre proteínas controlados ópticamente, es decir, fotoconmutables, permitiría manipular mediante luz las interacciones entre proteínas con la selectividad farmacológica de un inhibidor y el control y resolución espacio-temporal de una herramienta óptica. De este modo, sería posible establecer patrones temporales de inhibición de interacciones específicas en las localizaciones subcelulares de interés para los estudios funcionales. Este tipo de herramientas sería apropiado para la

investigación y validación de los mecanismos moleculares que dan lugar a las funciones que los métodos convencionales de la biología molecular asignan a las interacciones . También abrirían la puerta a estudios funcionales de las redes y vías de interacciones moleculares con alta resolución temporal y espacial.

Fotoconmutadores químicos

Desde finales del siglo XIX se conocen moléculas que experimentan transformaciones reversibles entre dos estados en función de la longitud de onda de la luz que reciben, conocidas como fotoconmutadores. Cada estado tiene una cierta banda de absorción de luz que promueve la conversión al otro estado. Así, bajo unas condiciones dadas de iluminación, un fotoconmutador alcanzará un equilibrio en las conversiones con proporción constante de ambos estados, denominado estado fotoestacionario. Además, con frecuencia uno de los dos estados es más estable, de forma que en ausencia de iluminación la composición evolucionará hacia un 100% de ese estado, lo que se conoce como relajación térmica del fotoconmutador. Para aplicar la fotoconmutación a moléculas biológicas es necesario disponer de fotoconmutadores que sean compatibles con las condiciones en que se desarrolla la vida y que además de los cambios en su espectro de absorción experimenten al interconvertirse entre estados cambios fisicoquímicos que puedan afectar a las propiedades de las biomoléculas que determinan su función. En otras palabras, se necesitan fotoconmutadores que incorporen un mecanismo de transducción de su fotoconmutación a las moléculas biológicas que se desea fotocontrolar.

Tres tipos de moléculas destacan por haberse aplicado como fotoconmutadores en contextos biológicos: los azobencenos, los diariletenos y los espiropiranos. Entre ellos los azobencenos son los más extensamente utilizados. Se trata de moléculas con un núcleo común consistente en un doble enlace N=N que une dos anillos bencénicos, cuyas substituciones en diferentes posiciones dan lugar a una amplia y creciente familia de moléculas con diferentes propiedades entre las se puede seleccionar la más adecuada para la aplicación deseada. El doble enlace N=N isomeriza entre cis y trans en función de la iluminación, dando lugar a importantes diferencias en distancia entre los extremos y en momento dipolar entre los isómeros de la molécula que se han explotado como mecanismo de transducción. El isómero trans suele ser el más estable y la forma relajada del azobenceno. Bajo luz intensa de 360-380 nm el azobenceno sin sustituyentes alcanza un estado fotoestacionario con más de 90% de cis-azobenceno. Es

importante tener en cuenta en aplicaciones biológicas el efecto que el trans-azobenceno restante pueda tener en el sistema estudiado.

El azobenceno es un bloque químico muy versátil. Agentes entrecruzantes derivados de azobenceno simples e hidrosoluble se pueden preparar en poco tiempo en cualquier laboratorio convencional de química orgánica y la mayoría de laboratorios de bioquímica (Burns et al., 2007). Propiedades como el espectro de absorción , la estabilidad del isómero cis, la eficacia de la fotoconmutación con iluminación de dos fotones, la longitud, la rigidez estructural o la reactividad química se pueden ajustar mediante diseño racional, principalmente a través de la introducción de sustituciones en los anillos bencénicos.

Las aplicaciones relacionadas con la biología de los azobencenos suelen explotar sus cambios en geometría. Con ellos se han desarrollado ligandos fotocrómicos análogos de neurotransmisores, ligandos fotoconmutables "atados" (tethered) a sus receptores de membrana con una cadena que contiene azobenceno, o ácidos nucléicos, proteínas, péptidos y peptidomiméticos de conformación fotoconmutable. Cuando se aplica a péptidos y proteínas, la estrategia de uso más frecuente del azobenceno es acoplarlo como un puente intramolecular a cadenas laterales de aminoácidos (Flint et al., 2002). En péptidos también puede introducirse en la molécula como un bloque de construcción en un proceso de síntesis en fase sólida (Hoppmann et al., 2011; C Renner et al., 2005) y en proteínas puede introducirse como cadena lateral de un aminoácido sintético y expresar la proteína modificada en células mediante técnicas de supresión de codones stop (Bose et al., 2006; Hoppmann et al., 2014). Merece la pena tener en cuenta que tanto el acoplamiento dirigido de azobenceno o ligandos "atados" a posiciones específicas en una proteína como la introducción de azobenceno por supresión de codones stop requieren la manipulación genética del sistema vivo a estudiar.

Péptidos como inhibidores de interacción proteína-proteína

Ante la dificultad de tratar algunas dianas con fármacos convencionales, las interacciones proteína-proteína han visto aumentado su interés como diana terapéutica y como fuente de ligandos capaces de perturbarlas. Del estudio de las interacciones proteicas se han derivado metodologías sistemáticas de desarrollo de ligandos orientadas a interacciones mediadas por hélices α, y hojas β que han resultado en el descubrimiento de peptidomiméticos inhibidores de la

interacción que imitan esas estructuras (Becerril & Hamilton, 2007; Edwards & Wilson, 2011; Robinson, 2008). También se han empleado como fármacos moléculas propiamente peptídicas, incluso derivadas directamente de las secuencias de las proteínas que interaccionan. Dado que muchas interacciones de interés ocurren en el citoplasma celular, la administración puede ser un problema para la inhibición de interacciones. La aplicación de péptidos con la habilidad de cruzar membranas celulares como lanzaderas fusionando su secuencia a la secuencia inhibidora puede superar ese obstáculo (Bechara & Sagan, 2013; Svensen et al., 2012). En algunos casos la propia secuencia inhibidora puede ser a la vez un péptido capaz de cruzar membranas biológicas, como en el caso de los péptidos helicoidales estabilizados mediante entrecruzamiento de cadenas laterales, o péptidos "grapados", capaces de inhibir interacciones proteína-proteína intracelulares relacionadas con el cáncer (Grossmann et al., 2012; Moellering et al., 2009; Verdine & Hilinski, 2012; Walensky et al., 2004).

Péptidos inhibidores fotoconmutables

Las posibilidades de usar secuencias derivadas de las regiones de interacción de complejos diana se pueden combinar con la introducción de restricciones conformacionales fotocontroladas en biomoléculas mediante acoplamiento de fotoconmutadores para llegar a obtener inhibidores competitivos fotoconmutables. Un paso intermedio en esta estrategia es el establecimiento de metodologías generales para lograr la fotoconmutación de la estructura de biomoléculas. Los motivos de plegamiento conocidos como las estructuras secundarias y los folds son el terreno natural para el desarrollo de esas metodologías. El grupo de G.A. Woolley ha dedicado muchas publicaciones al fotocontrol de péptidos con conformación de hélice α mediante acoplamiento de puentes de azobenceno entre dos de sus cadenas laterales. Además de estudiar el control óptico de la helicidad en péptidos modelo, ese grupo ha desarrollado variantes de agentes entrecruzantes de azobenceno con diferentes propiedades, como longitudes de onda de fotoconmutación más largas (Chi et al., 2006; Sadovski et al., 2009; Samanta et al., 2013) o longitudes mayores del puente de azobenceno (Fuzhong Zhang et al., 2008). También ha aplicado estas moléculas y principios en sistemas biológicos in vitro. Estas investigaciones proporcionan un conjunto de herramientas de diseño que ha contribuido a la popularidad del entrecruzamiento de péptidos helicoidales con azobenceno como fotoconmutador para el control

óptico de la estructura. Los estudios donde el fotocontrol estructural se traduce en fotocontrol de la afinidad por una diana son menos numerosos. Destacan el trabajo de Allemann y colaboradores, que aplicaron azobenceno a péptidos del dominio BH3 y demostraron in vitro que tanto su helicidad como su afinidad por la diana Bcl-XL eran diferentes antes y después de irradiarlos con luz, aunque no demostraron reversibilidad térmica ni controlada por iluminación de esta fotodependencia (Kneissl et al., 2008). el grupo de Renner logró fotocontrolar el ensamblaje de triples hélices de colágeno, en este caso sin mostrar efectos funcionales fotodependientes en un sistema vivo (Kusebauch et al., 2007). Estos estudios son ejemplos de fotocontrol de estructuras moleculares de orden mayor, pero no alcanzan el objetivo del fotocontrol funcional a través de la estructura. Por otro lado, un trabajo reciente del grupo de Woolley demuestra el fotocontrol estructural de péptidos fluorescentes entrecruzados con azobenceno y microinyectados en embriones de pez cebra (Samanta et al., 2013). Aunque demuestra que el fotocontrol de péptidos sintéticos con azobenceno es realizable in vivo , no pone ninguna función biomolecular bajo control óptico. Los trabajos presentados en esta tesis demuestran el fotocontrol funcional mediante péptidos con azobenceno en células y la habilidad de estos péptidos para cruzar la membrana celular. Junto con el reciente desarrollo de una metodología de presentación en fagos para la obtención de péptidos fotoconmutables con azobenceno, estos estudios abren la puerta a la aplicación de la tecnología de péptidos entrecruzados con azobenceno a virtualmente cualquier interacción objetivo.

Endocitosis mediada por clatrina y el péptido BAP-long

El sistema utilizado para desarrollar esta tesis es la interacción entre las proteínas β-arrestina y β-adaptina 2. Esta interacción es uno de los mecanismos moleculares implicados en la endocitosis mediada por clatrina de los receptores de membrana acoplados a proteína G (GPCRs). Estos receptores ponen en marcha cascadas de señalización intracelular cuando sus ligandos específicos se unen en su porción extracelular. Existen mecanismos de desensibilización de la respuesta de los GPCRs ante exposición prolongada a sus ligandos que evitan respuestas exacerbadas o demasiado extendidas en el tiempo. Uno de ellos es la internalización del receptor mediante endocitosis dependiente de clatrina, que retira los receptores activados de la membrana, impidiendo que respondan al ligando. La proteína β-arrestina media esta función uniéndose a la

porción intracelular de los GPCRs activados. Esta unión provoca la disociación de la proteína G asociada al receptor, que lo inhabilita para responder de nuevo al ligando (Johnson, 2006; R. J. Lefkowitz & Whalen, 2004). Además, la unión induce un cambio conformacional en la β-arrestina, que expone su región C-terminal . Esta región es capaz de unirse a los complejos proteicos que capturan proteínas de membrana y las concentran en las zonas de la membrana donde se produce endocitosis, los adaptadores asociados a clatrina (CLASPs). En concreto, la región C-terminal de β-arrestina se une al apéndice β del complejo adaptador canónico de la endocitosis mediada por clatrina, AP-2 (Edeling et al., 2006; Schmid et al., 2006). Este apéndice está constituido por la proteína β-adaptina 2. Así, la disrupción de la interacción β-arrestina /β-adaptina 2 debería inhibir la endocitosis de GPCRs activados y potencialmente afectar la endocitosis mediada por clatrina al ocupar sitios de interacción en su adaptador canónico, que media la endocitosis de otras proteínas de membrana además de los GPCRs. La interacción β-arrestina /β-adaptina 2 se produce entre una secuencia continua de 20 aminoácidos de la β-arrestina (DDDIVFEDFARQRLKGMKDD, denominada BAP-long) y un sitio de unión de la β-adaptina 2. BAP-long adopta estructura helicoidal cuando se une a β-adaptina 2 y se mantiene desestructurada cuando está libre en solución. Esta moderada tendencia a formar hélices facilitada por la interacción hace de BAP-long un buen candidato para el fotocontrol estructural y potencialmente para el de la afinidad y la función de la interacción.

Objetivos de la tesis

A partir de la literatura revisada, la hipótesis principal de este trabajo es que es posible poner bajo control óptico las actividades celulares mediadas por interacciones proteína-proteína mediante el tratamiento de las células donde la interacción tiene lugar con péptidos artificiales de estructura fotoconmutable derivados de la superficie de interacción y la aplicación de condiciones de iluminación adecuadas. A fin de probar esta hipótesis principal, se han fijado los siguientes objetivos para esta tesis:

- Establecer una estrategia para la exploración de interacciones proteína-proteína y la obtención de secuencias peptídicas candidatas para su modificación con el fotoconmutador azobenceno.

- Encontrar principios de diseño molecular que aplicados a la modificación con azobenceno de las secuencias candidatas faciliten la obtención de péptidos cuya estructura y afinidad por su diana de interacción sean dependientes de la iluminación que se les aplique.
- Buscar métodos sencillos de administración de las moléculas obtenidas al citoplasma celular, a fin de facilitar la aplicación de la tecnología desarrollada.
- Verificar si los procesos biológicos en los que está implicada la interacción β-arrestina/β-adaptina 2 se ven afectados por los péptidos obtenidos con la misma dependencia de la luz que su estructura y su afinidad.
- Intentar cumplir todos los objetivos anteriores en el sistema modelo de la interacción β-arrestina/β-adaptina 2 y su contexto funcional, la endocitosis mediada por clatrina.

Los dos primeros objetivos se desarrollan principalmente en la sección 2 de esta tesis, mientras que el tercero y cuarto se desarrollan en la sección 3 y el quinto en ambas.

5.2. **Diseño de inhibidores fotoconmutables de la interacción de β-adaptina 2 con β-arrestina**

En esta sección de la tesis hemos utilizado un panel de 14 péptidos modificados con azobenceno derivados de la secuencia BAP-long para evaluar la importancia de la estructura secundaria y la flexibilidad en su interacción con β-adaptina 2 y determinar los requisitos para el diseño de inhibidores fotoconmutables de la interacción proteína-proteína. Hemos analizado varias posiciones y distancias de acoplamiento del azobenceno y probado dos tipos de aminoácidos no proteinogénicos como herramientas de diseño. Los resultados muestran que las estructuras flexibles tienen una mayor capacidad de inhibición de la interacción observada y una mayor capacidad de fotoconmutación de la afinidad que las estructuras rígidas. Por lo tanto, identificamos la flexibilidad es identificado como un criterio adicional a tener en cuenta para la selección de candidatos a inhibidores de interacciones similares a la de β-arrestina con β-adaptina 2.

Los péptidos son estudiados mediante dicroísmo circular en solución para determinar su estructura secundaria y si tiene dependencia con la luz. También se determina su tiempo de relajación térmica mediante espectroscopía de absorción y se compara con el del azobenceno libre como una medida de la rigidez estructural de cada molécula. Se observan niveles de helicidad muy bajos en ausencia de proteína con cierta fotoconmutación estructural. A continuación, se determina para cada péptido la constante de inhibición competitiva de la interacción BAP-long/ β-adaptina 2 en ensayos de competición de fluorescencia polarizada, observándose un amplio rango de comportamientos desde la no interacción hasta la interacción fotocontrolada con ejemplos de péptidos cuya interacción está favorecida en la oscuridad y péptidos cuya interacción está favorecida en el estado fotoestacionario. De la comparación de secuencias, de datos determinados y de simulaciones estructurales de dinámica molecular se obtienen varios principios de diseño aplicables a este sistema y potencialmente a sistemas similares. Adicionalmente, se desarrolla un modelo simple para interacciones fotocontroladas que permite inferir las constantes de interacción intrínsecas de los péptidos en cis, que no pueden medirse directamente en el estado fotoestacionario, e informa posibles optimizaciones de inhibidores fotoconmutables.

Las conclusiones principales de esta sección son las siguientes:

- Existen 3 posiciones óptimas para la modificación con azobenceno en la cara del péptido opuesta a la superficie de interacción con la β-adaptina 2, estas posiciones definen una superficie de actuación (llamada así porque es donde se ubicará el actuador, el azobenceno) de 7 residuos. Cuando el azobenceno se coloca en esas posiciones, se obtienen péptidos capaces de unirse a β-adaptina 2 y cuya afinidad es fotodependiente.

- Para este sistema se recomiendan separaciones entre los puntos de acoplamiento del azobenceno de 7 y 11 residuos en la secuencia con preferencia sobre la separación de 4 residuos (que es la tercera posibilidad para péptidos helicoidales y con el azobenceno empleado). La restricción conformacional impuesta por esta última separación resulta en la abolición de la interacción con β-adaptina 2.

- La inserción del motivo inductor de helicidad valina-ácido α-aminoisobutírico en la secuencia peptídica tiene efectos grandes sobre la

afinidad, pero éstos dependen de la posición de inserción y del rol que esa parte del péptido desarrolle en la interacción molecular. Se ha encontrado el caso de que esta inserción transforma péptidos que no interaccionan en péptidos inhibidores en una posición mientras que en otra elimina la capacidad de interacción del péptido.

- La sustitución de fenilalaninas por naftilalaninas en la superficie de interacción facilita la interacción al aumentar la hidrofobicidad del péptido, pero la hace menos dependiente de la estructura, aboliendo la fotoconmutación de la actividad.

- La optimización de inhibidores activos en cis pasa por buscar un aumento de la ratio entre las constantes de afinidad del inhibidor inactivo y del inhibidor activo (ratio de fotoconmutación). Esto se puede lograr modificando la superficie de interacción.

- La optimización de inhibidores activos en trans pasa por buscar una disminución del contenido residual de inhibidor en trans en el estado fotoestacionario. Esto se puede lograr modificando el fotoconmutador.

- Los péptidos con mejor fotoconmutación de la inhibición tienen estructuras poco helicoidales en solución y tiempos de relajación que sugieren flexibilidad en la molécula. Por tanto, para el sistema β-arrestina/β-adaptina 2 los péptidos flexibles son más fáciles de fotocontrolar con azobenceno y mejores inhibidores.

- Aunque el diseño molecular se ha realizado asumiendo una estructura helicoidal de los péptidos y estos no la tienen en solución, la fotoconmutación de la afinidad es la esperada por el diseño. Esto sugiere que la fotoconmutación de la estructura como medio para fotoconmutar la afinidad de péptidos se puede aplicar también en péptidos sin una estructura secundaria fuertemente definida. Esta novedad expande el campo de péptidos e interacciones que se pueden abordar mediante esta aproximación.

- Cuatro péptidos que forman una sub-familia de diseño con fotoconmutaciones opuestas (unos activos en oscuridad y otros en estado fotoestacionario) han sido identificados como candidatos para el

fotocontrol de actividades celulares y se prueban en la siguiente sección con el nombre "traffic lights" (por su potencial papel como controladores del tráfico de membrana de las células por medio de luz).

5.3. **Control óptico de la endocitosis mediada por clatrina**

En esta sección aplicamos la estrategia y algunos de los péptidos descritos en la sección anterior para fotoregular la endocitosis mediada por clatrina en células vivas. La endocitosis mediada por clatrina es un proceso clave en todas las células eucariotas. La principal molécula adaptadora de esta maquinaria es el complejo AP-2, que media la unión de la clatrina a la membrana y a receptores de carga. La endocitosis se puede inhibir mediante interferencia con si-RNA (Boucrot et al., 2010; Motley et al., 2006) o inhibidores de tipo molécula pequeña contra clatrina (von Kleist et al., 2011) y dinamina (Joshi et al., 2010; Lee et al., 2010; Macia et al., 2006). Aunque son potentes y capaces de cruzar la membrana plasmática, la acción de estos inhibidores no puede localizarse a regiones de la célula y sólo se puede revertir con largos lavados de horas de duración. Para superar esta limitación se podría actuar selectivamente sobre interacciones entre proteínas para apagar y encender la endocitosis en poblaciones o regiones subcelulares de interés. En esta sección aplicamos péptidos traffic light dirigidos contra AP-2. Estos péptidos son capaces de cruzar la membrana celular y fotoregular la endocitosis mediada por clatrina en células vivas.

Los estudios de interacción mediante fluorescencia polarizada se extienden en esta sección para demostrar la reversibilidad de la fotoconmutación cuando se iluminan los péptidos con luz de diferentes longitudes onda. Hemos probado los péptidos que interaccionan reversiblemente con el apéndice β de AP-2 en ensayos de internalización del receptor de transferrina mediante microscopía óptica y citometría. A continuación, hemos comprobado la internalización espontánea de estos péptidos mediante ensayos de microscopía y citometría con péptidos marcados con fluorescencia y realizado también tests de toxicidad en diferentes tipos celulares. Finalmente, hemos comprobado la afectación de la dinámica de estructuras ricas en clatrina mediante experimentos de microscopía de reflexión total interna (TIRF) en células HeLa que expresaban la cadena ligera de clatrina marcada con mRFP y procesado los vídeos resultantes para observar

el tamaño, número, velocidad lateral y tiempo de vida de las partículas identificables con pozos o vesículas recubiertos de clatrina.

Las dos moléculas TL-1 y TL-2 son capaces de cruzar membranas celulares y perturbar luna interacción proteína-proteína de forma fotocontrolada y reversible en células vivas. La evaluación semicuantitativa de la potencia de la inhibición de la endocitosis mediada por clatrina y la capacidad de apagar y encender este proceso con luz coloca a los péptidos traffic light como reguladores del tráfico celular que responden a la iluminación y permiten el control de la endocitosis mediada por clatrina en patrones espacio-temporales definidos. Es esperable que este descubrimiento químico, aplicado a un proceso biológico de la relevancia de la endocitosis, tenga un impacto considerable en la comunidad científica dedicada a la biología celular. Los péptidos traffic light constituyen un ejemplo de estrategia optofarmacológica directa para la manipulación del ensamblaje y actividad de complejos proteicos endógenos sin necesidad de modificación química o genética de las células y moléculas diana que puede ser extendido a otras aplicaciones para la inhibición de otras interacciones proteína-proteína.

Las principales conclusiones de esta sección son las siguientes:

- La interacción de los péptidos TL-1 y TL-2 con β-adaptina 2 se puede controlar mediante aplicación de luz de 360-380 nm o de 500 nm para hacerlos conmutar entre alta y baja afinidad a lo largo de varios ciclos.
- En concordancia con el diseño molecular, TL-1 es un inhibidor activo en oscuridad y tiene menor actividad en el estado fotoestacionario bajo luz de 360-380nm. TL-2 funciona en sentido inverso.
- Tanto TL-1 como TL-2 son internalizados espontáneamente por células de mamífero de varios tipos celulares. Concentraciones menores que 100 μM y tiempos de incubación de 30 min son suficientes para que se produzca la internalización.
- TL-1 y TL-2 presentan una toxicidad aguda despreciable en ensayos de MTT de 3h y muy baja en ensayos de 24h, con variabilidad entre tipos celulares.

- TL-1 y TL-2 disminuyen la cantidad de receptor de transferrina internalizado en concordancia con su estado de activación (mayor disminución en estado activado y menor en el estado inactivo).
- TL-1 conserva una actividad residual importante en el estado fotoestacionario, siguiendo el modelo de inhibición fotoconmutable de la sección anterior.
- TL-1 y TL-2 activos afectan a las estructuras de clatrina aumentando su tamaño y tiempo de residencia en la membrana y, disminuyendo su velocidad lateral y su número por unidad de superficie de membrana. Esto sugiere un atasco general de la maquinaria endocítica que enlentece sin bloquear completamente la endocitosis por vía de clatrina.
- El procedimiento informático automatizado empleado para analizar los vídeos de los ensayos de TIRF produce resultados comparables a los de un experimentador que siguiese manualmente las trayectorias de las partículas detectadas en los vídeos.

5.4. **Conclusiones**

Las conclusiones generales de este trabajo son:

- Es posible utilizar péptidos entrecruzados con azobenceno con secuencias de la interfaz de una interacción proteína-proteína como inhibidores fotoconmutables de esa interacción.
- La fotoconmutación estructural del azobenceno se puede aplicar a fotocontrol de la afinidad y la actividad biológica de péptidos aunque carezcan de una estructura secundaria fuertemente definida.
- Los inhibidores peptídicos fotoconmutables de la interacción proteína-proteína β-arrestina/β-adaptina 2 desempeñan mejor su función cuando tienen mayor libertad conformacional. Esta conclusión se puede extender a la inhibición fotocontrolada de interacciones proteína-proteína similares, es decir, caracterizadas por la adaptación conformacional entre superficies de interacción flexibles.
- La secuencia de aminoácidos natural de un péptido que constituye una superficie de interacción puede soportar cierta cantidad de modificaciones,

adicionales a la introducción de cisteínas para el acoplamiento de azobenceno a sus cadenas laterales, sin perder su capacidad de interactuar con la molécula diana y su función como un inhibidor. Para ello, los residuos que forman la zona activa interacción deben ser conservados y disponer de libertad conformacional para llegar a las mismas posiciones relativas que ocupan en la interacción natural.

- En las interacciones mediadas por una sola cara de una molécula helicoidal, los residuos de esa cara conforman una superficie de interacción y tienen que ser conservados en el diseño de inhibidores, mientras que los residuos de la cara opuesta, o superficie de actuación, son el lugar ideal para introducir modificaciones (como el acoplamiento de azobenceno o la mutación de aminoácidos para mejorar la fotoconmutación).

- Para optimizar péptidos activos en el estado fotoestacionario, diseño molecular se debe aplicar para promover altas diferencias en la afinidad entre el estado activo y el estado inactivo.

- Para optimizar péptidos activos en oscuridad, el diseño molecular se debe aplicar para fomentar el mayor contenido posible del péptido inactivo en el estado fotoestacionario.

- Los aminoácidos no proteinogénicos como el ácido α-aminoisobutírico y la naftilalanina se pueden introducir en los péptidos inhibidores para mejorar la fotoconmutación de su afinidad, pero su efecto dependerá de la posición y de la interacción concreta que se desee controlar. Para emplearlos es recomendable considerar tanta información sobre los detalles moleculares de la interacción como se pueda conseguir.

- El acoplamiento intramolecular de azobenceno es una forma de "grapado" (stapling) de péptidos que promueve la penetración celular del péptido resultante, lo cual permite su aplicación contra dianas citoplasmáticas de células vivas.

- La disrupción de la interacción proteína-proteína β-arrestina/β-adaptina 2 con péptidos TL en células vivas produce una inhibición de la endocitosis

mediada por clatrina fotocontrolada de forma reversible con resolución celular y potencialmente subcelular.

- Los péptidos TL afectan al tamaño y a la dinámica de estructuras supramoleculares que contienen clatrina caracterizadas como vesículas recubiertas de clatrina, probablemente actuando sobre el complejo AP-2.
- Los péptidos TL en estado activo inducen la acumulación de maquinaria endocítica bloqueada, como muestra la formación de estructuras ricas en clatrina de mayor tamaño y dinámica más lenta en células expuestas a péptidos TL activos.
- Los péptidos fotoconmutables permiten el fotocontrol de actividades celulares con alta resolución espacial y temporal, con la especificidad de las interacciones biomoleculares y sin la necesidad de una modificación química o genética del sistema de destino.
- La posibilidad teórica de usar péptidos modificados con azobenceno de estructura fotoconmutable en optofarmacología se ha verificado por primera vez y es en principio aplicable a múltiples sistemas biológicos diferentes al empleado en este trabajo.

Appendix I - Technical notes

Azobenzene crosslinker synthesis

BSBCA was prepared following a published protocol (Burns et al., 2007) with adaptations to the available facilities and materials.

1. **Protection of amine 2 of 2,5-diaminobenzenesulfonic acid**

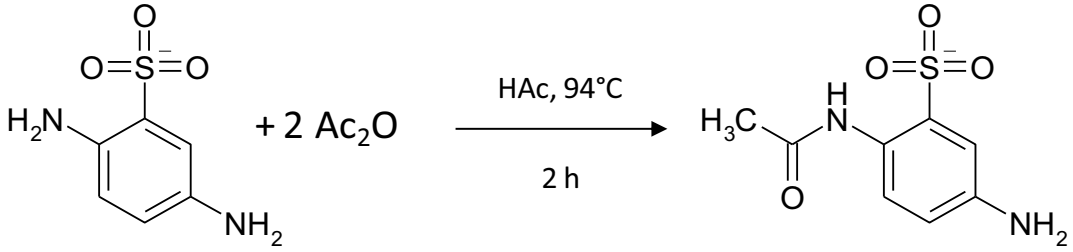

The starting material was 2,5-diaminobenzenesulfonic acid. (DABS, purchased from Sigma-Aldrich). The first synthetic step was protection of amine 2. 5 g of DABS were heated to 94°C in acetic acid (from Sigma-Aldrich) in a round flask using a heating plate with magnetic stirring and sand as a heat-conducing medium. 2 molar equivalents of acetic anhydride (from Sigma-Aldrich) were then added and a reflux apparatus mounted on the flask. The mixture was left to reflux for 2h, then filtered with paper filter on a Hirsch funnel, washed with hot acetic acid and afterwards with ether (anhydrous >99% from Sigma-Aldrich). The solid obtained was left to dry and further cleaned by resuspending in ethanol (absolute, from Panreac), filtering again and washing with ether. 2-acetylamino-5-aminobezenesulfonic acid was then dried and weighted.

2. **Condensation of 2-acetylamino-5-aminobezenesulfonic acid at the free amine**

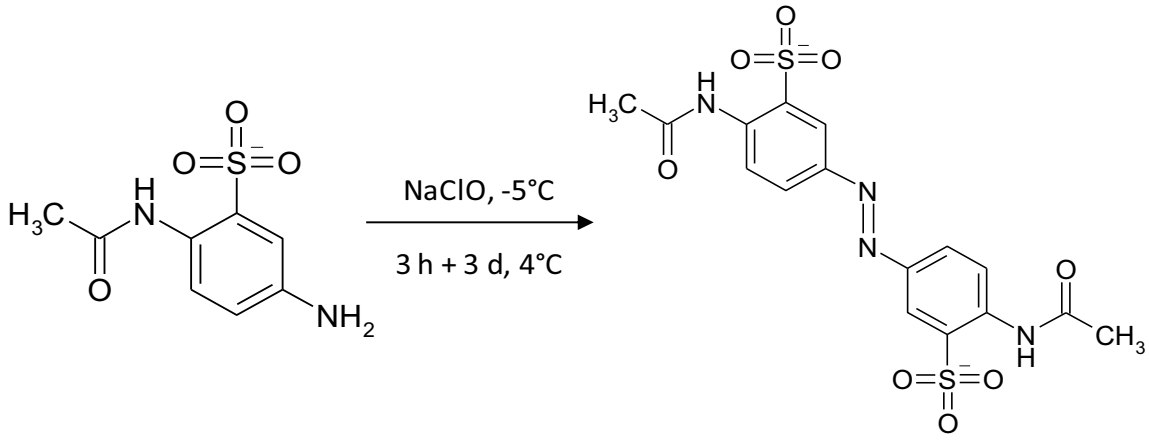

2 g of the product from the previous step were resuspended in water and the pH of the suspension was carefully adjusted to 8.5 by dropwise addition of dilute sodium carbonate (from Sigma-Aldrich) in order to facilitate amine oxidation. The pH-adjusted suspension was then cooled to -5°C in an ice/saturated sodium chloride solution bath and sealed with a rubber septum. 20 mL sodium hypochlorite (Sigma-Aldrich) was then added dropwise with a syringe. The mixture was stirred for 3h and left to precipitate at 4°C for 3 days. After precipitation, it was filtered and the resulting solid was washed with hot ethanol and washed again with ether before drying 3,3'-bis(sulfonato)- 4,4'-bis(acetamido)-azobenzene and weighting.

3. Deprotection of amines 4 and 4'

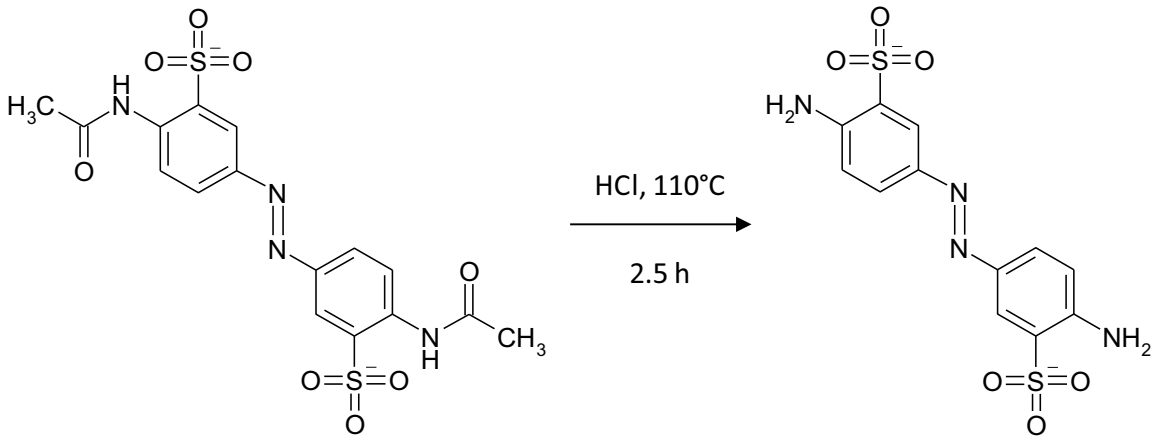

200 mg of the product from the previous step were suspended in 5.5 mL of water and 1.1 mL of hydrochloric acid (37%, from Sigma) were added. The

mixture was refluxed at 110°C for 2.5 h. The solvent was then evaporated in a rotary evaporator under aspirator vacuum . The remaining solid was resuspended in 16 mL of water and its pH adjusted to 8.5 by dropwise addition of 0.1 M sodium hydroxide (purchased as solid pellets from Panreac). The aqueous medium was then evaporated in a rotary evaporator under aspirator vacuum. The solid 3,3'-bis(sulfonato)-4,4'-bis(amino)-azobenzene was then dried and recovered.

4. Addition of chloroacetyl on amines 4 and 4'

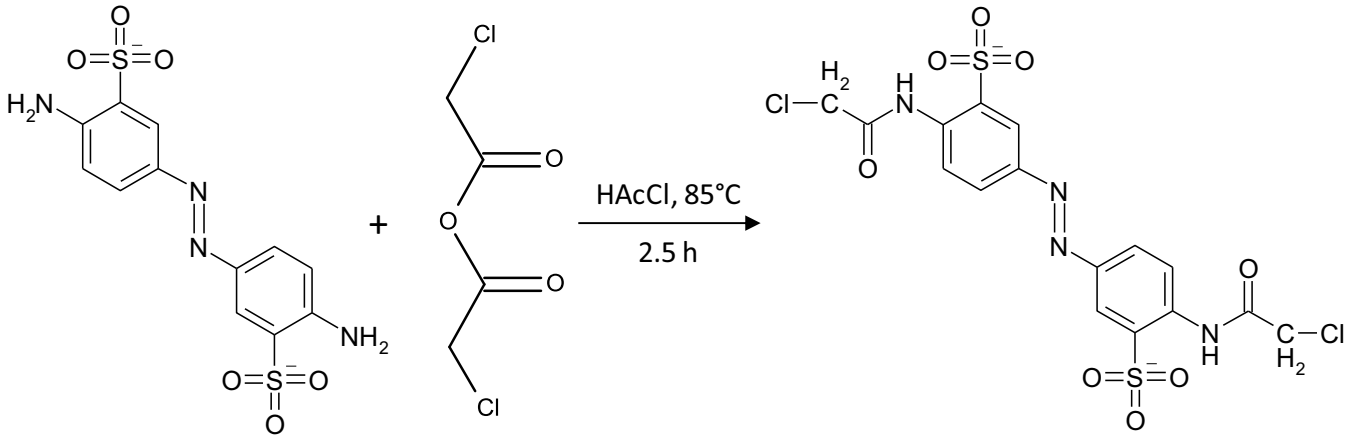

25 molar equivalents of both chloroacetic acid (Sigma-Aldrich) and chloroacetic anhydride (Sigma-Aldrich) were added to all the solid from the previous step (estimated 30 mg). The mixture was heated until complete melting (85-90°C) and refluxed for 9 h to overnight. The mixture was then cooled over ice to precipitate the product. Excess chloroacetic acid and chloroacetic anhydride were removed by washing with dichloromethane (Sigma-Aldrich) and filtering repeatedly. The resulting solid was then dried under vacuum and weighted. The overall mass yield of 3,3'-bis(sulfonato)-4,4'-bis(chloroacetamido)-azobenzene (BSBCA) was 9.4%.

Every step was confirmed by proton NMR (kindly recorded by Peter Tremmel).

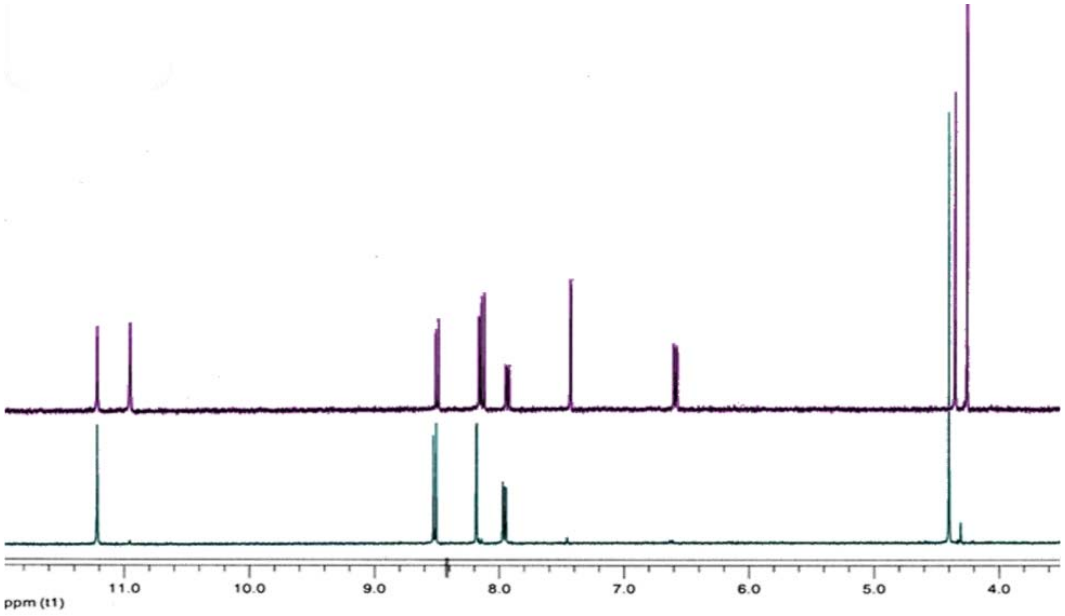

Figure A- 1 Proton NMR spectra of BSBCA in the dark (teal) and after 1 min illumination at 360 nm (purple). Increase of the *cis*-isomer can be appreciated as an increase in the purple spectrum of the minor family of peaks in the teal spectrum.

Peptide preparation

1. Non-crosslinked peptide synthesis

Non-crosslinked peptides were either prepared in the laboratory by Laura Nevola or purchased from a custom peptide synthesis service (GL Biochem, Shanghai). When synthesized in the laboratory, peptides were synthesized by standard 9-fluorenylmethoxycarbonyl/tertbutyl (Fmoc/tBu) solid-phase peptide synthesis. 2-chlorotrityl chloride or Rink amide resin (depending on the peptides) were loaded with the first amino acid (0.3 mmol/g) using DIPEA in DCM and TBTU/DIPEA in DCM respectively. The peptide elongation was performed using TBTU/DIPEA in DMF (all single couplings except for Arg which required double coupling). Fmoc group removal was performed each time by treating the resin with piperidine (20%) in DMF (3 x 5min.). 5(6)-carboxyfluorescein or rhodamine were coupled at the N-terminal, depending on the case, using PyBOP/HOAt/DIPEA in DMF/DCM (9:1) for 2 h. Both labeled and non-labeled peptides were cleaved from the resin by treatment with TFA (95 %), TIPS (2.5 %) and water (2.5%) for 3 h. Peptides were purified to >95% purity by RP-HPLC (Waters 2545 binary gradient module, Waters 2998 photodiode detector equipped with a Waters 2767 sample manager) using a XBridge™ Prep C18 or a Sunfire™ Semiprep C18 column

(Waters). HPLC conditions: flow = 3 mL/min, different gradient optimized depending on the profile of the crude product (from 10%of B to70% of B) A=0.1% TFA in H_2O, B=0.05% TFA in acetonitrile. 5(6)-carboxyfluorescein or rhodamine was coupled to the N-terminal when required.

2. Peptide crosslinking with BSBCA

Non-crosslinked peptides were dissolved in 200 mM Tris buffer supplemented with 10mM tris-(2-carboxyethyl)phosphine (TCEP). TCEP is a mild reducing agent that ensures the availability of the sulfhydryl group in cysteine amino acids for reaction with chloroacetamide. The pH of the supplemented buffer was carefully adjusted to 8.5, as it is critical for the crosslinking reaction. The peptide solution was allowed to reduce in a closed vial for 10 min and a total of 3 molar equivalents of BSBCA were added over 4 h (one equivalent every 1-2 h). The reaction mixture was stirred overnight protected from light and at room temperature. Formation of the desired product was verified by MALDI-TOF mass spectrometry. Samples of 1 μL were desalted with C18 desalting resin mounted into 2 μL pipette tips (ZipTip, Millipore) and eluted with MALDI medium (saturated α-cyano-4-hydroxycinnamic acid in a 1:1 acetonitrile/water mixture supplemented with 0.1% trifluoroacetic acid) directly on a MALDI plate. If the reaction was not complete, either additional TCEP and BSBCA were added to the crude or a new reaction batch was started with higher Tris and TCEP concentrations and higher molar excess of BSBCA (up to 9 equivalents). If the desired reaction product was detected, the reaction crude was freeze-dried and purified to >95% purity with the HPLC conditions described in section 2 (see Figure 8).

All peptides were identified by MALDI-TOF or ESI-MS (for peptides in Section 2, see Figure 9; for peptides in Section 3: Bap-long [MW=2413 (calc.2412.12)]; Bap-short [MW=1924.36(calc. 1924.08)]; CF-Bap-long [MW= 2772 .23 (calc. 2771.69)]; TL-1[MW=2930.2 (calc. 2928.8)]; TL-2 [MW=2830.8 (calc. 2829.4); TL-3[MW=2728 (calc. 2729.12)];TL-4[MW=2788 (calc. 2788.03)]; CF-TL-1[MW=3189.04 (calc. 3187.82)]; CF-TL-2 [MW=3185.76 (calc. 3187.56)]; Rd-TL-2 [MW= 3251.46 (calc 3251.48)]).

Irradiation systems

Two different light sources were used to photoswitch azobenzene in this work. For plate or cuvette experiments (circular dichroism and fluorescence polarization) an 8 Watt 365 nm transilluminator lamp (Biostep, Jahnsdorf) was inverted and placed over the samples and irradiation was performed at room temperature. During live microscopy experiments. TIRF and Confocal Microscopy were performed under CO_2 and temperature control to guarantee imaging of living cells. For the same reason irradiation was performed with a custom-made multi-LED dual wavelength (380 nm and 500 nm) lamp (FC Tècnics, Barcelona). The plate was directly introduced and retained in the microscope cabin —located above the cell preparation— during the whole experiment. In order to assure the right irradiation energy, cells were simultaneously exposed to local irradiation provided by a 380 nm laser in the same microscope.

Determination of cis-to-trans relaxation τ of azobenzene.

Azobenzene relaxation τ (mean lifetime of the *cis* isomer) at room temperature was determined by measuring absorption every 5 min over the 2 h following exposure to intense 380 nm light. All measurements were carried out in parallel in a 96-well clear bottomed plate using a micro-plate multimode reader (Infinite M200 pro, Tecan). Simultaneous excitation was achieved by placing the multi-well plate under the light emitted by a standard nucleic acid gel transilluminator. Data were normalized to obtain the percent relaxation and their complementary (100-X) was calculated to obtain the percentage of excitation. This percent excitation was fitted to one-phase exponential decay curves using Prism software (GraphPad 5). τ values were calculated as the inverses of the decay constants K obtained from the curve fit. The relaxation of TL-1 in Section 3 was measured independently and is expressed as cis isomer half-life($t_{1/2}$), corresponding to $\tau \cdot \ln(2)$.

Circular dichroism measurements

Circular dichroism is the differential absorption of left and right circularly polarized light. It is exhibited in the absorption bands of optically active chiral molecules. CD in the UV range of the electromagnetic spectrum is used to investigate the secondary structure of proteins. Usually the difference of absorption or molar extinction coefficient of left- and right-polarized light is measured, but frequently

most measurements are reported in degrees of ellipticity. Since total ellipticity is proportional to concentration of the measured molecule and the light path length, it has to be corrected by concentration to compare different molecules, resulting in molar ellipticity [θ]. When comparing biomolecules to make inferences about their secondary structures, molar ellipticity is further corrected by the number of residues in the polymer (the number of amino acids minus one in the case of proteins, as the CD is the result of regularly ordered amide bonds in the polypeptide backbone), resulting in molar, per residue, ellipticity (MRE).

Dichroism and MRE present characteristic signature spectra for common secondary structures such as α-helix and β-sheet. Complex spectra of molecules containing different secondary structures can be seen as a linear composition of the characteristic CD spectra of "pure" secondary structures and decomposed in order to estimate the fraction of the molecule represented by every secondary structure. In the case of α-helical peptides, this can be further simplified and the value of MRE at 222 nm can be compared to that of a model helix with the expression:

$$MRE_{222nm}(100\%\ helix) = -40000 \cdot \frac{n-4}{n}\ deg \cdot cm^2 \cdot dmol^{-1}$$

where n is the number of residues on the peptide (Flint et al., 2002) to estimate the proportion of residues that form part of an α-helix. So MRE_{222nm} values close to -40000 indicate an almost completely helical peptide. It must be noted, though, that CD is a cumulative property of an ensemble of molecules and that the values obtained will rarely represent a single molecular conformation, but the integration of the conformations present in the sample.

Circular dichroism measurements in this work were performed on a Jasco Model J-810 spectropolarimeter (a Jasco Model J-715 spectropolarimeter was used for peptide **12**). All measurements were made in thermostatized quartz cuvettes (0.01-cm path length) at 4 ºC. Temperatures were measured using a microprobe directly in the sample cell. All samples were dissolved in PBS (pH 7). Spectra reported are the averages of three scans. A scan speed of 10 nm/min, with a 0.5-nm bandwidth and a 4-s response time was used. Peptide concentrations were determined by measuring the absorption of the azobenzene moiety at 363 nm (ε_{363nm} of 24000 $M^{-1} \cdot cm^{-1}$ was used as molar extinction coefficient).

Molecular dynamics simulations

Computerized structural molecular dynamics simulations in this work were conducted by Sergio Madurga and are presented here for reference. The object of the simulations was to detect tendencies to form α-helix that could be related to the observed affinities, as free peptides in solution presented little helicity by CD. All the simulated peptides were initially built in α-helix conformation. Each peptide was immersed in a dodecahedron cell of more than 3400 water molecules. The appropriate amount of sodium and chlorine ions were introduced to neutralize the system and to achieve a bulk concentration of 0.1 M NaCl. All simulations were performed with GROMACS using the SPC model of water and the gromos53a6.ff force field for peptide atoms (http://www.gromacs.org) and adding the parameters for the azobenzene group of the crosslink. Full periodic boundary conditions were applied. The cut-off for non-bonded interactions was set to 1 nm. Long-range electrostatics were computed using the Particle Mesh Ewald method (Essmann et al., 1995). The Settle and LINCS algorithm was used to constrain bonds to allow an integration time step of 2.0 fs (Hess, 2008; Miyamoto & Kollman, 1992). For each peptide and for *cis* and *trans* conformation of the azobenzene group, the system was first subjected to a equilibration procedure using classical molecular dynamics simulations at 300 K. First, 100 ps of MD simulations were performed at constant volume and temperature (NVT ensemble) with position restraints applied to the heavy atoms of the peptide. Then, 100 ps of classical MD at constant pressure (1 atm) and temperature (NPT ensemble) with position restraints was done. Then, 200 ps of unrestrained NPT simulation allowed the relaxation of the peptide structure. Then, 20 to 40 ns of REMD simulations at 8 temperatures, ranging from 300 to 357 K, were carried out to equilibrate the system. Production runs were performed with 80 ns of REMD simulations. Only the conformation of the azobenzene group was restrained to *trans* or *cis* to prevent the interconversion between these two conformers during the simulation. Conformational analyses were performed with the GROMACS tools. A single residue criterion to determine the α-helix content was used. When a residue had the pairs of dihedral angles in a range close to the canonical α-helix (Φ between -90 and -30 and Ψ between -75 and -15 degrees), it was considered to be in an α-helix conformation.

Below are collected the results of molecular dynamics simulations, including a table with the simulation-predicted helicities of the peptides in *cis* and *trans*

conformation of the azobenzene moiety and graphs of the frequency of helical conformation for every amino acid in the simulations. The graphs show the relative frequency of the α-helical conformation in the sampled ensemble of structures for every amino acid position in each of the peptides. The same representation is shown for imposition of both *cis* and *trans* conformations of the azobenzene in the simulation.

Peptide	*trans*	*cis*	Variation
1	11±1	12±2	-1±3
2	10±2	17±2	-7±4
3	12±1	17±1	-5±2
4	ND	ND	ND
5	13±1	26±6	-13±7
6	15±2	25±2	-10±4
7	17±1	18±2	-1±3
8	ND	ND	ND
9	ND	ND	ND
10	16±1	30±1	-14±2
11	10±1	11±1	-1±2
12	12±5	12±1	0±6
13	22±3	32±1	-10±4
14	32±4	19±2	12±6

Figure A- 2 Helicity of the peptides in MD simulations. Proportion of residues in α-helical conformation for very peptide when *cis* and *trans* isomers of the azobenzene are imposed in the simulation. Peptides containing Aib (5 and 11) don't show difference in predicted helicity when compared to their Aib-free versions (6 and 12). REMD simulations of 80 ns with 8 temperatures between 300 and 357 K. Conformational analysis performed with GROMACS. A residue is considered α-helical if its predicted dihedral angles are $\Phi \in [-90°, -30°]$ and $\Psi \in [-75°, -15°]$. ND = Not determined.

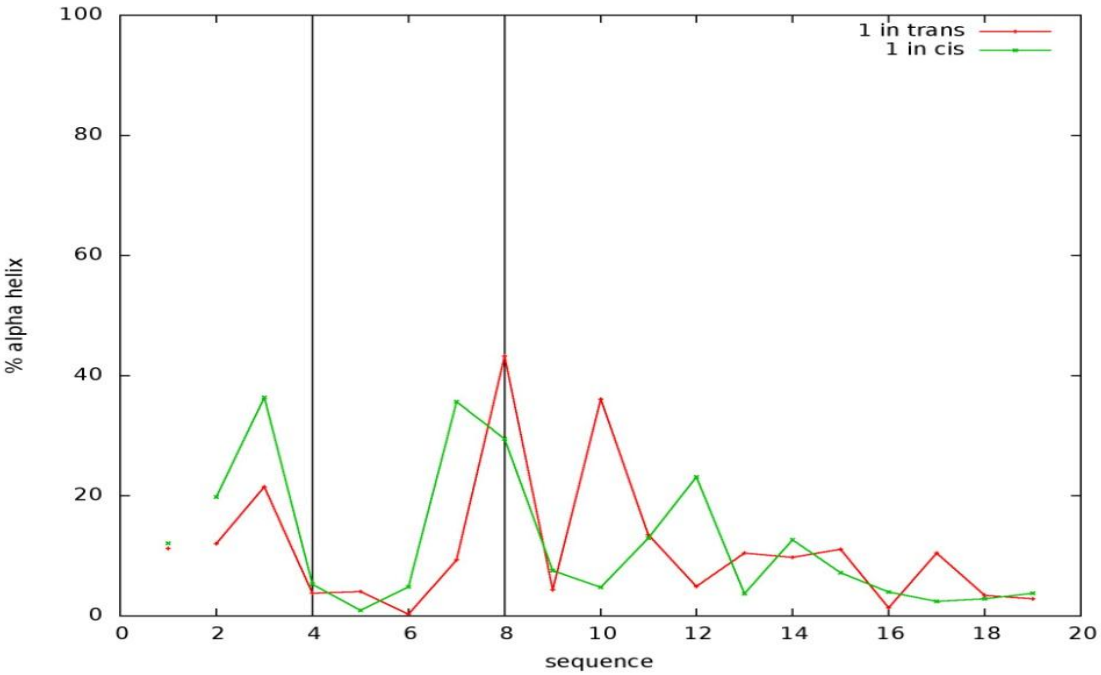

Figure A- 3 Peptide 1. Sequence DDDCVFECFARQRLKGMKDD.

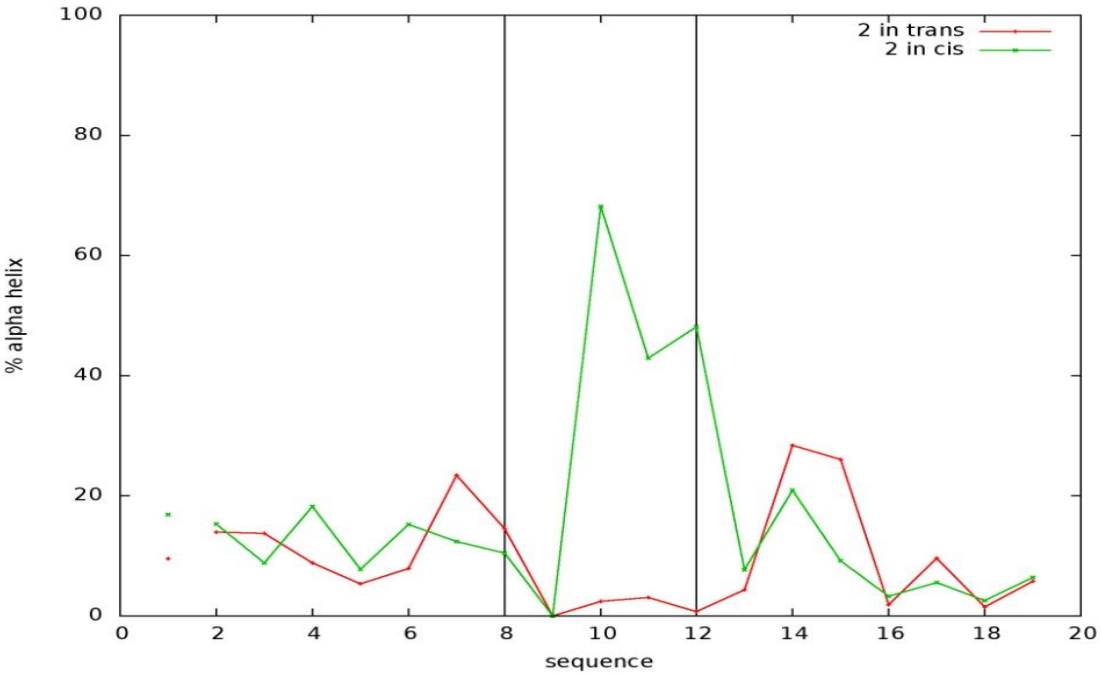

Figure A- 4 Peptide 2. Sequence DDDIVFECFARCRLKGMKDD.

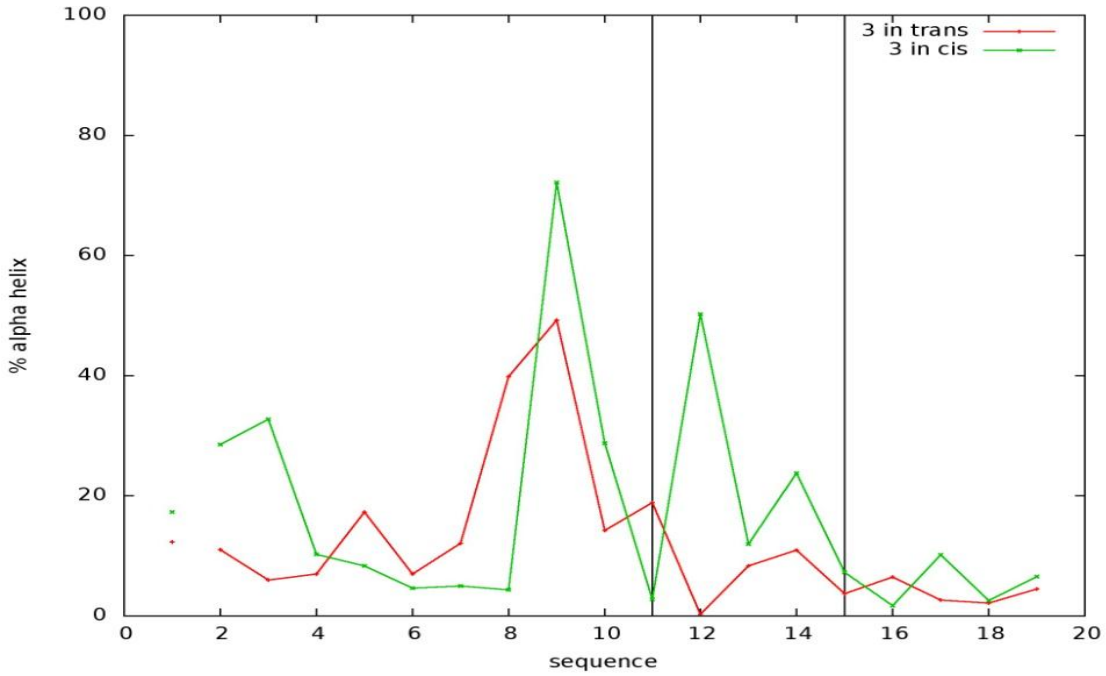

Figure A- 5 Peptide 3. Sequence DDDIVFEDFACQRLCGMKDD.

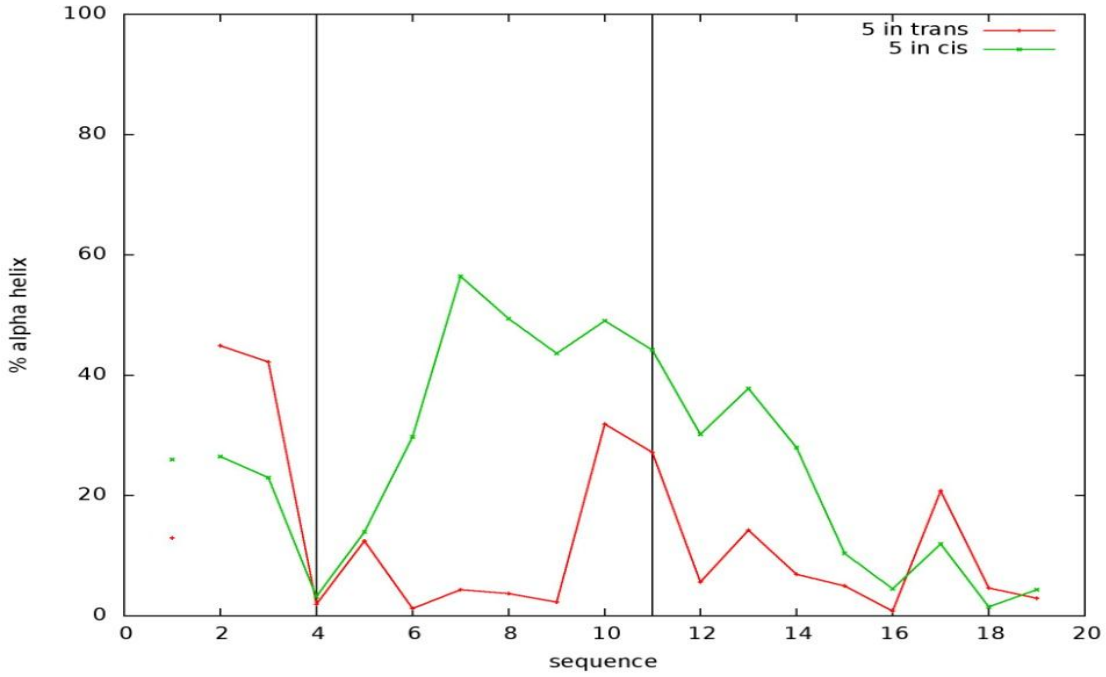

Figure A- 6 Peptide 5. Sequence DDDCVFEDFACQRLKGMKDD.

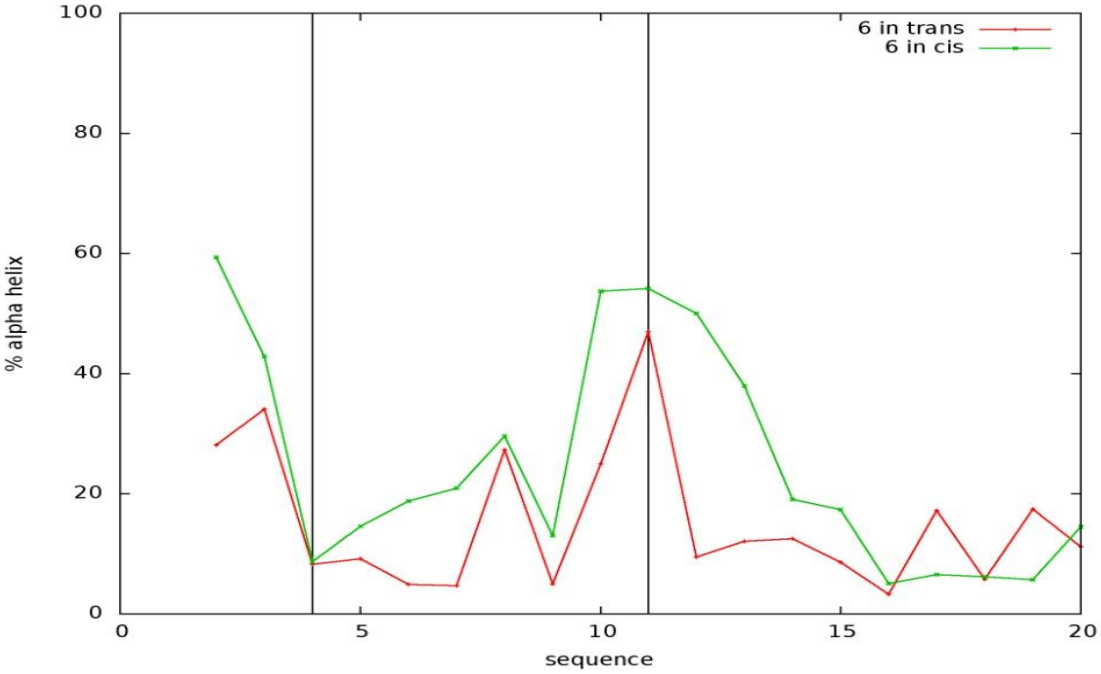

Figure A- 7 Peptide 6. Sequence (Succinyl)DDDCVFV(Aib)FACQRLKGMKDD.

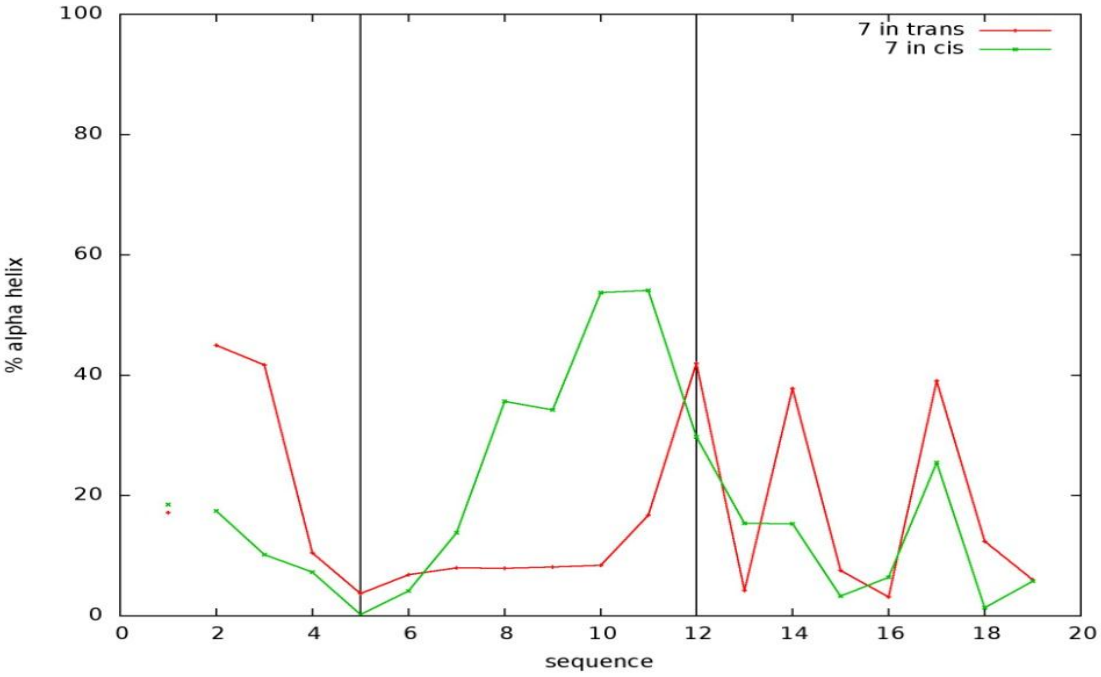

Figure A- 8 Peptide 7. Sequence DDDICFEDFARCRLKGMKDD

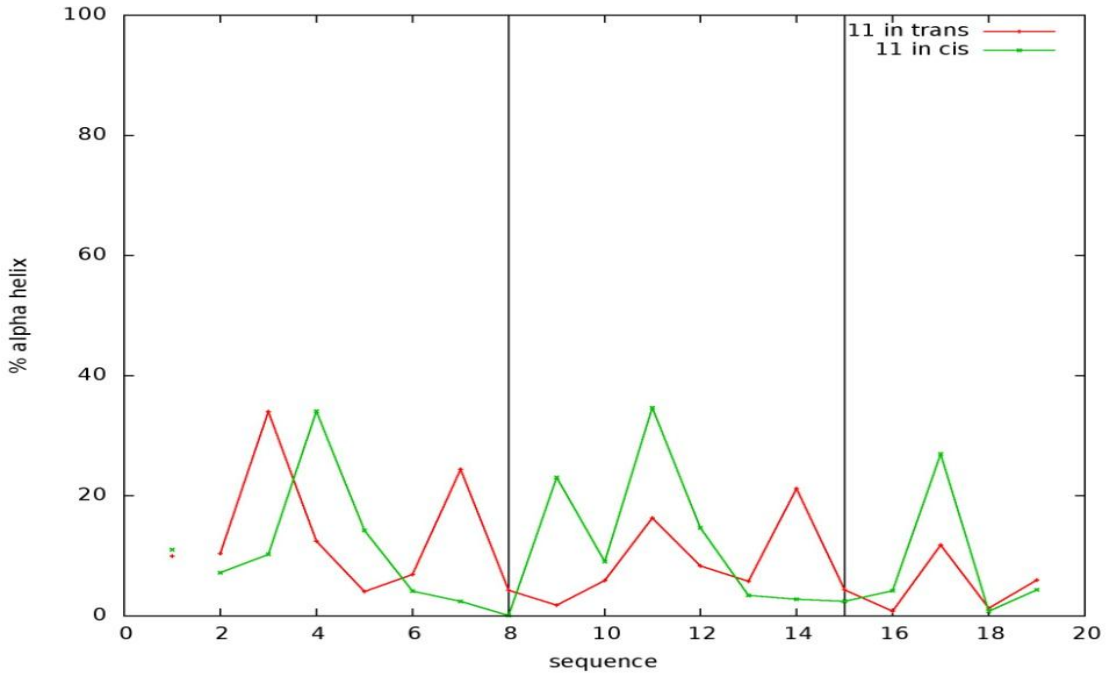

Figure A- 9 Peptide 11. Sequence DDDIVFECFARQRLCGMKDD.

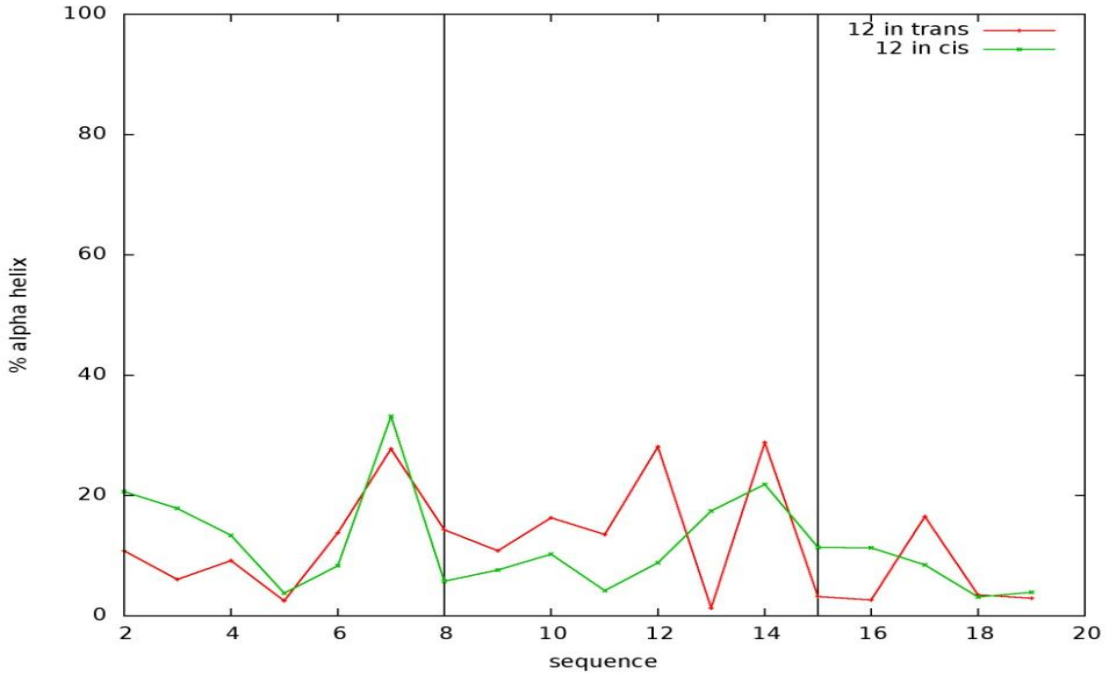

Figure A- 10 Peptide 12. Sequence DDDIVFECFAV(Aib)RLCGMKDD.

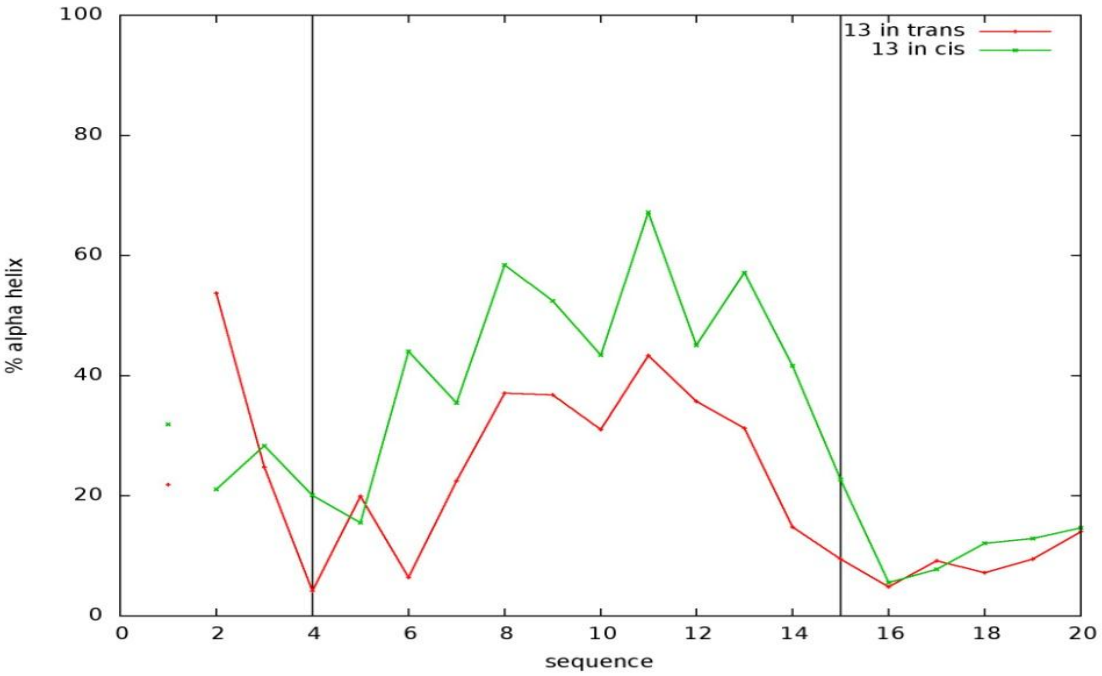

Figure A- 11 Peptide 13. Sequence (Succinyl)DDDCVFEDFARQRLCGMKDD.

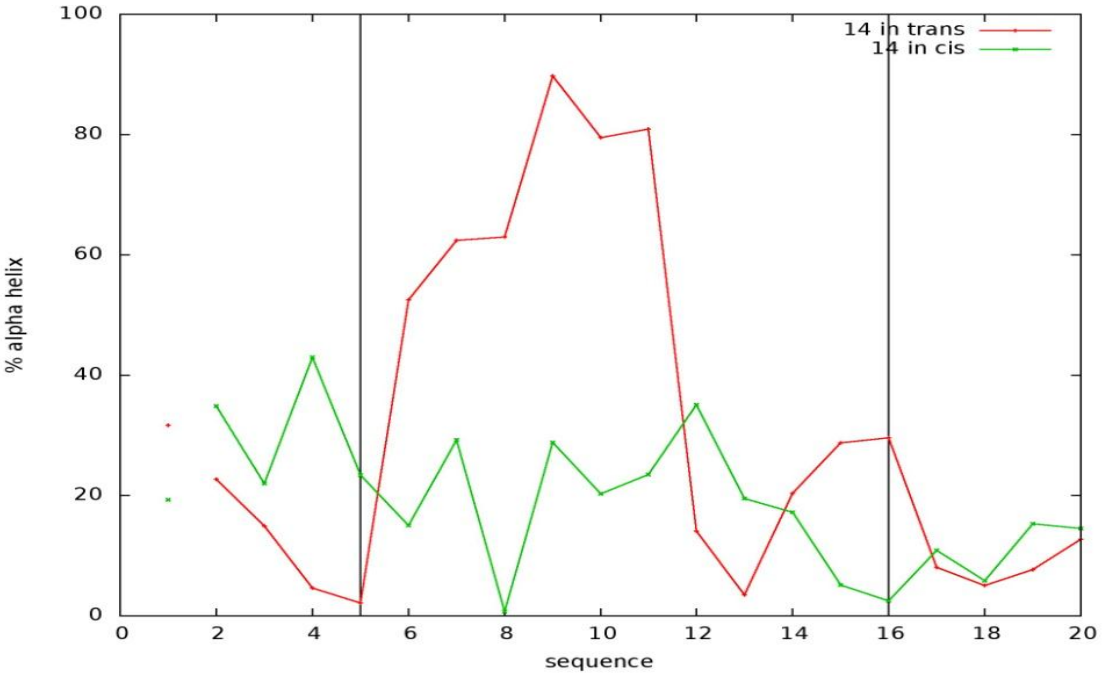

Figure A- 12 Peptide 14. Sequence (Succinyl)DDDICFEDFARQRLKCMKDD.

Fluorescence polarization binding assay.

Fluorescence polarization is a technique that exploits the relatively slower rotational motion of bigger molecules and complexes when compared to smaller ones to detect molecular binding. It requires that the molecules to be analyzed differ considerably in size, as is the case of many ligand-receptor pairs. The smaller molecule (the ligand) must be fluorescently tagged. Since a fluorochrome excited with polarized light will emit polarized fluorescence, a solution of fluorochromes excited with polarized light will emit polarized light if all the molecules are in the same orientation and don't rotate between the excitation and the emission. The molecules will not be in the same orientation at any given moment, so the degree of polarization will always decrease, but this decrease will be more important the faster the molecules rotate in solution. Conversely, more polarization will be retained if the fluorochromes are bound to bigger, slower rotating molecules. Thus, in an FP assay the degree of polarization of the emitted fluorescence is proportional to the binding. This allows constructing binding isotherms with a homogeneous assay (i.e. without the need to separate the bound ligand from the free ligand).

FP assays can be made in a competition configuration, were a fluorescent tracer ligand forming a complex with the receptor is displaced from the binding site by increasing concentrations non-fluorescent problem molecules and their apparent competitive inhibition constants can be determined. This configuration has the advantages of allowing testing many different molecules without the need for tagging them with a fluorochrome and of bypassing the effect of the fluorochrome on the binding affinity of the problem molecules. On the other hand, competition FP assays require a previous direct binding assay of the tracer molecule in order to determine the parameters of the binding equilibrium and the concentration ranges to be used in the competition assays. The competition configuration was used in this work to test the inhibition of the binding between β-arrestin and β-adaptin 2 by the assayed peptides.

Measurements were performed in half area 96-well plates (Corning) in PBS buffer (pH 7.5). For direct binding assays, a fixed concentration of N-terminal carboxyfluorescein labeled BAP-long (CF-BAP-long, final concentration 26 nM)

was added to serial dilutions of β-appendage protein. β-appendage was expressed in E. Coli at Protein Production Platform of CIBER-BBN at UAB using the plasmid kindly provided by Prof. H. McMahon (Schmid et al., 2006). For competition assays, serial dilutions of peptides were added to a pre-incubated mixture of CF-BAP-long (26 nM) and β-appendage (1 μM). Multiwell plates were incubated in the dark at room temperature until equilibrium was reached, and FP (mP units) was measured by micro-plate multimode reader (InfiniteF200Pro, Tecan). Dissociation constants (K_D) were calculated by non-linear regression analysis of one-site saturation curves using Prism software (GraphPad 5). For competition experiments, K_I values, related to the calculated affinity of CF-BAP-long for the β-appendage (K_D= 0.33 μM), were determined by non-linear regression using a one-site competition model.

Cell lines and gene constructs

HeLa, HEK293 and COS7 cell lines were obtained from ATCC (Manassas, VA); the MCF-7 and BSC-1 cell lines were kind gifts from A. Manzano and of T. Kirchhausen, respectively. Cells were cultured in DMEM (1000 mg/mL or 4000 mg/mL glucose, Biological Industries) containing fetal calf serum (10% FCS), glutamine (2 mm), penicillin (50 U/mL), and streptomycin (0.05 g/mL). Exponentially growing cells were detached from the culture flasks by using a trypsin/EDTA (0.25%) solution, and the cell suspension was seeded at specific concentration onto suitable surfaces, depending on the techniques used. Experiments were carried out 24 h or 48 h later, when the desired cell density was reached. LCa-mRFP (a kind gift from S. J. Royle) was made by fusing DNA encoding clathrin light chain to the mRFP1-N1 expression vector (Campbell et al., 2002). Transient expression of LCa-mRFP1-N1 was achieved in HeLa cells by X-tremeGene 9 (Roche) transfection of plasmid in serum-free medium.

TL uptake assays in living cells

For flow cytometry analysis, cells were seeded on a plastic well (35 x 10^3 cells/cm^2) and cultured for 48 h. The culture medium was discarded, and cells were incubated for 30 min at 37ºC under 5% CO_2 with fresh medium containing carboxyfluorescein or rhodamine labeled peptides. Cells were then rinsed twice, treated with trypsin, collected, centrifuged at 4ºC, filtered and re-suspended in cold medium. Fluorescence measurement of individual cells was performed with a Gallios Beckman Coulter flow cytometer.

For confocal microscopy analysis, cells were seeded (4-12x10^3 cells/cm^2) on glass chamber coverslips (poly-L-lysine treated for HEK293) and cultured for 48 h before being incubated as described before. Cells were washed twice, and fresh medium was introduced to perform experiments with living cells in CO_2 and temperature-controlled conditions. Time-lapse images were collected with a Leica SP5 Spectral confocal microscope attached to an inverted Leica DMI 6000, using a 63x/1.3 Glyc HCX PL APO objective.

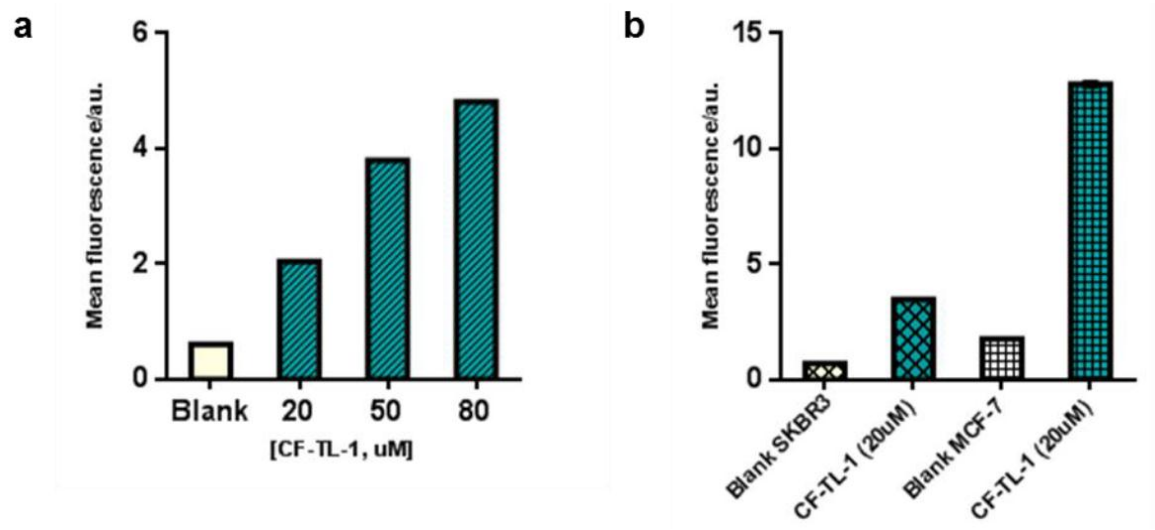

Figure A- 13 Flow cytometry uptake assay. a) Dose-dependent internalization of carboxyfluorescein-TL-1 in HeLa cells. b) Comparison between the amounts of carboxyfluorescein-TL-1 internalized in different cell lines (SKBR3 and MCF-7). Assay by Laura Nevola.

MTT cell viability assay

The toxicity assay was carried out as described in (von Kleist et al., 2011). HeLa cells were transferred to 96-well plates (100µl medium/well) at a density of 5000 cell/well. After 24 h, cells in triplicate were treated with or without TL-1 or TL-2 at a range of concentrations. After 3 h and 24 h of exposure to the inhibitor, cytotoxicity was evaluated using the MTT assay. The results are summarized below.

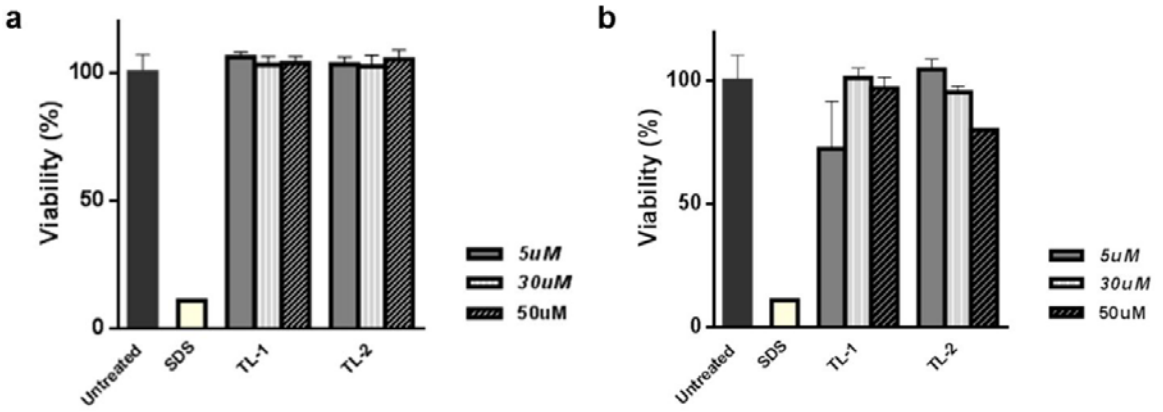

Figure A- 14 MTT toxicity assay in HeLa cells. a) Viability after exposure to different concentrations of TL-1 or TL-2 at 37°C for 3 h (a) or 24 h (b). Assay by Laura Nevola.

Transferrin receptor uptake

For flow cytometry analysis, HeLa, HEK293 and MCF-7 cell lines were prepared as described above and incubated with TLs (20 μM, illuminated at 380 nm or not) in serum-free medium for 30 min at 37ºC. Cells were then allowed to cool at 20ºC, the medium was removed, and a solution of Alexa647-Tf (5ug/ml) was added for 2 min. This strategy allows the interaction with the receptor but slows down internalization (Macia et al., 2006). Afterward, the medium was discarded and the inhibitor solution (illuminated at 380 nm or not) was re-added, while promoting internalization at 37ºC for 10 min. Finally, cells were washed with medium at room temperature, acid washed twice (0.1M NaCl, 0.1M Glycine pH 3.3), trypsin-treated, and collected at 4ºC. Fluorescence sorting was performed with a Gallios Beckman Coulter flow cytometer. For Confocal Microscopy experiments, HeLa cells were seeded on MatTek glass-bottom 14-mm microwell 35-mm Petri dishes and treated as for flow cytometry (excluding trypsin treatment). Images were recorded in CO2 and temperature-controlled conditions with a Leica SP5 Spectral Confocal microscope attached to an inverted DMI 6000, using a 63x/1.3 Glyc HCX PL APO objective. For time-lapse experiments, movies were recorded every 15 sec (5 stacks of 0.3 μm each) at 37ºC. Alexa647-Tf was added dropwise with a home-made perfusion system inside the isolated microscope in order to allow image recording from the first moment of the experiment.

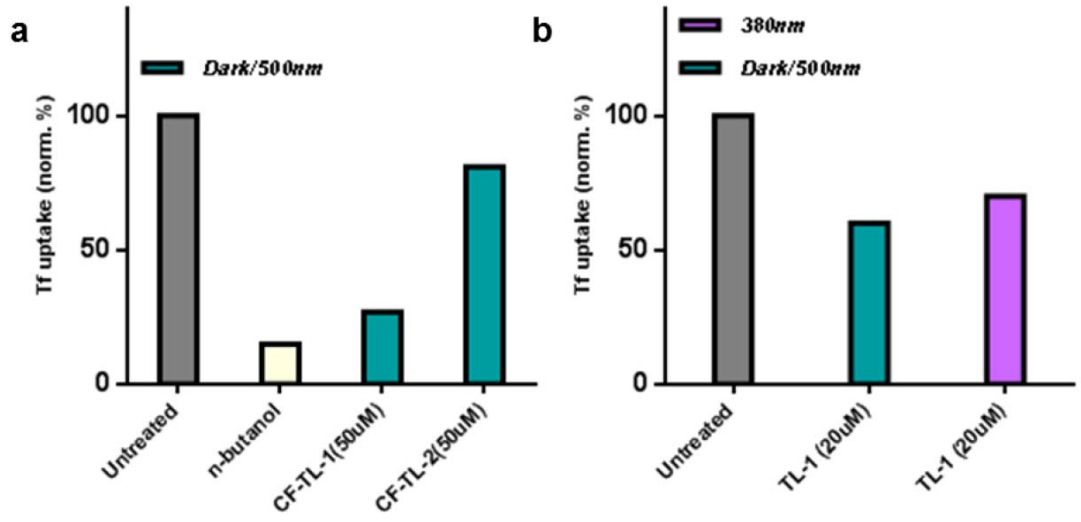

Figure A- 15 Transferrin uptake assay in different cell lines. a) Uptake in HEK293 cells treated with 50μM dark-adapted carboxyfluorescein-TL-1 or carboxyfluorescein-TL-2. b) Uptake in MCF-7 cells treated with 20μM TL-1, either dark-adapted or after irradiation at 380nm

.

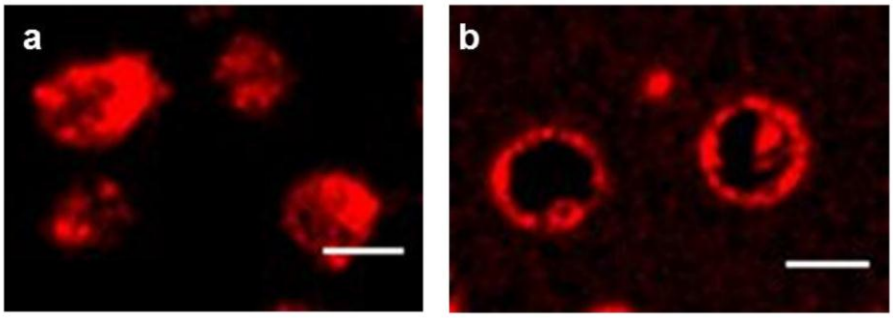

Figure A- 16 TLs inhibit CME in living cells. Final frame of experiments following Alexa647-transferrin uptake in real time. Fluorescence accumulates in the membrane in cells treated with TL-1 (b) when compared to untreated control cells (a). Scale bar: 5μm.

TIRF Microscopy

For live cell microscopy, HeLa cells transiently expressing LCa-mRFP were used. CCP dynamics were captured by Laura Nevola with a TIRFM capable microscope (Olympus) with a 100x/1.45 oil Plan Apo objective, under the control of Xcellence Software. Depending on the experiment, movies between 2 and 15 min long were acquired at 0.5 Hz, using a 12-bit Hamamatsu Orca-ER camera, after incubation for 30 min at 37ºC with TL-1 or TL-2 (both 20μM) in the three conditions: dark, 380 nm and 500 nm.

Appendix II - Publications and communications

The works of this thesis have been and will be presented in the international publications, conferences and visits listed below:

- Martín-Quirós, A., Nevola, L. (shared first authorship), Eckelt, K., Madurga, S., Giralt, E., Gorostiza, P. (2014) Flexibility as key feature of photoswitchable inhibitors of protein-protein interactions (Submitted to the Journal of the American Chemical Society).

- Nevola, L., Martín-Quirós, A. (shared first authorship), Eckelt, K., Camarero, N., Tosi, S., Llobet, A., Giralt, E., Gorostiza, P. (2013). Light-regulated stapled peptides to inhibit protein-protein interactions involved in clathrin-mediated endocytosis. Angewandte Chemie (International Ed. in English), 52(30), 7704–8. doi:10.1002/anie.201303324 Granted Very Important Paper status and highlighted in the cover of the journal.

- Nevola, L., Martín-Quirós, A., Eckelt, K., Madurga S., Giralt E., Gorostiza P. Nanoengineering cell-permeable, photoswitchable peptide inhibitors (Manuscript in preparation).

- Light-regulated stapled peptides to inhibit protein-protein interactions involved in clathrin-mediated endocytosis. Poster presentation in the European Molecular Biology Organization's *Systems Dynamics in Endocytosis*. Villars-sur-Ollon (Switzerland) 2013.

- Traffic light peptides: regulation of clathrin-mediated endocytosis by photo-control of protein-protein interactions. Poster presentation in the Royal Society of Chemistry's *11th International Symposium on Advancing the Chemical Sciences (ISACS11) - Challenges in Chemical Biolo*gy. Boston (Massachusetts) 2013.

- Nanoengineering Photoswitchable Inhibitors of Protein-Protein Interactions. Poster presentation in the Royal Society of Chemistry's *11th International Symposium on Advancing the Chemical Sciences (ISACS11) - Challenges in Chemical Biolo*gy. Boston (Massachusetts) 2013.

- Light-regulated stapled peptides to inhibit protein-protein interactions involved in clathrin-mediated endocytosis. Poster presentation in the Institute for Research in Biomedicine's *5th European Conference in Chemistry for Life Sciences (ECCLS5)*. Barcelona (Spain) 2013.

- Photocontrol of endocytosis through engineered inhibitory peptides. Poster presentation in the Spanish Biophysics Society (SBE) *XII International Congress.* Barcelona (Spain) 2012.

- Spatiotemporal regulation of clathrin-mediated endocytosis with light. Oral communication in the Spanish Biophysics Society (SBE) *XII International Congress.* Barcelona (Spain) 2012.

- Spatiotemporal regulation of clathrin-mediated endocytosis with light. Poster presentation in the Institute for Bioengineering of Catalonia's *5th IBEC Symposium on Bioengineering and Nanomedicine*. Barcelona (Spain) 2012.

- Traffic Lights: azobenzene-based photoswitchable peptides for clathrin-mediated endocytosis. Oral communication in visit at the Frances Brodsky laboratory in the G.W. Hooper Foundation, University of California at San Francisco. San Francisco (California) 2014.

- Traffic Lights: azobenzene-based photoswitchable peptides for clathrin-mediated endocytosis. Oral communication in visit at the Christian Heinis laboratory in the École Polytechnique Fédérale de Lausanne. Lausanne (Switzerland) 2013.

Appendix III - References

Angelini, N., Corrias, B., Fissi, A., Pieroni, O., & Lenci, F. (1998). Photochromic polypeptides as synthetic models of biological photoreceptors: a spectroscopic study. *Biophysical Journal*, *74*(5), 2601–10. doi:10.1016/S0006-3495(98)77966-4

Arkin, M. R., & Wells, J. A. (2004). Small-molecule inhibitors of protein-protein interactions: progressing towards the dream. *Nature Reviews. Drug Discovery*, *3*(4), 301–17. doi:10.1038/nrd1343

Asanuma, H., Liang, X., Nishioka, H., Matsunaga, D., Liu, M., & Komiyama, M. (2007). Synthesis of azobenzene-tethered DNA for reversible photo-regulation of DNA functions: hybridization and transcription. *Nature Protocols*, *2*(1), 203–12. doi:10.1038/nprot.2006.465

Azzarito, V., Long, K., Murphy, N. S., & Wilson, A. J. (2013). Inhibition of α-helix-mediated protein-protein interactions using designed molecules. *Nature Chemistry*, *5*(3), 161–73. doi:10.1038/nchem.1568

Babii, O., Afonin, S., Berditsch, M., Reiβer, S., Mykhailiuk, P. K., Kubyshkin, V. S., … Komarov, I. V. (2014). Controlling biological activity with light: diarylethene-containing cyclic peptidomimetics. *Angewandte Chemie (International Ed. in English)*, *53*(13), 3392–5. doi:10.1002/anie.201310019

Banghart, M., Borges, K., Isacoff, E., Trauner, D., & Kramer, R. H. (2004). Light-activated ion channels for remote control of neuronal firing. *Nature Neuroscience*, *7*(12), 1381–6. doi:10.1038/nn1356

Bartels, E., Wassermann, N. H., & Erlanger, B. F. (1971). Photochromic activators of the acetylcholine receptor. *Proceedings of the National Academy of Sciences of the United States of America*, *68*(8), 1820–3.

Becerril, J., & Hamilton, A. D. (2007). Helix mimetics as inhibitors of the interaction of the estrogen receptor with coactivator peptides. *Angewandte Chemie (International Ed. in English)*, *46*(24), 4471–3. doi:10.1002/anie.200700657

Bechara, C., & Sagan, S. (2013). Cell-penetrating peptides: 20 years later, where do we stand? *FEBS Letters*, *587*(12), 1693–702. doi:10.1016/j.febslet.2013.04.031

Beharry, A. A., Chen, T., Al-Abdul-Wahid, M. S., Samanta, S., Davidov, K., Sadovski, O., … Woolley, G. A. (2012). Quantitative analysis of the effects of photoswitchable distance constraints on the structure of a globular protein. *Biochemistry*, *51*, 6421–6431. doi:dx.doi.org/10.1021/bi300685a

Beharry, A. A., & Woolley, G. A. (2011). Azobenzene photoswitches for biomolecules. *Chemical Society Reviews*, *40*(8), 4422–37. doi:10.1039/c1cs15023e

Bellmann-Sickert, K., & Beck-Sickinger, A. G. (2010). Peptide drugs to target G protein-coupled receptors. *Trends in Pharmacological Sciences*, *31*(9), 434–41. doi:10.1016/j.tips.2010.06.003

Bellotto, S., Chen, S., Rentero Rebollo, I., Wegner, H. A., & Heinis, C. (2014). Phage selection of photoswitchable peptide ligands. *Journal of the American Chemical Society*, *136*(16), 5880–3. doi:10.1021/ja501861m

Bose, M., Groff, D., Xie, J., Brustad, E., & Schultz, P. G. (2006). The incorporation of a photoisomerizable amino acid into proteins in E. coli. *Journal of the American Chemical Society*, *128*(2), 388–9. doi:10.1021/ja055467u

Bosshard, H. R. (2001). Molecular recognition by induced fit: how fit is the concept? *News in Physiological Sciences : An International Journal of Physiology Produced Jointly by the International Union of Physiological Sciences and the American Physiological Society*, *16*(August), 171–3.

Boucrot, E., Saffarian, S., Zhang, R., & Kirchhausen, T. (2010). Roles of AP-2 in clathrin-mediated endocytosis. *PloS One*, *5*(5), e10597. doi:10.1371/journal.pone.0010597

Boyden, E. S., Zhang, F., Bamberg, E., Nagel, G., & Deisseroth, K. (2005). Millisecond-timescale, genetically targeted optical control of neural activity. *Nature Neuroscience*, *8*(9), 1263–8. doi:10.1038/nn1525

Browne, L. E., Nunes, J. P. M., Sim, J. A., Chudasama, V., Bragg, L., Caddick, S., & Alan North, R. (2014). Optical control of trimeric P2X receptors and acid-sensing ion channels. *Proceedings of the National Academy of Sciences of the United States of America*, *111*(1), 521–6. doi:10.1073/pnas.1318582111

Bullock, B. N., Jochim, A. L., & Arora, P. S. (2011). Assessing helical protein interfaces for inhibitor design. *Journal of the American Chemical Society*, *133*(36), 14220–3. doi:10.1021/ja206074j

Burns, D. C., Zhang, F., & Woolley, G. A. (2007). Synthesis of 3,3'-bis(sulfonato)-4,4'-bis(chloroacetamido)azobenzene and cysteine cross-linking for photo-control of protein conformation and activity. *Nature Protocols*, *2*(2), 251–8. doi:10.1038/nprot.2007.21

Campbell, R. E., Tour, O., Palmer, A. E., Steinbach, P. A., Baird, G. S., Zacharias, D. a, & Tsien, R. Y. (2002). A monomeric red fluorescent protein. *Proceedings of the National Academy of Sciences of the United States of America*, *99*(12), 7877–82. doi:10.1073/pnas.082243699

Canagarajah, B. J., Ren, X., Bonifacino, J. S., & Hurley, J. H. (2013). The clathrin adaptor complexes as a paradigm for membrane-associated allostery, *22*, 517–529. doi:10.1002/pro.02235

Chen, L., Wu, J., Schmuck, C., & Tian, H. (2014). A switchable peptide sensor for real-time lysosomal tracking. *Chemical Communications (Cambridge, England)*, *50*(49), 6443–6. doi:10.1039/c4cc00670d

Chi, L., Sadovski, O., & Woolley, G. A. (2006). A blue-green absorbing cross-linker for rapid photoswitching of peptide helix content. *Bioconjugate Chemistry*, *17*(3), 670–6. doi:10.1021/bc050363u

Doherty, G. J., & McMahon, H. T. (2009). Mechanisms of endocytosis. *Annual Review of Biochemistry*, *78*, 857–902. doi:10.1146/annurev.biochem.78.081307.110540

Dürr, H., & Bouas-Laurent, H. (Eds.). (2003). *Photochromism: Molecules and Systems* (2nd ed., p. 1218). Elsevier B.V.

Edeling, M. a, Mishra, S. K., Keyel, P. a, Steinhauser, A. L., Collins, B. M., Roth, R., … Traub, L. M. (2006). Molecular switches involving the AP-2 beta2 appendage regulate endocytic cargo selection and clathrin coat assembly. *Developmental Cell*, *10*(3), 329–42. doi:10.1016/j.devcel.2006.01.016

Edwards, T. A., & Wilson, A. J. (2011). Helix-mediated protein--protein interactions as targets for intervention using foldamers. *Amino Acids*, *41*(3), 743–54. doi:10.1007/s00726-011-0880-8

Ehrlich, M., Boll, W., Van Oijen, A., Hariharan, R., Chandran, K., Nibert, M. L., & Kirchhausen, T. (2004). Endocytosis by random initiation and stabilization of clathrin-coated pits. *Cell*, *118*(5), 591–605. doi:10.1016/j.cell.2004.08.017

Essmann, U., Perera, L., Berkowitz, M. L., Darden, T., Lee, H., & Pedersen, L. G. (1995). A smooth particle mesh Ewald method. *The Journal of Chemical Physics*, *103*(19).

Fenno, L., Yizhar, O., & Deisseroth, K. (2011). The development and application of optogenetics. *Annual Review of Neuroscience*, *34*, 389–412. doi:10.1146/annurev-neuro-061010-113817

Ferreira, T., & Rasband, W. (2012). *ImageJ User Guide User Guide* (pp. 1–185). Retrieved from http://imagej.nih.gov/ij/docs/guide/

Flint, D. G., Kumita, J. R., Smart, O. S., & Woolley, G. A. (2002). Using an azobenzene cross-linker to either increase or decrease peptide helix content upon trans-to-cis photoisomerization. *Chemistry & Biology*, *9*(3), 391–7.

Fujimoto, K., Amano, M., Horibe, Y., & Inouye, M. (2006). Reversible photoregulation of helical structures in short peptides under indoor lighting/dark conditions. *Organic Letters*, *8*(2), 285–7. doi:10.1021/ol0526524

Fujimoto, K., Kajino, M., Sakaguchi, I., & Inouye, M. (2012). Photoswitchable, DNA-binding helical peptides assembled with two independently designed sequences for photoregulation and DNA recognition. *Chemistry (Weinheim an Der Bergstrasse, Germany)*, *18*(32), 9834–40. doi:10.1002/chem.201201431

Gorostiza, P., & Isacoff, E. Y. (2008a). Nanoengineering ion channels for optical control. *Physiology (Bethesda, Md.)*, *23*, 238–47. doi:10.1152/physiol.00018.2008

Gorostiza, P., & Isacoff, E. Y. (2008b). Optical switches for remote and noninvasive control of cell signaling. *Science*, (October), 395–399.

Grossmann, T. N., Yeh, J. T.-H., Bowman, B. R., Chu, Q., Moellering, R. E., & Verdine, G. L. (2012). Inhibition of oncogenic Wnt signaling through direct targeting of β-catenin. *Proceedings of the National Academy of Sciences of the United States of America*, *109*(44), 17942–7. doi:10.1073/pnas.1208396109

Guerrero, L., Smart, O. S., Weston, C. J., Burns, D. C., Woolley, G. A., & Allemann, R. K. (2005). Photochemical regulation of DNA-binding specificity of MyoD. *Angewandte Chemie (International Ed. in English)*, *44*(47), 7778–82. doi:10.1002/anie.200502666

Guglielmetti, R. J. (2003). 4n+2 Systems: Spiropyrans. In H. Dürr & H. Bouas-Laurent (Eds.), *Photochromism: Molecules and Systems* (2nd ed., pp. 314–465). Elsevier Inc.

Hess, B. (2008). P-LINCS: A Parallel Linear Constraint Solver for Molecular Simulation. *Journal of Chemical Theory and Computation*, *4*(1), 116–122. doi:10.1021/ct700200b

Hoppmann, C., Lacey, V. K., Louie, G. V, Wei, J., Noel, J. P., & Wang, L. (2014). Genetically encoding photoswitchable click amino acids in Escherichia coli and mammalian cells. *Angewandte Chemie (International Ed. in English)*, *53*(15), 3932–6. doi:10.1002/anie.201400001

Hoppmann, C., Schmieder, P., Heinrich, N., & Beyermann, M. (2011). Photoswitchable click amino acids: light control of conformation and bioactivity. *Chembiochem : A European Journal of Chemical Biology*, *12*(17), 2555–9. doi:10.1002/cbic.201100578

Hoppmann, C., Seedorff, S., Richter, A., Fabian, H., Schmieder, P., Rück-Braun, K., & Beyermann, M. (2009). Light-directed protein binding of a biologically relevant beta-sheet. *Angewandte Chemie (International Ed. in English)*, *48*(36), 6636–9. doi:10.1002/anie.200901933

Ihalainen, J. a, Paoli, B., Muff, S., Backus, E. H. G., Bredenbeck, J., Woolley, G. A., … Hamm, P. (2008). Alpha-Helix folding in the presence of structural constraints. *Proceedings of the National Academy of Sciences of the United States of America*, *105*(28), 9588–93. doi:10.1073/pnas.0712099105

Irie, M. (2000). *Diarylethenes for Memories and Switches. Chemical reviews* (Vol. 100, pp. 1685–1716).

Ivanov, A. A., Khuri, F. R., & Fu, H. (2013). Targeting protein-protein interactions as an anticancer strategy. *Trends in Pharmacological Sciences*, *34*(7), 393–400. doi:10.1016/j.tips.2013.04.007

Izquierdo-Serra, M., Gascón-Moya, M., Hirtz, J. J., Pittolo, S., Poskanzer, K. E., Ferrer, E., … Gorostiza, P. (2014). Two-photon neuronal and astrocytic stimulation of azobenzene-based photoswitches. *Journal of the American Chemical Society*, *0*(ja), 140523112951005. doi:10.1021/ja5026326

Johnson, M. (2006). Molecular mechanisms of beta(2)-adrenergic receptor function, response, and regulation. *The Journal of Allergy and Clinical Immunology*, *117*(1), 18–24; quiz 25. doi:10.1016/j.jaci.2005.11.012

Joshi, S., Perera, S., Gilbert, J., Smith, C. M., Mariana, A., Gordon, C. P., … Chircop, M. (2010). The dynamin inhibitors MiTMAB and OcTMAB induce cytokinesis failure and inhibit cell proliferation in human cancer cells. *Molecular Cancer Therapeutics*, *9*(7), 1995–2006. doi:10.1158/1535-7163.MCT-10-0161

Kienzler, M. a, Reiner, A., Trautman, E., Yoo, S., Trauner, D., & Isacoff, E. Y. (2013). A red-shifted, fast-relaxing azobenzene photoswitch for visible light control of an ionotropic glutamate receptor. *Journal of the American Chemical Society*, *135*(47), 17683–6. doi:10.1021/ja408104w

Kneissl, S., Loveridge, E. J., Williams, C., Crump, M. P., & Allemann, R. K. (2008). Photocontrollable peptide-based switches target the anti-apoptotic protein Bcl-xL. *Chembiochem : A European Journal of Chemical Biology*, *9*(18), 3046–54. doi:10.1002/cbic.200800502

Kuil, J., van Wandelen, L. T. M., de Mol, N. J., & Liskamp, R. M. J. (2008). A photoswitchable ITAM peptidomimetic: synthesis and real time surface plasmon resonance (SPR) analysis of the effects of cis-trans isomerization on binding. *Bioorganic & Medicinal Chemistry*, *16*(3), 1393–9. doi:10.1016/j.bmc.2007.10.049

Kuil, J., van Wandelen, L. T. M., de Mol, N. J., & Liskamp, R. M. J. (2009). Switching between low and high affinity for the Syk tandem SH2 domain by irradiation of azobenzene containing ITAM peptidomimetics. *Journal of Peptide Science : An Official Publication of the European Peptide Society*, *15*(10), 685–91. doi:10.1002/psc.1173

Kumita, J. R., Flint, D. G., Smart, O. S., & Woolley, G. A. (2002). Photo-control of peptide helix content by an azobenzene cross-linker: steric interactions with underlying residues are not critical. *Protein Engineering*, *15*(7), 561–9.

Kumita, J. R., Flint, D. G., Woolley, G. A., & Smart, O. S. (2003). Achieving photo-control of protein conformation and activity: producing a photo-controlled leucine zipper. *Faraday Discussions*, *122*, 89–103. doi:10.1039/b200897a

Kumita, J. R., Smart, O. S., & Woolley, G. A. (2000). Photo-control of helix content in a short peptide. *Proceedings of the National Academy of Sciences of the United States of America*, *97*(8), 3803–8.

Kumita, J. R., Weston, C. J., Choo-Smith, L.-P., Woolley, G. A., & Smart, O. S. (2003). Prevention of peptide fibril formation in an aqueous environment by mutation of a single residue to Aib. *Biochemistry*, *42*(15), 4492–8. doi:10.1021/bi026856t

Kusebauch, U., Cadamuro, S. A., Musiol, H.-J., Moroder, L., & Renner, C. (2007). Photocontrol of the collagen triple helix: synthesis and conformational characterization of bis-cysteinyl collagenous peptides with an azobenzene clamp. *Chemistry (Weinheim an Der Bergstrasse, Germany)*, *13*(10), 2966–73. doi:10.1002/chem.200601162

Laarhoven, W. H. (2003). 4n+2 Systems: Molecules derived from Z-hexa-1,3,5-triene/cyclohexa-1,3-diene. In H. Dürr & H. Bouas-Laurent (Eds.), *Photochromism: Molecules and Systems* (2nd ed., pp. 270–313). Elsevier Inc.

Lee, S., Jung, K.-Y., Park, J., Cho, J.-H., Kim, Y.-C., & Chang, S. (2010). Synthesis of potent chemical inhibitors of dynamin GTPase. *Bioorganic & Medicinal Chemistry Letters*, *20*(16), 4858–64. doi:10.1016/j.bmcl.2010.06.092

Lefkowitz, R. (2007). Seven transmembrane receptors: something old, something new. *Acta Physiologica*, 9–19. doi:10.1111/j.1748-1716.2007.01693.x

Lefkowitz, R. J., & Whalen, E. J. (2004). Beta-Arrestins: Traffic Cops of Cell Signaling. *Current Opinion in Cell Biology*, *16*(2), 162–8. doi:10.1016/j.ceb.2004.01.001

Lemoine, D., Habermacher, C., Martz, A., Méry, P.-F., Bouquier, N., Diverchy, F., … Grutter, T. (2013). Optical control of an ion channel gate. *Proceedings of the National Academy of Sciences of the United States of America*, *110*(51), 20813–8. doi:10.1073/pnas.1318715110

Lin, J. Y. (2011). A user's guide to channelrhodopsin variants: features, limitations and future developments. *Experimental Physiology*, *96*(1), 19–25. doi:10.1113/expphysiol.2009.051961

Lougheed, T., Borisenko, V., Hennig, T., Ruck-Braun, K., & Woolley, G. A. (2004). Photomodulation of ionic current through hemithioindigo-modified gramicidin channels. *Organic & Biomolecular Chemistry*, *2*(19), 2798–801. doi:10.1039/B408485C

Macia, E., Ehrlich, M., Massol, R., Boucrot, E., Brunner, C., & Kirchhausen, T. (2006). Dynasore, a cell-permeable inhibitor of dynamin. *Developmental Cell*, *10*(6), 839–50. doi:10.1016/j.devcel.2006.04.002

Mackay, J. P., Sunde, M., Lowry, J. A., Crossley, M., & Matthews, J. M. (2007). Protein interactions: is seeing believing? *Trends in Biochemical Sciences*, *32*(12), 530–531.

Mao, T., Kusefoglu, D., Hooks, B. M., Huber, D., Petreanu, L., & Svoboda, K. (2011). Long-range neuronal circuits underlying the interaction between sensory and motor cortex. *Neuron*, *72*(1), 111–23. doi:10.1016/j.neuron.2011.07.029

McMahon, H. T., & Boucrot, E. (2011). Molecular mechanism and physiological functions of clathrin-mediated endocytosis. *Nature Reviews. Molecular Cell Biology*, *12*(8), 517–33. doi:10.1038/nrm3151

Meijering, E., Dzyubachyk, O., & Smal, I. (2012). *Methods for cell and particle tracking. Methods in enzymology* (1st ed., Vol. 504, pp. 183–200). Elsevier Inc. doi:10.1016/B978-0-12-391857-4.00009-4

Merino, E., & Ribagorda, M. (2012). Control over molecular motion using the cis-trans photoisomerization of the azo group. *Beilstein Journal of Organic Chemistry*, *8*, 1071–90. doi:10.3762/bjoc.8.119

Merrifield, C. J., Feldman, M. E., Wan, L., & Almers, W. (2002). Imaging actin and dynamin recruitment during invagination of single clathrin-coated pits. *Nature Cell Biology*, *4*(9), 691–8. doi:10.1038/ncb837

Miller, G. (2006). Optogenetics. Shining new light on neural circuits. *Science (New York, N.Y.)*, *314*(5806), 1674–6. doi:10.1126/science.314.5806.1674

Miyamoto, S., & Kollman, P. A. (1992). Settle: An analytical version of the SHAKE and RATTLE algorithm for rigid water models. *Journal of Computational Chemistry*, *13*(8), 952–962. doi:10.1002/jcc.540130805

Moellering, R. E., Cornejo, M., Davis, T. N., Bianco, C. Del, Aster, J. C., Blacklow, S. C., … Bradner, J. E. (2009). Direct inhibition of the NOTCH transcription factor complex. *Nature*, *462*(7270), 182–188. doi:http://www.nature.com/nature/journal/v462/n7270/suppinfo/nature08543_S1.html

Morgan, S.-A., Al-Abdul-Wahid, S., & Woolley, G. A. (2010). Structure-based design of a photocontrolled DNA binding protein. *Journal of Molecular Biology*, *399*(1), 94–112. doi:10.1016/j.jmb.2010.03.053

Motley, A., Berg, N., Taylor, M. J., Sahlender, D. A., Hirst, J., Owen, D. J., & Robinson, M. S. (2006). Functional analysis of AP-2 α and μ2 subunits. *Molecular Biology of …*, *17*(December), 5298–5308. doi:10.1091/mbc.E06–05–0452

Mullard, A. (2012). Protein–protein interaction inhibitors get into the groove. *Nat Rev Drug Discov*, *11*(3), 173–175. Retrieved from http://dx.doi.org/10.1038/nrd3680

Nagel, G., Ollig, D., Fuhrmann, M., Kateriya, S., Musti, A. M., Bamberg, E., & Hegemann, P. (2002). Channelrhodopsin-1: a light-gated proton channel in green algae. *Science (New York, N.Y.)*, *296*(5577), 2395–8. doi:10.1126/science.1072068

Nagel, G., Szellas, T., Huhn, W., Kateriya, S., Adeishvili, N., Berthold, P., … Bamberg, E. (2003). Channelrhodopsin-2, a directly light-gated cation-selective membrane channel. *Proceedings of the National Academy of Sciences of the United States of America*, *100*(24), 13940–5. doi:10.1073/pnas.1936192100

Neduva, V., Linding, R., Su-Angrand, I., Stark, A., de Masi, F., Gibson, T. J., … Russell, R. B. (2005). Systematic discovery of new recognition peptides

mediating protein interaction networks. *PLoS Biology*, *3*(12), e405. doi:10.1371/journal.pbio.0030405

Nevola, L., Martín-Quirós, A., Eckelt, K., Camarero, N., Tosi, S., Llobet, A., … Gorostiza, P. (2013). Light-regulated stapled peptides to inhibit protein-protein interactions involved in clathrin-mediated endocytosis. *Angewandte Chemie (International Ed. in English)*, *52*(30), 7704–8. doi:10.1002/anie.201303324

Packer, A. M., Peterka, D. S., Hirtz, J. J., Prakash, R., Deisseroth, K., & Yuste, R. (2012). Two-photon optogenetics of dendritic spines and neural circuits. *Nature Methods*, *9*(12), 1202–5. doi:10.1038/nmeth.2249

Parisot, J., Kurz, K., Hilbrig, F., & Freitag, R. (2009). Use of azobenzene amino acids as photo-responsive conformational switches to regulate antibody-antigen interaction. *Journal of Separation Science*, *32*(10), 1613–24. doi:10.1002/jssc.200800698

Petreanu, L., Mao, T., Sternson, S. M., & Svoboda, K. (2009). The subcellular organization of neocortical excitatory connections. *Nature*, *457*(7233), 1142–5. doi:10.1038/nature07709

Petsalaki, E., & Russell, R. B. (2008). Peptide-mediated interactions in biological systems: new discoveries and applications. *Current Opinion in Biotechnology*, *19*(4), 344–50. doi:10.1016/j.copbio.2008.06.004

Poloni, C., Szymański, W., Hou, L., Browne, W. R., & Feringa, B. L. (2014). A fast, visible-light-sensitive azobenzene for bioorthogonal ligation. *Chemistry (Weinheim an Der Bergstrasse, Germany)*, *20*(4), 946–51. doi:10.1002/chem.201304129

Ponka, P., & Lok, C. N. (1999). The transferrin receptor: role in health and disease. *The International Journal of Biochemistry & Cell Biology*, *31*(10), 1111–37.

Pozhidaeva, N., Cormier, M.-E., Chaudhari, A., & Woolley, G. A. (2004). Reversible photocontrol of peptide helix content: adjusting thermal stability of the cis state. *Bioconjugate Chemistry*, *15*(6), 1297–303. doi:10.1021/bc049855h

Rau, H. (1989). Photoisomerization of Azobenzenes. In J. F. Rabek (Ed.), *Photochemistry and Photophysics*. CRC Press.

Rau, H. (2003). Azo compounds. In H. Dürr & H. Bouas-Laurent (Eds.), *Photochromism: Molecules and Systems* (2nd ed., pp. 165–192). Elsevier Inc.

Reisinger, B., Kuzmanovic, N., Löffler, P., Merkl, R., König, B., & Sterner, R. (2014). Exploiting protein symmetry to design light-controllable enzyme inhibitors. *Angewandte Chemie (International Ed. in English)*, *53*(2), 595–8. doi:10.1002/anie.201307207

Reiter, A., Skerra, A., Trauner, D., & Schiefner, A. (2013). A photoswitchable neurotransmitter analogue bound to its receptor. *Biochemistry*, *52*(50), 8972–4. doi:10.1021/bi4014402

Renner, C., Kusebauch, U., Löweneck, M., Milbradt, A. G., & Moroder, L. (2005). Azobenzene as photoresponsive conformational switch in cyclic peptides. *The Journal of Peptide Research : Official Journal of the American Peptide Society*, *65*(1), 4–14. doi:10.1111/j.1399-3011.2004.00203.x

Renner, C., & Moroder, L. (2006). Azobenzene as conformational switch in model peptides. *Chembiochem : A European Journal of Chemical Biology*, *7*(6), 868–78. doi:10.1002/cbic.200500531

Robinson, J. A. (2008). Beta-hairpin peptidomimetics: design, structures and biological activities. *Accounts of Chemical Research*, *41*(10), 1278–88. doi:10.1021/ar700259k

Sadovski, O., Beharry, A. A., Zhang, F., & Woolley, G. A. (2009). Spectral tuning of azobenzene photoswitches for biological applications. *Angewandte Chemie (International Ed. in English)*, *48*(8), 1484–6. doi:10.1002/anie.200805013

Samanta, S., Beharry, A. A., Sadovski, O., McCormick, T. M., Babalhavaeji, A., Tropepe, V., & Woolley, G. A. (2013). Photoswitching Azo Compounds in Vivo with Red Light. *Journal of the American Chemical Society*, *135*(26), 9777–9784. doi:10.1021/ja402220t

Samanta, S., & Woolley, G. A. (2011). Bis-azobenzene crosslinkers for photocontrol of peptide structure. *Chembiochem : A European Journal of Chemical Biology*, *12*(11), 1712–23. doi:10.1002/cbic.201100204

Sbalzarini, I. F., & Koumoutsakos, P. (2005). Feature point tracking and trajectory analysis for video imaging in cell biology. *Journal of Structural Biology*, *151*(2), 182–95. doi:10.1016/j.jsb.2005.06.002

Schierling, B., Noël, A.-J., Wende, W., Hien, L. T., Volkov, E., Kubareva, E., … Pingoud, A. (2010). Controlling the enzymatic activity of a restriction enzyme by light. *Proceedings of the National Academy of Sciences of the United States of America*, *107*(4), 1361–6. doi:10.1073/pnas.0909444107

Schindelin, J., Arganda-Carreras, I., Frise, E., Kaynig, V., Longair, M., Pietzsch, T., … Cardona, A. (2012). Fiji: an open-source platform for biological-image analysis. *Nature Methods*, *9*(7), 676–82. doi:10.1038/nmeth.2019

Schmid, E. M., Ford, M. G. J., Burtey, A., Praefcke, G. J. K., Peak-Chew, S.-Y., Mills, I. G., … McMahon, H. T. (2006). Role of the AP2 β-Appendage Hub in Recruiting Partners for Clathrin-Coated Vesicle Assembly. *PLoS Biol*, *4*(9), e262. doi:10.1371/journal.pbio.0040262

Schmidt, D., Tillberg, P. W., Chen, F., & Boyden, E. S. (2014). A fully genetically encoded protein architecture for optical control of peptide ligand concentration. *Nature Communications*, *5*, 3019. doi:10.1038/ncomms4019

Schrader, T. E., Schreier, W. J., Cordes, T., Koller, F. O., Babitzki, G., Denschlag, R., … Zinth, W. (2007). Light-triggered beta-hairpin folding and unfolding. *Proceedings of the National Academy of Sciences of the United States of America*, *104*(40), 15729–34. doi:10.1073/pnas.0707322104

Shiraishi, Y., Itoh, M., & Hirai, T. (2010). Thermal isomerization of spiropyran to merocyanine in aqueous media and its application to colorimetric temperature indication. *Physical Chemistry Chemical Physics : PCCP*, *12*(41), 13737–45. doi:10.1039/c0cp00140f

Stawski, P., Sumser, M., & Trauner, D. (2012). A photochromic agonist of AMPA receptors. *Angewandte Chemie (International Ed. in English)*, *51*(23), 5748–51. doi:10.1002/anie.201109265

Strickland, D., Lin, Y., Wagner, E., Hope, C. M., Zayner, J., Antoniou, C., … Glotzer, M. (2012). TULIPs: tunable, light-controlled interacting protein tags for cell biology. *Nature Methods*, *9*(4), 379–84. doi:10.1038/nmeth.1904

Strickland, D., Yao, X., & Gawlak, G. (2010). Rationally improving LOV domain-based photoswitches. *Nature …*, *7*(8), 623–626. doi:10.1038/nmeth.1473.Rationally

Svensen, N., Walton, J. G. a, & Bradley, M. (2012). Peptides for cell-selective drug delivery. *Trends in Pharmacological Sciences*, *33*(4), 186–92. doi:10.1016/j.tips.2012.02.002

Tompa, P., & Fuxreiter, M. (2008). Fuzzy complexes: polymorphism and structural disorder in protein-protein interactions. *Trends in Biochemical Sciences*, *33*(1), 2–8. doi:10.1016/j.tibs.2007.10.003

Traub, L. M. (2009). Tickets to ride: selecting cargo for clathrin-regulated internalization. *Nature Reviews. Molecular Cell Biology*, *10*(9), 583–96. doi:10.1038/nrm2751

Vasudevan, N. T., Mohan, M. L., Goswami, S. K., & Prasad, S. V. N. (2011). Regulation of β -adrenergic receptor function An emphasis on receptor resensitization. *Cell Cycle*, *10*(21), 3684–3691. doi:10.4161/cc.10.21.18042

Verdine, G. L., & Hilinski, G. J. (2012). Stapled peptides for intracellular drug targets. In *Methods in enzymology* (1st ed., Vol. 503, pp. 3–33). Elsevier Inc. doi:10.1016/B978-0-12-396962-0.00001-X

Volgraf, M., Gorostiza, P., Numano, R., Kramer, R. H., Isacoff, E. Y., & Trauner, D. (2006). Allosteric control of an ionotropic glutamate receptor with an optical switch. *Nature Chemical Biology*, *2*(1), 47–52. doi:10.1038/nchembio756

Volgraf, M., Gorostiza, P., Szobota, S., Helix, M. R., Isacoff, E. Y., & Trauner, D. (2007). Reversibly caged glutamate: a photochromic agonist of ionotropic glutamate receptors. *Journal of the American Chemical Society*, *129*(2), 260–1. doi:10.1021/ja067269o

Vomasta, D., Högner, C., Branda, N. R., & König, B. (2008). Regulation of human carbonic anhydrase I (hCAI) activity by using a photochromic inhibitor. *Angewandte Chemie (International Ed. in English)*, *47*(40), 7644–7. doi:10.1002/anie.200802242

Von Kleist, L., Stahlschmidt, W., Bulut, H., Gromova, K., Puchkov, D., Robertson, M. J., … Haucke, V. (2011). Role of the clathrin terminal domain in regulating coated pit dynamics revealed by small molecule inhibition. *Cell*, *146*(3), 471–84. doi:10.1016/j.cell.2011.06.025

Walensky, L. D., Kung, A. L., Escher, I., Malia, T. J., Barbuto, S., Wright, R. D., … Korsmeyer, S. J. (2004). Activation of Apoptosis in Vivo by a Hydrocarbon-Stapled BH3 Helix. *Science*, *305*(5689), 1466–1470. doi:10.1126/science.1099191

Woolley, G. A. (2005). Photocontrolling Peptide α Helices. *Accounts of Chemical Research*, *38*(6), 486–493. doi:10.1021/ar040091v

Woolley, G. A., Jaikaran, A. S. I., Berezovski, M., Calarco, J. P., Krylov, S. N., Smart, O. S., & Kumita, J. R. (2006). Reversible photocontrol of DNA binding by a designed GCN4-bZIP protein. *Biochemistry*, *45*(19), 6075–84. doi:10.1021/bi060142r

Yin, H., Lee, G., Park, H. S., Payne, G. a, Rodriguez, J. M., Sebti, S. M., & Hamilton, A. D. (2005). Terphenyl-based helical mimetics that disrupt the p53/HDM2 interaction. *Angewandte Chemie (International Ed. in English)*, *44*(18), 2704–7. doi:10.1002/anie.200462316

Zhang, F., Sadovski, O., & Woolley, G. A. (2008). Synthesis and characterization of a long, rigid photoswitchable cross-linker for promoting peptide and protein conformational change. *Chembiochem : A European Journal of Chemical Biology*, *9*(13), 2147–54. doi:10.1002/cbic.200800196

Zhang, F., Timm, K. a, Arndt, K. M., & Woolley, G. A. (2010). Photocontrol of coiled-coil proteins in living cells. *Angewandte Chemie (International Ed. in English)*, *49*(23), 3943–6. doi:10.1002/anie.201000909

Zhang, F., Wang, L.-P., Brauner, M., Liewald, J. F., Kay, K., Watzke, N., … Deisseroth, K. (2007). Multimodal fast optical interrogation of neural circuitry. *Nature*, *446*(7136), 633–9. doi:10.1038/nature05744

Appendix IV - Abbreviations

	γ-ITAM	γ-immunoglobulin tyrosine based activation motif
	7MSR	Seven membrane-spanning helices-containing receptor
A	Aib	α-aminoisobutyric acid
	Alexa647-Tf	Transferrin labeled with the Alexa 647 fluorescent dye
	AMPA	α-amino-3-hydroxy-5-methyl-4-isoxazolepropionic acid
	AP	Adaptor protein complex
	AP180	Clathrin coat assembly protein 180 KDa
	AsLOV2	Light-oxygen-voltage-sensing domain 2 from *Avena sativa*
	ATA-3	Azobenzene tetrazolyl AMPA type 3
	ATCC	American Type Culture Collection
B	BAP	β-arrestin C-terminal region peptide
	BAP-long	β-arrestin C-terminal region peptide 20-mer DDDIVFEDFARQRLKGMKDD
	BAR	Bin-amphiphysin-Rvs domain
	Bcl-2	B-cell lymphoma protein 2
	Bcl-XL	B-cell lymphoma extra-large protein
	BH3	Bcl-2 homology domain type 3
	BisQ	*trans*-3,3'-bis[α-(trimethylammonium)-methyl]azobenzene bromide
	BSBCA	3,3'-bis(sulfonato)-4,4'-bis(chloroacetamido)-azobenzene
C	CCP	Clathrin-coated pit
	CCV	Clathrin-coated vesicle
	CD	Circular Dichroism
	Cell-permeable	capable of crossing the plasma membrane of cells

	CF-BAP-long	Carboxyfluorescein-labeled BAP-long
	CF-TL-1	Carboxyfluorescein-labeled TL 1
	CF-TL-2	Carboxyfluorescein-labeled TL 2
	ChR	Channelrhodopsin
	CLASP	Clathrin-associated sorting protein
	CME	Clathrin-mediated endocytosis
	COPI	Coat protein complex I
	COPII	Coat protein complex II
D	DABS	2,5-diaminobenzenesulfonic acid
	DCM	Dichloromethane
	DFM	Dimethylformamide
	DIPEA	*N,N*-Diisopropylethylamine
	DMEM	Dulbecco's modified Eagle's medium
E	EDTA	Ethylenediaminetetraacetic acid
	ESI	Electrospray Ionization
F	FCS	Fetal calf serum
	FcεRI	High affinity receptor for the Fc region of immunoglobulin E
	Fmoc/tBu	9-fluorenylmethoxycarbonyl/tertbutyl
	FP	Fluorescence polarization
G	Gluazo	(4R)-4-[(2E)-3-{4-[(E)-phenyldiazenyl]phenyl}prop-2-en-1-yl]-1-L-glutamic acid
	GPCR	G-protein coupled receptor
	GRK2	G-protein receptor kinase 2
H	HOAt	1-Hydroxy-7-azabenzotriazole
	HPLC	High-performance liquid chromatography
L	LCa	Clathrin light chain A
	Lca-mRFP	Clathrin light chain A fused to monomeric red fluorescent polarization
	LOV	Light-oxygen-voltage-sensing domain
M	MAG	Maleimide-azobenzene-glutamate
	MAL-AZO-QA	Maleimide-azobenzene-quaternary ammonium
	MALDI	Matrix-assisted laser desorption-ionization

	MRE	Molar per residue ellipticity
	mRFP	Monomeric red fluorescent protein
	MTT	3-(4,5-dimethylthiazol-2-yl)-2,5-diphenyltetrazolium bromide
N	Nal	Naphtylalanine
	NMR	Nuclear Magnetic Resonance
	nNOS	Neuronal isoform of nitric oxide synthase
	NpHR	Halorhodopsin from *Natromonas pharaonis*
P	PBS	Phosphate-buffered saline
	PCL	Photochromic ligand
	PDB	Protein Data Bank
	PIPPI	Photoswitchable inhibitor of protein-protein interaction
	PPI	Protein-protein interaction
	PSS	Photostationary state
	PTL	Photoswitchable tethered ligand
	PyBOP	benzotriazol-1-yl-oxytripyrrolidinophosphonium hexafluorophosphate
Q	QBr	3-(α-bromomethyl)-3'-[α-(trimethylammonium)methyl]azobenzene bromide
R	REMD	Replica-exchange molecular dynamics
	RP-HPLC	Reverse-phase high-performance liquid chromatography
S	S.E.M.	Standard error of the mean
	SNR	Signal-to-noise ratio
T	TBTU	*N,N,N′,N′*-Tetramethyl-*O*-(benzotriazol-1-yl)uronium tetrafluoroborate
	TCEP	tris-(2-carboxyethyl)phosphine
	Tf	Transferrin
	TFA	Trifluoroacetic acid
	TfR	Transferrin receptor
	TIPS	Triisopropylsilane
	TIRF	Total internal reflection

TIRFM	Total internal reflection microscopy
TL	Traffic light peptide
TOF	Time of flight
TrpZip2	β-hairpin tryptophan zipper 2 peptide
TULIP	Tunable, light-controlled interacting protein tag